Fisheries New Zealand
Tini a Tangaroa

Antipodean albatross multi-threat risk assessment

New Zealand Aquatic Environment and Biodiversity Report No. 332

Y. Richard,
K. Berkenbusch,
E. Crawford,
M. Tornquist,
K. Walker,
G. Elliott,
L. Tremblay-Boyer

ISSN 1179-6480 (online)
ISBN 978-1-991285-71-3 (online)

June 2024

Te Kāwanatanga o Aotearoa
New Zealand Government

Disclaimer

This document is published by Fisheries New Zealand, a business unit of the Ministry for Primary Industries (MPI). The information in this publication is not government policy. While every effort has been made to ensure the information is accurate, the Ministry for Primary Industries does not accept any responsibility or liability for error of fact, omission, interpretation, or opinion that may be present, nor for the consequence of any decisions based on this information. Any view or opinion expressed does not necessarily represent the view of Fisheries New Zealand or the Ministry for Primary Industries.

Requests for further copies should be directed to:

Fisheries Science Editor
Fisheries New Zealand
Ministry for Primary Industries
PO Box 2526
Wellington 6140
NEW ZEALAND

Email: Fisheries-Science.Editor@mpi.govt.nz
Telephone: 0800 00 83 33

This publication is also available on the Ministry for Primary Industries websites at:
http://www.mpi.govt.nz/news-and-resources/publications
http://fs.fish.govt.nz go to Document library/Research reports

© Crown Copyright – Fisheries New Zealand

Please cite this report as:

Richard, Y.; Berkenbusch, K.; Crawford, E.; Tornquist, M.; Walker, K.; Elliott, G.; Tremblay-Boyer, L. (2024). Antipodean albatross multi-threat risk assessment. *New Zealand Aquatic Environment and Biodiversity Report No. 332*. 62 p.

TABLE OF CONTENTS

EXECUTIVE SUMMARY 1

1 INTRODUCTION 2

2 METHODS 3
2.1 Review of threats to Antipodean albatross . . . 3
2.2 Antipodean albatross population model . . . 4
2.3 Impact of New Zealand fisheries . . . 5
2.4 Impact of international fisheries . . . 6
2.4.1 Comparison of catchabilities from survival rates and overlaps . . . 6
2.5 Impact of climate . . . 7
2.6 Management scenarios . . . 8

3 RESULTS 10
3.1 Literature review: threats to Antipodean albatross . . . 10
3.1.1 Fisheries . . . 10
3.1.2 Climate change . . . 12
3.1.3 Plastic pollution . . . 13
3.1.4 Contaminants . . . 14
3.1.5 Diseases . . . 15
3.2 Population model of Antipodean albatross . . . 15
3.3 Interactions with New Zealand fisheries . . . 22
3.4 Interactions with international fisheries . . . 26
3.4.1 Comparison of catchabilities from survival rates and overlaps . . . 28
3.5 Impact of climate . . . 30
3.6 Exploration of management scenarios . . . 34

4 DISCUSSION 35

5 ACKNOWLEDGEMENTS 37

6 REFERENCES 38

APPENDIX A STAN MODELS 43
A.1 Model of population dynamics of Antipodean albatross . . . 43
A.2 Estimation of captures in New Zealand fisheries . . . 51

APPENDIX B POPULATION MODEL DIAGNOSTICS 52

APPENDIX C AT-SEA DISTRIBUTION OF ANTIPODEAN ALBATROSS 58

APPENDIX D NEW ZEALAND FISHING EFFORT 59

APPENDIX E MODEL DIAGNOSTICS FOR NEW ZEALAND FISHERY IMPACT 60

APPENDIX F OVERLAP BY YEAR AND FLAG IN THE TASMAN SEA 61

APPENDIX G INTERNATIONAL FISHERIES CATEGORISED AS “OTHER” 62

Plain language summary

Antipodean albatross breed at Antipodes Islands, to the south of New Zealand. Its population has been declining since 2005. Data collected since 1994 were used to make a model of the albatross population. The model showed that the number of albatrosses, their survival rates (especially for females), and their breeding rates have all decreased. This study looked at whether fishing, climate change, plastic pollution, and diseases could be causing the population decline. To find out, the study looked at where the albatrosses go when they are away from Antipodes Island. Female albatrosses spend more time in the Tasman Sea and north-east of New Zealand than males do. The study didn't find one clear reason for the albatross decline. But, it suggested that an increase in tuna fishing in the Tasman Sea, after 2006, might be a factor. The study suggested that we need more information on albatross captures by tuna fishing vessels in the Tasman Sea.

EXECUTIVE SUMMARY

Richard, Y.[1]; Berkenbusch, K.[1]; Crawford, E.[1]; Tornquist, M.[1]; Walker, K.[2]; Elliott, G.[2]; Tremblay-Boyer, L.[3] (2024). Antipodean albatross multi-threat risk assessment.

***New Zealand Aquatic Environment and Biodiversity Report No. 332*. 62 p.**

Antipodean albatross (*Diomedea antipodensis antipodensis*) is one of two subspecies of wandering albatross *Diomedea antipodensis*, with Gibson's albatross *D. antipodensis gibsoni* forming the other subspecies. The species is endemic to New Zealand, with Antipodean albatross nesting primarily on Antipodes Island (and a few breeding pairs on Chatham and Campbell islands), whereas Gibson's albatross breeds at the Auckland Islands.

The Antipodean albatross population has undergone a considerable decline since 2005, but the underlying causes of this decline remain unknown. The at-sea distribution of Antipodean albatross covers an extensive area from Australia to South America and there are a number of potential threats that may impact the population. The goal of this study was to investigate the causes of the Antipodean albatross decline. The investigation included a literature review to collate information of the different threats to Antipodean albatross and similar species, followed by an analysis of data and modelling to assess the impacts of different threats.

The analysis included the development of a Bayesian model to estimate the principal demographic parameters of the population and how they varied over time. The estimated parameters confirmed previous results that the population decline was a result of a decrease in survival rate, mostly of adult females, and in the breeding probability and breeding success.

The threat of fisheries was assessed by estimating the annual number of captures in New Zealand trawl, bottom-longline, and surface-longline fisheries. The estimation highlighted a peak in captures prior to 2005, and around 22 estimated captures per year across these fisheries thereafter.

The overlap in the spatial distribution between Antipodean albatross and international surface-longline fisheries showed an overall decrease around 2005, due to an overall decrease in fishing effort. Nevertheless, the overlap with fleets flagged to China and minor countries increased after 2007, and was negatively correlated with female annual survival. This relationship was not evident with other fleets. In addition, the differences between male and female survival, and between the periods pre- and post-2006, in overlaps with the fleets flagged to China, Vanuatu, Fiji, and Solomon Islands, were also the most consistent with differences in survival rates.

A simulation tool based on the population model was developed and made publicly available. The development included an expert workshop that allowed participants to test different management scenarios in view of the potential impacts of different threats. In this workshop, the fisheries operating in the Tasman Sea were found to be the most likely cause of the observed population decline. Varying the impact of different international fisheries individually, the fleet flagged to China was the only fleet that could potentially explain both the change after 2006 and the female-biased impact. When the impact factor of this fleet was set to lead to around 1450 hypothetical deaths annually across the entire distributional range of the species, the simulation showed a stabilisation of the population, and an even survival rate between both sexes, at around 97%. Changes in oceanographic and climate parameters since 1995, and the overlap with plastic pollution in the Pacific Ocean, did not explain the patterns in demographic parameters.

These results suggest that further research on fisheries in the Tasman Sea would support an increased understanding of population declines of Antipodean albatross.

---

[1] Dragonfly Data Science, New Zealand

[2] Albatross Research, New Zealand.

[3] CSIRO, Australia

1. INTRODUCTION

Antipodean albatross (*Diomedea antipodensis antipodensis*) is one of two subspecies of wandering albatross *Diomedea antipodensis*, with Gibson's albatross *D. antipodensis gibsoni* forming the other subspecies (Elliott & Walker 2013). The species is endemic to New Zealand, with Antipodean albatross nesting primarily on Antipodes Island (and a few breeding pairs on Chatham and Campbell islands), whereas Gibson's albatross breeds at the Auckland Islands.

Internationally, the species is classified as "Endangered" (BirdLife International 2018), listed on Appendix I of the Convention on Migratory Species (Convention on Migratory Species 2020), and each subspecies is individually classified as "Nationally Critical" under the New Zealand Threat Classification System (Robertson et al. 2021). The latter ranking was based on criterion C of the classification system, indicating a very high (>70%) ongoing or predicted decline.

Long-term monitoring has documented the population decline of the Antipodean albatross subspecies since 2005, caused by high female mortality, reduced breeding success, and increased age-at-breeding (Walker & Elliott 2022). Demographic modelling based on earlier survey data identified the main factors influencing population dynamics, which were breeding rate, and success and age at first breeding (Edwards et al. 2017). A subsequent integrated population model estimated mortality separately for adult males and females (Richard 2021). This modelling found that female survival had declined from 2004 onwards, and subsequently increased from 2013 onwards. Breeding success also declined from the early 1990s to 2008, but has stabilised since then, with a slight increase in recent years. The most recent population survey on Antipodes Island indicated a stable number of breeding pairs, and also potential increases in female survival, but the overall number of chicks produced continued to be small (Parker et al. 2023).

Previous risk assessments estimated the population impacts from bycatch mortality of Antipodean albatross (and other seabirds) in commercial fisheries in New Zealand waters and in the Southern Hemisphere (Abraham et al. 2019, Richard & Abraham 2020, Edwards et al. 2023a). Based on these risk assessments, the species (i.e., both subspecies) was ranked to be at a "medium" risk in New Zealand waters (Richard & Abraham 2020); for surface- (pelagic) longline fisheries in Southern Hemisphere waters (including New Zealand), the estimated number of annual captures did not exceed the population sustainability threshold (Abraham et al. 2019).

Recent population monitoring on Antipodes Island has included tracking studies, providing information of the at-sea distribution of individual birds (e.g., Walker & Elliott 2022, Parker et al. 2023). These tracking data were used in recent analyses that focused on determining the spatial distribution of Antipodean albatross and its overlap with commercial fisheries (Bose & Debski 2020, 2021, Richard et al. 2024). Other potential threats to Antipodes albatross include impacts from exposure to plastics or debris in the marine environment, diseases, and climate change (Phillips et al. 2016, Dias et al. 2019).

The present study built on previous research by providing a risk assessment for Antipodean albatross. It focused on developing an updated population model, and assessing the risks of multiple threats to this subspecies, including spatial information. The Fisheries New Zealand funded project (number PRO2021-03) had the overall objective "to identify the sources of risk to Antipodean Albatross from both within New Zealand's EEZ and extending to the entire population distribution". The project had four specific objectives:

1. Construct a population model for the Antipodean albatross colony and sub-population.
2. Map fishery and non-fishery threats to Antipodean albatross and estimate the overlap between multi-year albatross distributions and threats.
3. Estimate fisheries impact and risk to Antipodean albatross.
4. Examine a range of spatial management scenarios through both modelling and outcomes from a multi-threat risk assessment workshop.

2. METHODS

2.1 Review of threats to Antipodean albatross

The scoping of key threats to Antipodean albatross was guided by existing reviews (e.g., Phillips et al. 2016, Dias et al. 2019), individual studies (e.g., Cherel et al. 2018, Jaeger et al. 2018, Roman et al. 2019), and suggestions from members of the Aquatic Environment Working Group (discussed at its meeting 9 June 2022). An important consideration for this scoping was the availability of spatial data that would allow the mapping of threats to estimate their overlap with multi-year Antipodean albatross distributions.

A review of threats to albatross and petrel species that are part of the Agreement on the Conservation of Albatrosses and Petrels considered fishery bycatch the greatest threat to these species (Phillips et al. 2016, Dias et al. 2019). Other identified threats included intentional take (or killing at sea), pollution (including debris, discarded fishing gear), introduced species at breeding sites, pathogens (e.g., diseases), and climate change. Similarly, a subsequent assessment of global threats to seabirds listed bycatch as the main threat to albatrosses in general, followed by invasive non-native species, climate change and severe weather events, and diseases (Dias et al. 2019).

Land-based impacts from introduced species were omitted from the present risk assessment. Although ranked amongst the top threats to albatrosses, the eradication of mice (*Mus musculus*) from Antipodes Island in 2016 has meant that impacts from invasive non-native species are no longer relevant to Antipodean albatross at its main breeding sites (Department of Conservation 2018, Horn et al. 2019).

Suggestions from members of the Aquatic Environment Working Group (9 June 2022) included impacts from nutritional stress, as indicated in previous population modelling of Antipodean albatross (Edwards et al. 2017). Other suggestions were the intentional take or killing of birds at sea, and contaminants, such as heavy metals (i.e., mercury), that may affect the population.

From the initial scoping, a literature review was carried out to identify and capture (where available) qualitative and quantitative information that may be used to identify and compare threats to Antipodean albatross, including data for the model to develop different scenarios of the threats.

The search for information was mostly based on published reviews and individual research publications (including cross-referencing). The search focused on a number of databases: Aquatic Sciences and Fisheries Abstracts (including Biological Sciences, Biology Digest, BioOne.1, Conference Papers Index, Ocean Abstracts, Scopus Natural Sciences), Science Direct, Ornithological Worldwide Literature (includes coverage of grey literature), Searchable Ornithological Research Archive, Google, and Google Scholar.

Keywords for each threat were searched individually or in combination; e.g., search terms for plastic debris included *seabird, plastic*, debris*,*Procellariiform, Diomedeidae, *Diomedea*, albatross, ingest*, Southern Hemisphere, New Zealand. Broadly-defined initial searches that returned a large number (>500) of results were narrowed down by adding or exchanging a search term (e.g., “seabird” was replaced by “Procellariiform” or “albatross”).

In addition to the literature review, information from seabird necropsy data (held by Wildlife Management International) were queried for evidence of plastic ingestion.

Where spatial information was available, the spatial extent of the threat and its effect were included in the subsequent analysis and visualisation.

2.2 Antipodean albatross population model

The Antipodean albatross colony at Antipodes Island has been monitored by Department of Conservation annually since 1994, except in 2006 (see most recent survey reports by Walker & Elliott 2022 and Parker et al. 2023).

The survey data were used in previous population modelling, including the integrated population model developed by Richard (2021). This model was updated for the Antipodean albatross colony, using data from the period between 1995 and 2021.

The structure of the updated model was similar to the previous model (Richard 2021), and consisted of modelling the transition between latent states of successive years for each bird, based on the observed states recorded in the field. There were nine latent states considered in the model: adults breeding inside the study area, adults breeding outside the study area, adults non-breeding inside the study area, adults non-breeding outside the study area, pre-breeders inside the study area, pre-breeders outside the study area, juveniles inside the study area, juveniles outside the study area, and dead birds. The transition probabilities between successive states were specified, depending on the biology of the species. There were nine observed states, assigned from the state of the birds as recorded in the field: adults breeding inside the study area, adults not breeding inside the study area, adults outside the study area (breeding or not), pre-breeder inside the study area, pre-breeder outside the study area, juvenile inside the study area, juvenile outside the study area, dead birds, and not seen. The probabilities of an observed state were dependent on the latent state and the detection probability of each state.

In the model, juveniles start at the colony, then spend time at sea for a few years, before returning to the colony at the age of first return, when they become pre-breeders; they then breed for the first time at the age of first breeding, when they become adults; they become non-breeders or breed again the following year, depending on the outcome of their breeding attempt. Non-breeders may become breeders if they were previously unsuccessful breeders. At any annual time step, individuals may die depending on their class (juvenile, pre-breeder, adult female, or adult male), and year.

The model used previously by Richard (2021) was improved in several ways. In particular:

- the probability of breeding varied among years, as it was modelled with an annual random effect;
- the age at first return to the colony and age at first breeding were re-parametrised with a probability increasing linearly with age, from zero at a minimum age, to one at a maximum age. In contrast to the previous model, this change constrained the individuals to all return to the colony and to all breed after a certain age, leading to a portion of the population to never return or never breed;
- the detection probability of pre-breeders was allowed to increase for years when field surveys started later than usual, to account for pre-breeders tending to arrive at the colony later in the season than adults; in addition, they may be seen more frequently during late surveys;
- the model code was refactored so that the calculations of the transition probabilities could be exported into R to run simulations more quickly and with the assurance that the simulation process was identical to that in the model, minimising the chance of errors.

The Stan model was fitted from R using the package *cmdstanr* (https://mc-stan.org/cmdstanr), using Markov chain Monte Carlo (MCMC) algorithms. Four MCMC chains were run for 1500 iterations each, after a warm-up period of 1000 iterations.

2.3 Impact of New Zealand fisheries

The number of annual fatalities of Antipodean albatross in New Zealand fisheries was estimated from data on observed captures and observed fishing effort, collected by fisheries observers, and total fisher-reported effort and at-sea bird distribution maps. The capture and fishing effort data covered the period 1993 to 2020, and all fishing in trawl, bottom-longline, and surface-longline fisheries was considered.

Because Antipodean albatross are difficult to distinguish from other wandering albatrosses, we also included captures and distributions of Gibson’s and wandering (*D. exulans*) albatrosses, and generic captures of wandering albatross (*Diomedea* spp.).

The at-sea distributions for the three species were derived for the Southern Hemisphere seabird risk assessment at a 5-degree resolution from tracking data and colony sizes (Abraham et al. 2019). The distribution for all wandering albatross species was obtained by summing the distributions across the three species.

Captures and fishing effort were gridded to match the distribution extent and resolution of the species, and the fishing effort was categorised into four groups according to the fishing method.

A Bayesian model was developed to estimate the vulnerability of the species to captures in fisheries, in which the number of observed captures in each grid cell was assumed to be following a Poisson distribution. The mean number of captures was modelled differently depending on whether the captures were recorded at the species level, or at the genus level. For captures that were identified at the species level (equation 1), the mean number of captures I_{sg} of species s in the fishery group g was the product of the overlap between the fishery group and the species (θ_{sg}, i.e., the product of bird density and fishing effort), the vulnerability of the species to the fishery group (v_{sg}), and the probability that a capture was identified at the species level (p_{ident}). For unidentified captures, i.e., captures recorded as being of a generic wandering albatross (equation 2), the mean number of captures U_g in the fishery group g was the probability of a capture to be recorded as generic ($1 - p_{\text{ident}}$), multiplied by the sum over the three species of the product of the overlap and vulnerability for each species within the fishery group.

$$I_{sg} = \text{Poisson}(p_{\text{ident}} v_{sg} \theta_{sg}), \tag{1}$$

$$U_g = \text{Poisson}((1 - p_{\text{ident}}) \sum_s v_{sg} \theta_{sg}), \tag{2}$$

The model was fitted to the capture and effort data between 2003 and 2020, when capture data were more reliable, but predictions were made using the reporting period from 1993 to 2020.

The model was written using the Stan language (Carpenter et al. 2017) and fitted in R (R Core Team 2021) using the package rstan (Stan Development Team 2020). Four Markov chain Monte Carlo chains were run over 6000 iterations, with a warm-up period of 1000 iterations (the model code is shown in Appendix A.2).

From the fitted model, the total number of observable captures for each species and fishery group was then predicted by drawing randomly from a Poisson distribution with a mean equal to the product of the vulnerability v_{sg}, as estimated in the model and by the total overlap, calculated using total fishing effort.

2.4 Impact of international fisheries

Suitable data on observed captures and observed fishing effort in international fisheries were not available for this assessment, so that an estimation of captures in international fisheries was not attempted. Instead, the present study included an examination of the variability in overlap across years and among population classes, which was related to the variability of demographic parameters among years.

Spatial layers of international surface-longline fishing effort in hooks and by flag were obtained from Regional Fisheries Management Organisations (RFMOs), gridded at a 5-degree resolution, between 1995 and 2019. These grids were re-sampled to a 1-degree resolution to match the extent and resolution of the Antipodean albatross distribution layers derived by Richard et al. (2024). For this approach, fishing effort was first converted to densities, taking into account the area of each grid cell, and re-converting the value to hooks after re-projection.

The Antipodean albatross distribution modelling by Richard et al. (2024) provided a distribution density layer for each class (juvenile, pre-breeder, non-breeding adult, successful breeder, unsuccessful breeder) and for each sex (male and female). Hereafter, the combination of class and sex are referred to as “class” for simplicity.

The total overlap between each population class and flag fishery was calculated for each year, by summing the product of the bird density and the fishing effort at each grid cell and each year, over the entire grid. The bird densities were first normalised so that the sum over all cells of the product of bird density and cell area was one.

The correlation between overlap and yearly estimates of annual survival rates was then assessed graphically and by calculating the Pearson’s correlation coefficient (Freedman et al. 2007), with and without the Bonferroni correction factor (Dunn 1961), for each combination of flag fishery and population class.

2.4.1 Comparison of catchabilities from survival rates and overlaps

A novel approach was developed to assess whether changes in fisheries overlap between sexes and between the pre- and post-2006 periods were sufficient to explain changes in survival rates between sexes and between periods. The approach was applied to each fishery individually, considering all other factors to be constant.

The total annual mortality rate m of the species can be expressed as the sum of the annual mortality rate in the fishery g and the annual mortality rate m_o from all other causes (including natural or from other human-related causes):

$$m = m_g + m_o. \tag{3}$$

Assuming that the natural mortality and the mortality from human-related activities other than fishery g is the same between males and females, then:

$$m_{♂} - m_{g,♂} = m_{♀} - m_{g,♀}. \tag{4}$$

Because the annual mortality rate is one minus the annual survival rate $(1 - \varphi)$ and the mortality rate in fishery g is the product of catchability (q_g) in the fishery and the per-capita overlap between the species and the fishery (O), Equation 4 becomes:

$$(1 - \varphi_{♂}) - q_{g,♂} O_{g,♂} = (1 - \varphi_{♀}) - q_{g,♀} O_{g,♀}. \tag{5}$$

Assuming that the catchability of males and females is the same, then q_g, is:

$$q_g = -\frac{\varphi_{♂} - \varphi_{♀}}{O_{g,♂} - O_{g,♀}}. \tag{6}$$

Following a similar reasoning, using the survival rates pre- and post-2006 (φ_{pre} and φ_{post}, respectively), and assuming that catchability, natural mortality, and other mortality did not change between the two periods, then q_g for each sex is:

$$q_g = -\frac{\varphi_{\text{pre}} - \varphi_{\text{post}}}{O_{g,\text{pre}} - O_{g,\text{post}}}. \tag{7}$$

Using the difference in survival rates between males and females, the difference in survival rates between the two periods for each sex, and their associated overlaps, this approach provided three estimates for the catchability in fishery g. If the change in the overlap with fishery g is the main cause for the change in survival rates, then the three estimates of catchability should be similar, positive, and credible. The three estimates using this approach were calculated for each fishery and then compared.

The plausibility of the catchability estimates was assessed by comparing the estimates to the catchability from New Zealand fisheries. The latter was estimated directly from the estimated number of captures in the New Zealand fleet and its overlap with Antipodean albatross. Because the number of captures C in the fishery is the product of its catchability q, its overlap with adults O, and the total number of adults in the population N, then $q = C/ON$. The number of observable captures estimated here, however, is likely to underestimate the total number of fatalities, because not all captures are observable. Based on 15 years of observations in surface-longline fisheries, it was estimated that only half the fatalities were recoverable on-board of fishing vessels (Brothers et al. 2010). The estimated number of observable captures in New Zealand surface-longline fisheries was, therefore, doubled to calculate the catchability.

2.5 Impact of climate

Using the bird density layers by population class from Richard et al. (2024), a weighted average of several climatic variables was calculated for each year and population class to assess whether a change over time could explain the variability in demographic parameters.

These climate variables were included in the analysis and downloaded from National Oceanic and Atmospheric Administration (NOAA)[4] using the R package *rerddap* (Chamberlain 2023):

- sea surface temperature (SST) and anomaly, monthly (ERDDAP dataset "NOAA_DHW_monthly_Lon0360");
- wind speed and direction, monthly (ERDDAP dataset "erdlasFnWPr");
- air temperature, sea-level pressure, surface Lifted Index (atmospheric instability), omega (atmospheric vertical motion), relative humidity, daily (ERDDAP dataset "esrlNcepRe").

The climatic and atmospheric layers were converted to gridded annual averages and then re-sampled to the same extent and resolution as the bird density layers.

The annual weighted average of a climatic variable ($\bar{\alpha}$) was then calculated by population class by taking the sum over all grid cells of the product of the climatic value ($\alpha_{x,y}$) of cell (x,y) and its bird density of the class ($d_{x,y}$), divided by the total of number of birds in the class (Equation 8):

$$\bar{\alpha} = \frac{\sum_{x,y} \alpha_{x,y} d_{x,y}}{\sum_{x,y} d_{x,y}}. \tag{8}$$

---

[4] https://coastwatch.pfeg.noaa.gov/erddap

In addition, the monthly Southern Oscillation Index (SOI), although not spatially resolved, indicates periods of El Niño or La Niña phases, and was obtained from Statistics NZ.[5]

The correlation between climatic variables and demographic estimates by year was then assessed graphically and by calculating the Pearson's correlation coefficient, with and without the Bonferroni correction factor (Dunn 1961). The demographic parameters that were considered were annual survival rate for each of the ten population classes, breeding probability, and breeding success.

2.6 Management scenarios

To explore the impact of different scenarios on the Antipodean albatross population, the current project also included the development of an interactive application using R Shiny (Figure 1).

The application allows users to simulate the potential impact of a threat to the species. Spatial threats can be imported from a vector or raster file, or drawn manually on an interactive map; these threats are then rasterised automatically to the extent, projection, and resolution of the Antipodean albatross distribution. The user can specify the bird classes and sexes that may be impacted by the threat, and also the impact value, which represents the probability that a fatality results from a bird being exposed to a unit of threat.

Once the spatial threat is defined with the impacted classes and the impact value, the overlap between the distribution (from Richard et al. 2024) of the impacted bird classes and the threat is calculated by multiplying the bird density and the threat density in each 1-degree cell; it is then multiplied by the impact value to derive the number of fatalities spatially. The resulting total number of fatalities by class and sex is then reported.

For threats that have no spatial extent, or for which spatial information is unavailable, their impact can be defined as an overall number of fatalities, or as a change in the value of the demographic parameters directly (survival rate of juveniles, pre-breeders, adult female, and adult male, breeding probability, or breeding success).

In the scenario explorer, both spatial or non-spatial threats can be defined as either potential or existing. For potential threats, the impact is added, and decreases the value of the demographic parameters. A potential threat should be chosen when assessing the effect of a new threat, such as a new fishery or a new pollution source. For existing threats, removing the impact from the population dynamics leads to an increase in the values of demographic parameters. This scenario is useful for assessing the removal of a threat or its effect on the current population dynamics, e.g., when considering the closure of a fishery or to assess if a given impact is realistic.

When the impact of a threat is defined as a number of fatalities, the associated change in the annual survival rate of the impacted classes is calculated by converting the number of fatalities to a mortality rate. This mortality rate is the ratio of fatalities to the number of individuals in the population class in the initial global population.

For the initial population in the simulations, the structure of the population in 2021 was derived from simulating each individual over time using the transition probabilities fitted in the population model, from their first sighting after 1994 to 2021. The predicted status of the birds in 2021 was replaced with their actual status as recorded in the field when it was known. The total number of birds in each class and sex was then scaled to the global population by dividing this number by the proportion of the global population that is within the study area (2.73%).

Multiple threats can be considered in a single scenario. In this case, the impact on each class is added to calculate the associated change in demographic parameters.

---

[5] https://statisticsnz.shinyapps.io/enso_oct20

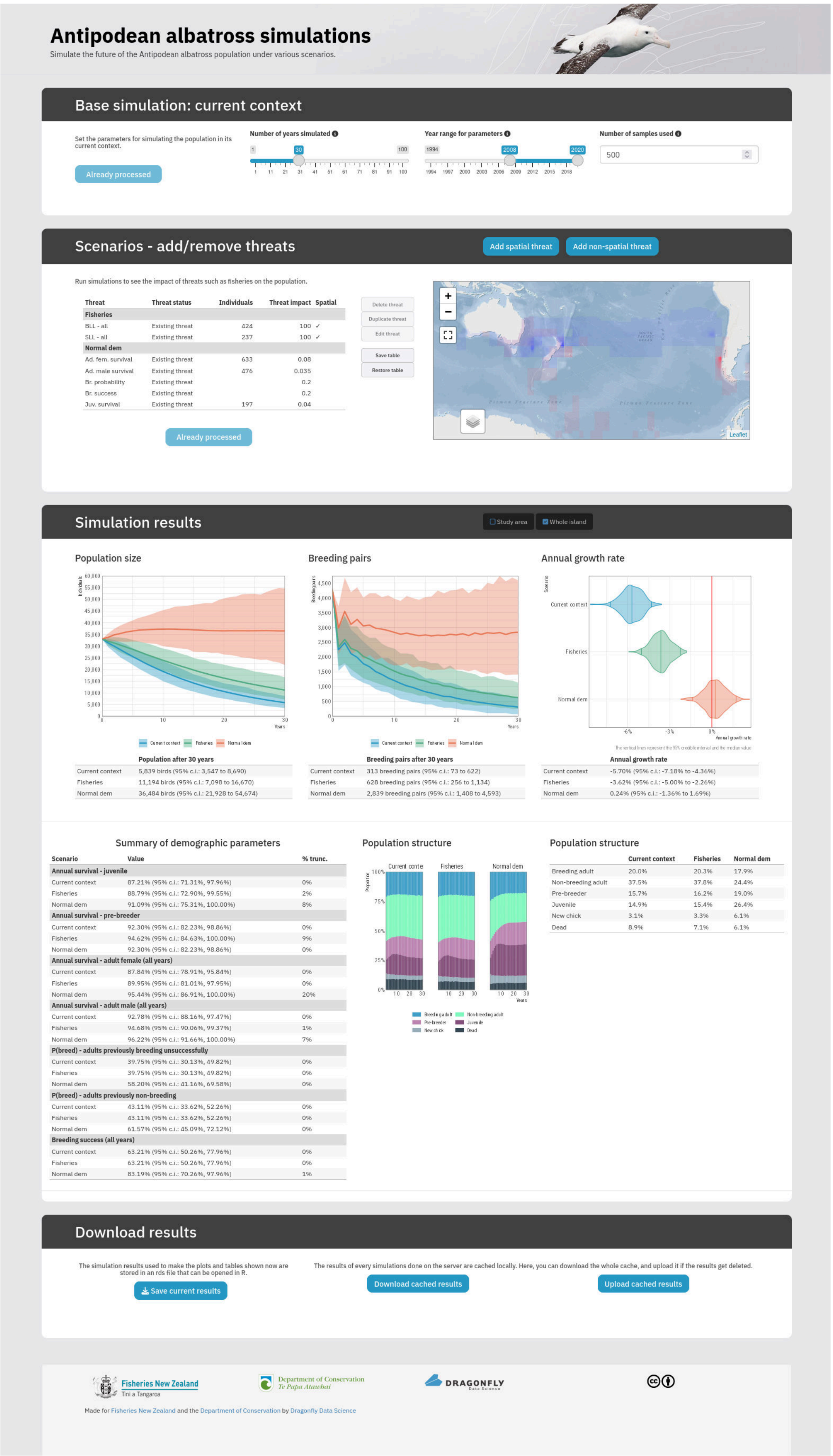
Already processed
Add spatial threat
Add non-spatial threat
Delete threat
Duplicate threat
Edit threat
Save table
Restore table
Already processed
Leaflet
☐ Study area
☑ Whole island
Individuals
Years
Breeding pairs
Scenario
Annual growth rate
Current context
Fisheries
Normal dem
Proportion
Breeding adult
Non-breeding adult
Pre-breeder
Juvenile
New chick
Dead
Save current results
Download cached results
Upload cached results
Fisheries New Zealand
Tini a Tangaroa
Department of Conservation
Te Papa Atawhai
DRAGONFLY
Data Science

Antipodean albatross simulations

Simulate the future of the Antipodean albatross population under various scenarios.

Base simulation: current context

Set the parameters for simulating the population in its current context.

Number of years simulated: 30 (range 1–100)

Year range for parameters: 2008 – 2020 (range 1994–2020)

Number of samples used: 500

Scenarios - add/remove threats

Run simulations to see the impact of threats such as fisheries on the population.

Threat	Threat status	Individuals	Threat impact	Spatial
Fisheries				
BLL - all	Existing threat	424	100	✓
SLL - all	Existing threat	237	100	✓
Normal dem				
Ad. fem. survival	Existing threat	633	0.08	
Ad. male survival	Existing threat	476	0.035	
Br. probability	Existing threat		0.2	
Br. success	Existing threat		0.2	
Juv. survival	Existing threat	197	0.04	

Simulation results

Population size

Breeding pairs

Annual growth rate

The vertical lines represent the 95% credible interval and the median value

	Population after 30 years
Current context	5,839 birds (95% c.i.: 3,547 to 8,690)
Fisheries	11,194 birds (95% c.i.: 7,098 to 16,670)
Normal dem	36,484 birds (95% c.i.: 21,928 to 54,674)

	Breeding pairs after 30 years
Current context	313 breeding pairs (95% c.i.: 73 to 622)
Fisheries	628 breeding pairs (95% c.i.: 256 to 1,134)
Normal dem	2,839 breeding pairs (95% c.i.: 1,408 to 4,593)

	Annual growth rate
Current context	-5.70% (95% c.i.: -7.18% to -4.36%)
Fisheries	-3.62% (95% c.i.: -5.00% to -2.26%)
Normal dem	0.24% (95% c.i.: -1.36% to 1.69%)

Summary of demographic parameters

Scenario	Value	% trunc.
Annual survival - juvenile		
Current context	87.21% (95% c.i.: 71.31%, 97.96%)	0%
Fisheries	88.79% (95% c.i.: 72.90%, 99.55%)	2%
Normal dem	91.09% (95% c.i.: 75.31%, 100.00%)	8%
Annual survival - pre-breeder		
Current context	92.30% (95% c.i.: 82.23%, 98.86%)	0%
Fisheries	94.62% (95% c.i.: 84.63%, 100.00%)	9%
Normal dem	92.30% (95% c.i.: 82.23%, 98.86%)	0%
Annual survival - adult female (all years)		
Current context	87.84% (95% c.i.: 78.91%, 95.84%)	0%
Fisheries	89.95% (95% c.i.: 81.01%, 97.95%)	0%
Normal dem	95.44% (95% c.i.: 86.91%, 100.00%)	20%
Annual survival - adult male (all years)		
Current context	92.78% (95% c.i.: 88.16%, 97.47%)	0%
Fisheries	94.68% (95% c.i.: 90.06%, 99.37%)	1%
Normal dem	96.22% (95% c.i.: 91.66%, 100.00%)	7%
P(breed) - adults previously breeding unsuccessfully		
Current context	39.75% (95% c.i.: 30.13%, 49.82%)	0%
Fisheries	39.75% (95% c.i.: 30.13%, 49.82%)	0%
Normal dem	58.20% (95% c.i.: 41.16%, 69.58%)	0%
P(breed) - adults previously non-breeding		
Current context	43.11% (95% c.i.: 33.62%, 52.26%)	0%
Fisheries	43.11% (95% c.i.: 33.62%, 52.26%)	0%
Normal dem	61.57% (95% c.i.: 45.09%, 72.12%)	0%
Breeding success (all years)		
Current context	63.21% (95% c.i.: 50.26%, 77.96%)	0%
Fisheries	63.21% (95% c.i.: 50.26%, 77.96%)	0%
Normal dem	83.19% (95% c.i.: 70.26%, 97.96%)	1%

Population structure

Population structure

	Current context	Fisheries	Normal dem
Breeding adult	20.0%	20.3%	17.9%
Non-breeding adult	37.5%	37.8%	24.4%
Pre-breeder	15.7%	16.2%	19.0%
Juvenile	14.9%	15.4%	26.4%
New chick	3.1%	3.3%	6.1%
Dead	8.9%	7.1%	6.1%

Download results

The simulation results used to make the plots and tables shown now are stored in an rds file that can be opened in R.

The results of every simulations done on the server are cached locally. Here, you can download the whole cache, and upload it if the results get deleted.

Made for Fisheries New Zealand and the Department of Conservation by Dragonfly Data Science

Figure 1: Screenshot of the online application to simulate scenarios of threats on the population dynamics of Antipodean albatross.

The consequence of each scenario on the population dynamics of Antipodean albatross is then simulated over 30 years (the default value).

The interactive tool provides several pre-loaded spatial datasets of:

- annual fishing effort for trawl, bottom-longline, surface-longline, and jig fisheries, for all the flag fleets that together contributed over 95% of the total overlap with Antipodean albatross, from Edwards et al. (2023b);
- spatial distribution of ocean plastics from Eriksen et al. (2014), and
- sea surface temperature anomaly for the periods 1995–2006 and 2007–2022, and for the entire period (1995–2022).

3. RESULTS

3.1 Literature review: threats to Antipodean albatross

Antipodean albatross are exposed to a range of diverse threats, including fisheries, climate change and severe weather events, plastic and other pollution (e.g., contaminants, oil spills), and diseases (Table 1). The spatial extent of these threats may be localised, e.g., affecting individual birds at nesting sites, or have an extensive spatial extent, e.g., impacting the foraging distribution of different life stages.

Some of the threats may have similar repercussions; for example, nutritional stress may be caused by the ingestion of plastic debris (preventing the uptake of food; e.g., Roman et al. 2021), prey depletion from fishing (e.g., Grémillet et al. 2018), or by climate change (through changes in the distribution of prey or in foraging efficiency; e.g., Carpenter-Kling et al. 2020). In addition, combined effects from different threats may be sequential or additive, exacerbating their overall impact on albatross populations (Pardo et al. 2017).

3.1.1 Fisheries

Threats posed by fisheries include population impacts from bycatch mortality, resource competition, and intentional take or killing at sea (Alfaro-Shigueto et al. 2016).

Records of Antipodean albatross bycatch in New Zealand waters are provided by fisheries observers on-board commercial fishing vessels. For example, recent observer data documented the incidental capture of five Antipodean albatross (four mortalities) in surface-longline fisheries in the 2019–20 fishing year, and the same number of captures (five mortalities) in 2018–19 (see https://protectedspeciescaptures.nz/). Observed captures in trawl fisheries appear to be rare, with one record in the period between 2002–03 and 2019–20.

Analyses of tracking data and spatial fishing information (from Global Fishing Watch) highlighted the bycatch threat posed by pelagic longline fisheries in the Pacific Ocean, including in New Zealand waters (Bose & Debski 2020, 2021). Impacts from other fisheries were considered to be minor, owing to the lack of overlap (bottom longlining, jigging), or few observed incidental captures (trawl fisheries in New Zealand waters).

Recent modelling of Antipodean albatross distributions highlighted the overlap between this subspecies and surface-longline fleets, particularly in the Tasman Sea, in waters north and east of New Zealand, and off the Chilean coast (Richard et al. 2024).

Table 1: Overview of key risks and associated threats to Antipodean albatross considered in the present risk assessment, including the availability of spatial information.

Risk	Threat	Quantitative, spatial data	Reference
Fisheries	Bycatch mortality.	Vessel locations, observed captures; tracking data, distribution modelling.	Bose & Debski (2021) and Richard et al. (2024)
	Intentional take, killing at-sea.	Data for other Procellariiformes species.	Alfaro-Shigueto et al. (2016), Gianuca et al. (2020)
	Resource competition, nutritional stress	Data for other species.	Bertrand et al. (2012)
Climate change	Availability & distribution of prey, foraging behaviour, body condition and reproduction.	Some data for other species.	Queirós et al. (2021), Weimerskirch et al. (2012), Pinaud & Weimerskirch (2002)
	Severe weather events: foraging, habitat impacts, nesting success.	Data for other species.	Wolfaardt et al. (2012), Ventura et al. (2023)
Pollution	Plastic debris: mortality, feeding & condition, breeding success.	Data for other species, some data for Antipodean albatross.	Xavier et al. (2014), Roman et al. (2016), Cherel et al. (2017)
	Oil spills: mortality, impacts on feeding & condition, foraging.	Data for other species, including in NZ waters.	Leighton (1993), King et al. (2021), Hunter et al. (2019)
	Contaminants (e.g., mercury).	Data for other species; ongoing research Department of Conservation.	Goutte et al. (2014), Cherel et al. (2018)
Disease	Avian influenza, avian cholera: mortality, reduced condition.	Data for other species.	Leotta et al. (2006), Jaeger et al. (2018)

Other fishery impacts may arise from the intentional take or killing of birds and through resource competition affecting the availability of prey. Mortality through the deliberate killing and intentional take of albatrosses has been reported for other species, such as waved albatross (*Phoebastria irrorata*) off the coast of Peru (Alfaro-Shigueto et al. 2016). Similarly, the intentional killing (and infliction of severe injuries) has also been reported for eight species of Procellariiformes in the southwestern Atlantic Ocean (Gianuca et al. 2020). Because these mortalities are rarely documented, data are generally lacking, including for Antipodean albatross.

Resource competition with fisheries has been documented to affect seabird populations worldwide through the reduction or local depletion of prey (Grémillet et al. 2018). Antipodean albatross feed on a variety of oceanic squid and octopod species, in addition to fish, as they forage across an extensive area throughout the Pacific Ocean (Cherel & Klages 1997, Nicholls et al. 2002, Xavier et al. 2014). Potential repercussions from reduced prey availability and lowered foraging success include lower body condition and nutritional stress, which in turn may lead to reduced breeding success (Fayet et al. 2021).

There is limited information available on the competition between fisheries and seabirds (e.g., see Bertrand et al. 2012), and there are no data for this type of fishery interaction with Antipodean albatross. Nevertheless, previous modelling of Antipodean albatross population dynamics suggested that nutritional stress impacted on breeding rates and success, explaining some of the population decline (Edwards et al. 2017).

3.1.2 Climate change

Climate change impacts arise from warming air and sea temperatures, including sea surface temperature anomalies (e.g., “marine heat waves”), changes in ocean circulation patterns and marine biogeochemistry, and severe weather events. These changes impact on the structure, functioning, and productivity of ecosystems, with repercussion for resident species and populations. For example, changes in climate and weather conditions may impact a population by affecting the distribution or abundance of prey species, which in turn can lead to food deprivation affecting an animal’s condition and its survival and reproduction.

For Antipodean albatross, one of the foraging areas (particularly for juveniles), the Tasman Sea, has undergone one of the highest rates of warming globally (outside the polar regions), including unprecedented marine heat waves (Oliver et al. 2017). Similarly, Antarctica and the Southern Ocean are among the world’s regions most impacted by climate change, which is predicted to affect (in combination with fisheries and other factors) the ecology and productivity of fish and squid species in the region (Caccavo et al. 2021).

Although there has been no formal assessment of the effect of climate change on Antipodean albatross, studies of other albatross species in the Southern Ocean reported impacts from changing environmental variables on demographic rates, with predicted shifts in future distributions (e.g., Rolland et al. 2010, Thomson et al. 2015, Krüger et al. 2018). For Southern Ocean squid species that form a significant part of the diet of Antipodean and Gibson’s albatrosses, climate change may lead to southward movement of adult squid, caused by changes in habitat (i.e., oceanic fronts), potentially affecting Antipodean albatross foraging (Queirós et al. 2021). Foraging may also be affected by changing wind patterns, with adverse conditions requiring more energy expenditure or different habits (Weimerskirch et al. 2012).

Changes in foraging efficiency can lead to adverse effects on body condition and reproduction, as documented in a a study of black-browed albatrosses (*Thalassarche melanophris*), which highlighted the influence of oceanographic conditions on breeding performance: during years of low resource availability, birds returned to their nest with lower body condition, and adults in low body condition were more likely to cease breeding (Pinaud & Weimerskirch 2002).

In addition to changes in oceanographic conditions and wind patterns, the increased frequency and severity of weather events caused by climate change have the potential to significantly impact albatross colonies (Wolfaardt et al. 2012, Ventura et al. 2023). Effects from severe weather events include damage to seabird nesting sites, the loss of eggs and chicks, increased adult mortality, and preventing adults from foraging and feeding their offspring. Examples include storm damage to a breeding colony of *Thalassarche melanophris* that included high mortality rates, leading to a predicted population decline of 2% per year (Ventura et al. 2023).

At Antipodes Island, an extreme weather event in January 2014 caused severe landslips that affected several erect-crested penguin (*Eudyptes sclateri*) colonies on the island (Chilvers & Hiscock 2019). Although landslips at Antipodean albatross nesting sites are unlikely owing to their location, it is possible that other impacts from severe weather events may affect their breeding sites in the future.

3.1.3 Plastic pollution

Plastic pollution has become a significant conservation challenge in marine ecosystems, where the accumulation of increasing amounts of plastic debris poses a considerable threat to marine life (Cózar et al. 2014, Gall & Thompson 2015). For seabirds, risks associated with plastic pollution include entanglement and ingestion of particles leading to direct mortality, and also internal injuries and the filling or blockage of digestive organs, reducing the ability to feed sufficiently and to build fat deposits.

The latter is also relevant for breeding birds that regurgitate plastic particles to feed their young, leading to an “inter-generational transfer” of plastic particles (Ryan 2015).

Other adverse effects are caused by leaching of organic contaminants (e.g., persistent organic pollutants) that are part of the production of plastic (i.e., additives) or absorbed by plastic particles while floating in marine waters (Arthur et al. 2008, Yamashita et al. 2021).

Plastic pollution has not been formally recognised as a threat to Antipodean albatross by the Agreement on the Conservation of Albatrosses and Petrels (Agreement on the Conservation of Albatrosses and Petrels 2009), and *Diomedea* species are considered to rarely ingest plastic particles. Nevertheless, fragments and pieces of plastic were found during dietary studies that examined stomach contents of wandering albatross *Diomedea exulans* (Cherel et al. 2017), and boluses from Antipodean and Gibson’s albatrosses (Xavier et al. 2014).

Records of plastic ingested by Antipodean albatross are also documented in autopsy reports of seabirds killed in New Zealand fisheries (Robertson et al. 2001).

Although these records are relatively rare, mortality following plastic ingestion is likely to be under-reported, given few stranded albatrosses are encountered each year (and are unlikely to undergo a post-mortem examination). As Antipodean albatross feed by surface seizing and shallow diving, their foraging behaviour puts them at relatively high risk of ingesting marine plastics (Roman et al. 2016).

At the same time, the Southern Ocean boundary with the Tasman Sea between New Zealand and Australia has been identified as a “hotspot” for increased risk of plastic ingestion due to the high plastic concentration and high seabird diversity (Wilcox et al. 2015). In addition, the foraging distribution of Antipodean albatross overlaps with the spatial extent of one of the five great “garbage patches” in the world’s oceans, associated with the South Pacific subtropical gyre (Eriksen et al. 2013). With increasing concentrations of plastic in the marine environment (Ostle et al. 2019), it is likely that encounter rates with seabirds will also increase, including for Antipodean albatross.

3.1.4 Contaminants

Contamination from acute and chronic oil spills arises from internal and external exposure to oil at sea (Leighton 1993, King et al. 2021). In addition to direct mortality, documented repercussions include vulnerability to hypothermia through the loss of waterproofing in feathers, the loss of body condition, and starvation. For albatrosses and petrels, their large body size means that they may initially survive light exposure to oil, but they may be unable to fly or feed, leading to subsequent mortality (Chilvers & Ruoppolo 2019).

Potential impacts of oil spills are dependent on the location, duration, and spatial overlap with seabird distributions (Rodríguez et al. 2019), and may include spills from exploratory drilling such as in the Southern Basin off south-eastern New Zealand (Chilvers & Ruoppolo 2019). Recorded seabird mortalities from a significant oil spill in New Zealand waters following the grounding of the container ship MV Rena near Tauranga in October 2011 affected 49 species, including *Diomedea exulans*, *Thalassarche eremita*, and *Thalassarche cauta steadi* (Hunter et al. 2019).

Other contamination risks for Antipodean albatross arise from exposure to toxins, such as heavy metals (e.g., mercury, cadmium, lead) persistent organic pollutants, and organochlorines (e.g., Thompson & Hamer 2000, Blévin et al. 2013). Similar to other long-lived apex predators, albatrosses are susceptible to bioaccumulation of toxins through the consumption of prey (Tavares et al. 2013). Potential impacts from chronic exposure to pollutants include reduced survival rates and lower reproductive outputs, leading to population declines (e.g., Goutte et al. 2014).

Mercury occurs naturally in the environment, and human activities have increased mercury cycling three- to five-fold on a global scale, including in the ocean (Selin 2009). In addition, climate change warming Southern Ocean waters may increase the bioavailability of mercury to the Antarctic marine food web by releasing ice-stored mercury and increasing methylation rates by microorganisms, thereby increasing its toxicity (Matias et al. 2022).

Diomedeidae have been recognised as the most mercury-contaminated bird family, with the wandering albatross complex representing the most mercury-contaminated taxa within the family (Cherel et al. 2018). Examples of adverse effects from mercury exposure include decreased egg mass, embryo malformations, and decreased chick growth and survival.

In wandering albatross *Diomedea exulans*, high blood mercury concentrations (and of persistent organic pollutants) had negative effects on long-term breeding, hatching, and fledging probabilities (Goutte et al. 2014). In male grey-headed albatrosses (*Thalassarche chrysostoma*), mercury exposure appeared to negatively influence breeding success (Mills et al. 2020).

For Antipodean albatross, an analysis of mercury, cadmium, zinc, and copper concentrations in organ tissue documented high concentrations of cadmium and mercury in liver and kidney tissue of bycaught individuals (Stewart et al. 1999). Ongoing research by the Department of Conservation is further investigating mercury contamination of Antipodean albatross (J. Fischer, pers. comm.).

Other studies have documented the presence and increases in pollutants such as persistent organic pollutants and organochlorines in different species of albatross (e.g., Yamashita et al. 2021, and see for example reviews by Thompson & Hamer 2000, Phillips et al. 2016). In addition to the level of contamination in foraging areas, the risks posed by contaminants is also dependent on the dietary preference of albatross species.

3.1.5 Diseases

Another potential risk to Antipodean albatross are diseases, most prominently avian cholera and avian influenza (Phillips et al. 2016). A recent review of disease information for 31 species of albatrosses and large petrels listed under ACAP focused on viral pathogens, bacterial and fungal pathogens, protozoa, helminths, and ectoparasites (Uhart et al. 2018). Across these diseases and pathogens, avian cholera, caused by the bacterium *Pasteurella multocida*, was considered the most serious threat. Avian cholera can lead to large-scale outbreaks, some recurrent, with significant mortality events reported, particularly in the Northern Hemisphere (e.g., Wille et al. 2016).

For endangered yellow-nosed albatross (*Thalassarche carteri*) on Amsterdam Island (southern Indian Ocean), low breeding success and a decreasing population trend since the 1980s were attributed to high chick mortality induced by the bacterial agent of avian cholera *Pasteurella multocida* (Weimerskirch 2004, Jaeger et al. 2018). Reported cases of avian cholera also include mortalities of different species of seabird in Antarctica, including giant petrel (*Macronectes giganteus*), with the infections across species tentatively linked to transmission through water (Leotta et al. 2006).

Avian influenza has been linked to high bird mortalities, caused by strains of the highly pathogenic avian influenza (HPAI), whereas its counterpart (low pathogenicity avian influenza , LPAI) causes a milder disease (Alexander 2003). There are currently no documented Procellariiformes mortalities linked to HPAI; however, one of the HPAI strains (subtype H5N1) has spread rapidly across Northern Hemisphere seabirds, with over 1000 reported outbreaks (Uhart et al. 2022). Its unprecedented impact over a short period of time (in 2021 and 2022) included high-mortality events of cormorants, cranes, geese, shorebirds, terns, gannets, and skua across a wide geographical spread of countries. The rapid spread and unprecedented impact of this strain on seabird populations prompted the study authors to highlight its potential risk to ACAP-listed species, including their exposure via migratory birds or accidental introduction via humans (Uhart et al. 2022). In February 2024, the virus was found in dead skua on the Antarctic Peninsula (Wong 2024).

3.2 Population model of Antipodean albatross

The dataset used to fit the population model consisted of 13 908 sighting events of 3176 Antipodean albatross between 1994 and 2020, including 5294 sightings of 1073 females, 7500 sightings of 1037 males, and 1114 sightings of 1066 birds of unknown sex, predominantly of birds seen only once (Figure 2). The number of sightings by individual varied between one and 23 (Figure 2).

The sightings were classified into eight observed states, as well as a state of birds not being seen. Adults breeding within the study area represented almost half of all sightings, followed by non-breeding adults within the study area representing a quarter of all sightings. The remaining sightings were mostly of pre-breeders and juveniles within the study area, in similar numbers (juvenile sightings were in their first year before fledging) (Table 2).

The convergence of the fitted model was satisfactory, as evident in the MCMC traces of the model chains for all parameters showing a lack of trend and considerable mixing of the chains (see Appendix B).

When the model was used to simulate the trajectory of all birds between 1994 and 2020, only considering their initial state, the number of breeding birds within the study area corresponded closely to the number of nests recorded within the study area (Figure 3). Both the simulated numbers of males and females followed a similar trend over time. The number of breeding females was slightly lower than the number of nests, but consistent across years.

According to the model, half of the juveniles returned to the colony by the age of 6, and 90% of juveniles returned by the age of 11 (Figure 4). Half of the individuals had bred at least once by the age of 14, and 90% of birds by the age of 21 (Figure 5).

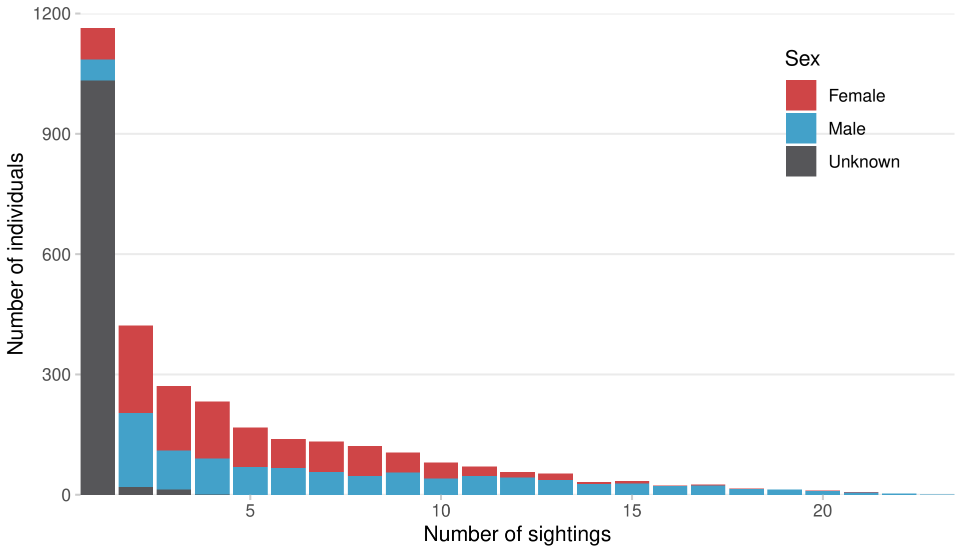

Figure 2: Distribution of the number of sightings across individual histories recorded between 1994 and 2020, used to fit the population model of Antipodean albatross.

Table 2: Number of sightings of each observed state considered in the population model of Antipodean albatross (the state of unseen birds was also considered, but is not shown here). SA: study area.

Observed state	Females	Males	Unknown	Total
Adult breeding in SA	3 197	3 232	38	6 467
Adult non-breeding in SA	850	2 405	4	3 259
Adult outside SA	176	147	3	326
Pre-breeder inside SA	529	1 259	11	1 799
Pre-breeder outside SA	214	78	11	303
Juvenile inside SA	323	367	1 040	1 730
Juvenile outside SA	0	0	0	0
Dead	5	12	7	24
All	5 294	7 500	1 114	13 908

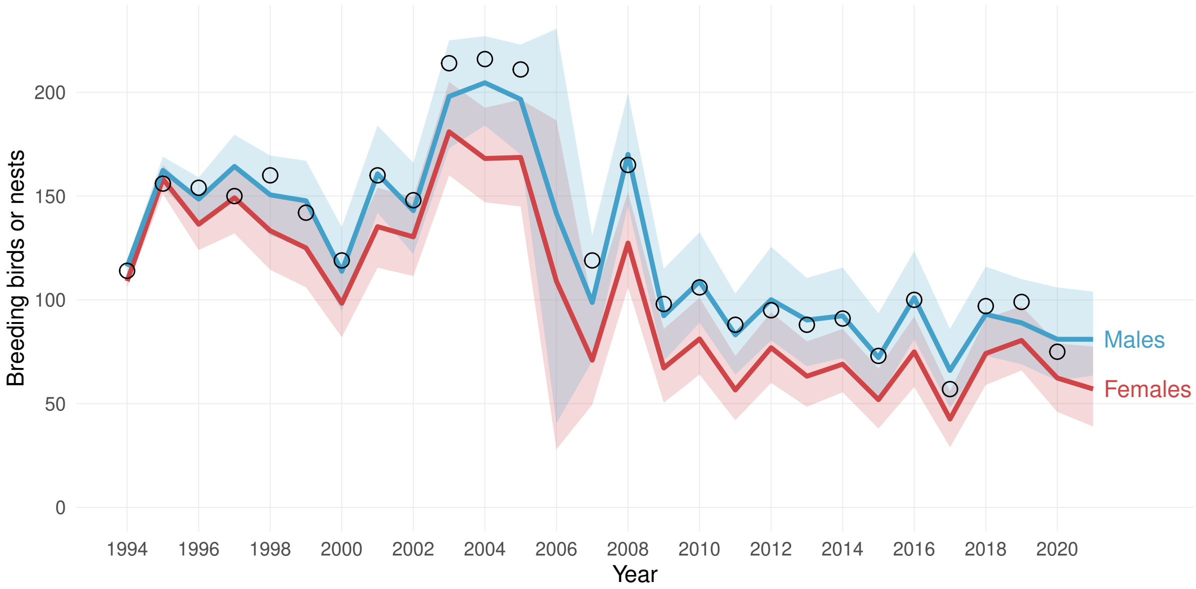

Figure 3: Simulation of the number of breeding male and female Antipodean albatross within the study area between 1994 and 2021, represented by their mean (line) and 95% credible interval (shading). Black circles show the counts of active nests within the same study area.

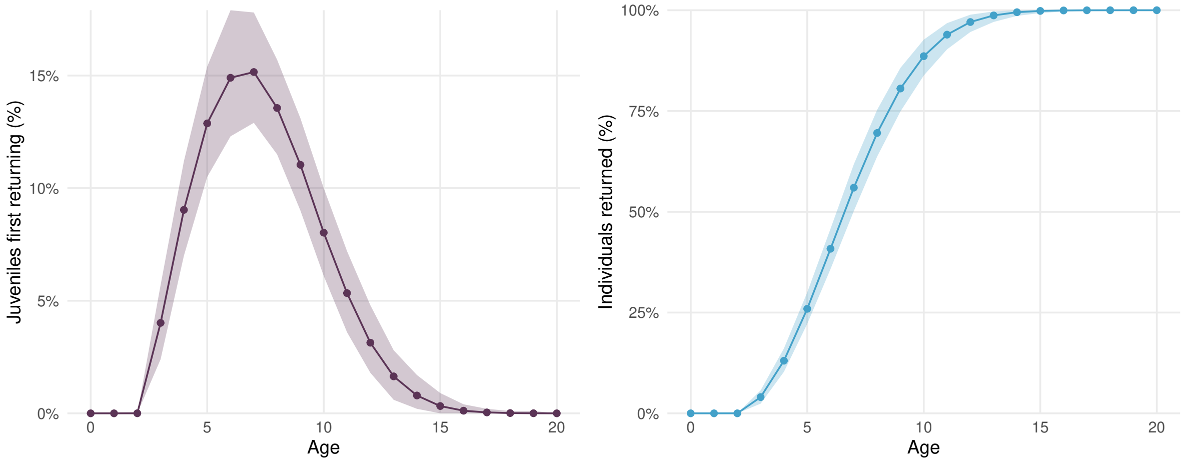

Figure 4: Age at first return to the colony, estimated by the population model. Annual probability that a juvenile returns to the colony for the first time (left), and cumulative proportion of juveniles that returned to the colony (right).

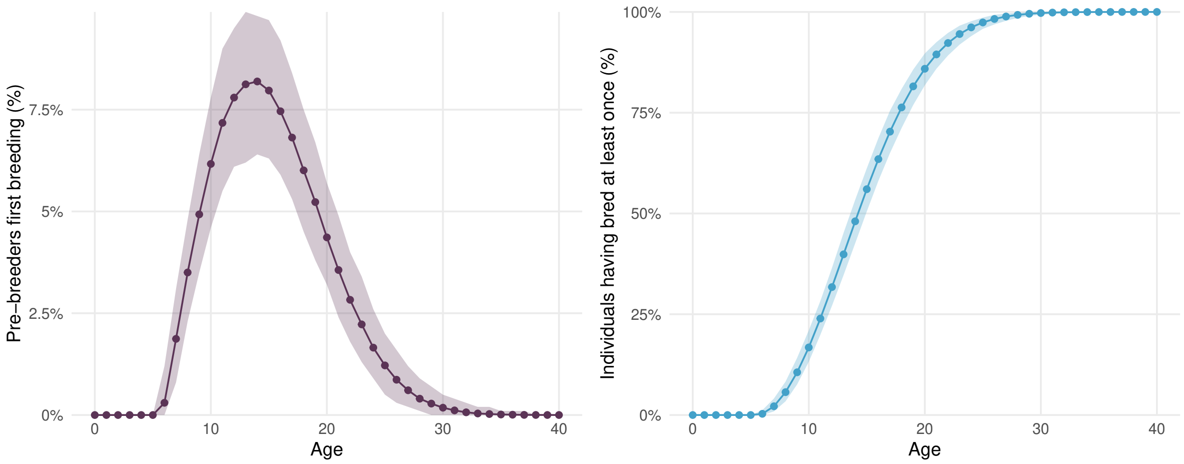

Figure 5: Age at first breeding, estimated by the population model. The annual probability that an individual breeds for the first time is shown on the left, and the cumulative proportion of individuals that have bred at least once is shown on the right.

The annual breeding probability of adults varied across years, but was similar for adults that were previously unsuccessful breeders and other adults (Figure 6). For the former grouping, annual breeding probability declined from a mean of 0.77 before 2005 to a mean of 0.42 after 2006. For other breeders, it declined from a mean of 0.79 before 2005 to a mean 0.45 after 2006. Although annual breeding probability showed a slight increase from 2009 onwards, but it remained low overall.

Breeding success, as defined as the probability that a nest produces a fledgling, followed a similar decline as breeding probability, followed by a potential increase (Figure 7). It declined from a mean of 0.72 before 2006, to a mean of 0.63 after 2006. Nevertheless, there was considerable variation around mean breeding success over time.

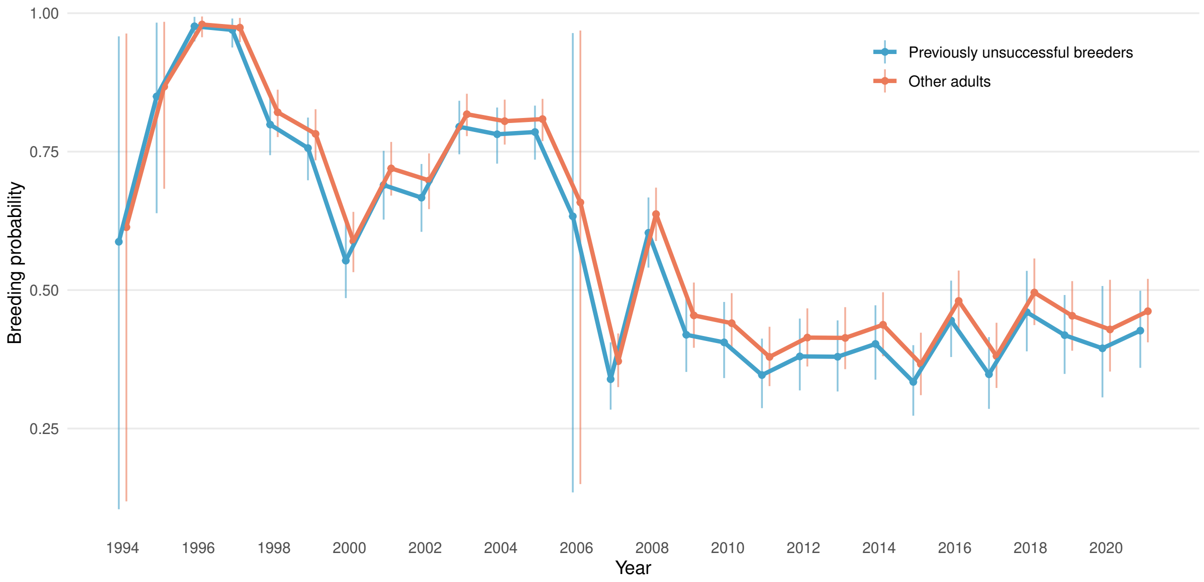

Figure 6: Annual breeding probability for adults that were previously unsuccessful breeders and for other breeders (successful breeders do not breed the following year). The points and lines indicate the mean values, and the vertical bars show the 95% credible interval.

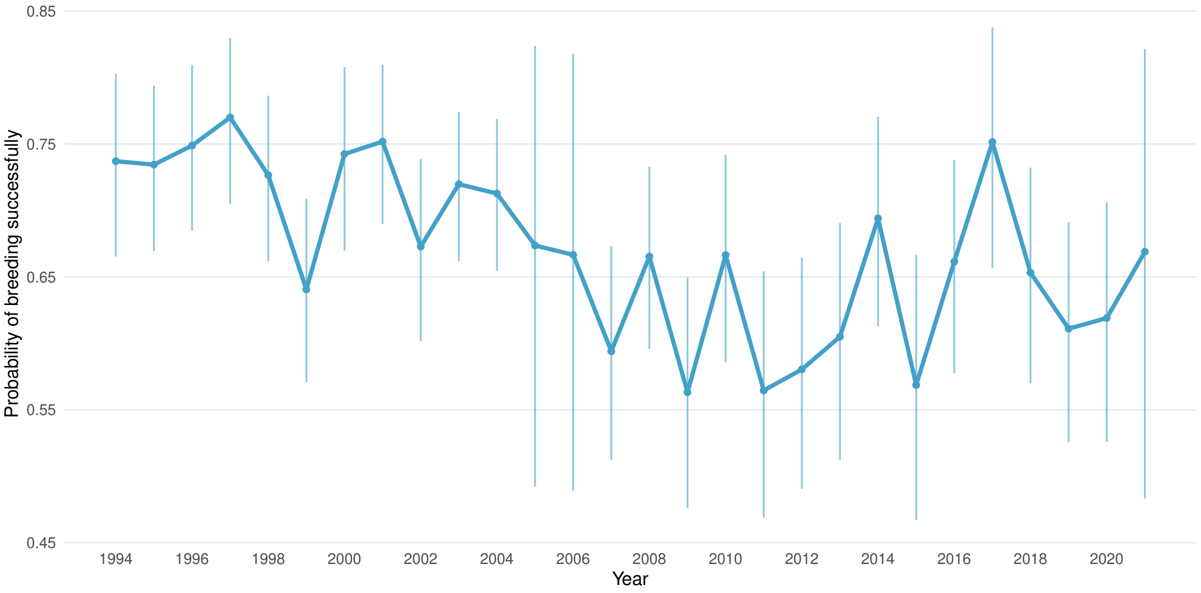

Figure 7: Annual breeding success of Antipodean albatross, the probability that a breeding attempt leads to a surviving fledgling, as estimated by the population model. The points and lines indicate the mean values, and the vertical bars show the 95% credible interval.

Annual survival (φ) also declined for the four classes considered in the model—adult females, adult males, pre-breeders, and juveniles (Figure 8). The decline was most apparent for adult females, from a mean survival rate pre-2006 of 0.95 (95% c.i.: 0.9– 0.98) to a mean survival rate of 0.88 (95% c.i.: 0.79–0.96) after 2006. The finding documented that the adult female life expectancy, $(1-\varphi_a)^{-1}$, declined from a mean of 19.1 years to a mean of 8.3 years. In contrast, the smallest decline in survival rate was for adult males, from a mean of 0.95 (95% c.i.: 0.9– 0.98) to a mean of 0.93 (95% c.i.: 0.88– 0.97) after 2006. This decrease corresponded to a change in adult male life expectancy from a mean of 18.4 years to a mean of 13.6 years.

The annual detection probability for all five classes considered in the model did not show a trend over time, but it did reflect variations in the timing and length of field surveys (Figure 9). In the model, the same annual variability in detection probability was applied to all classes, except for pre-breeders inside the study area. Pre-breeders generally arrive at the colony later than adults and are, therefore, more likely to be recorded at the colony when surveys are delayed. This factor was included in the model by allowing the detectability of pre-breeders to vary for years when the surveys started later than in previous years. The model estimates confirmed the hypothesis, as their estimated detectability increased to above 0.75 in years of late surveys, whereas it remained just above 0.5 in standard years. (Figure 9). The detection probability of juveniles and of dead individuals was constant among years in the model due to the lack of data, and was estimated to be between 0.018% (95% c.i.: 0.001– 0.067%) and 0.084% (95% c.i.: 0.054–0.12%), respectively.

In the population model, individuals were allowed to move outside the study area between years, and to return to it, to account for potential biases in survival rates. Females had a mean annual probability of leaving the study area of 0.095 (95% c.i.: 0.084– 0.106) (Figure 10). Their probability was significantly higher than it was for males (mean of 0.041 (95% c.i.: 0.035– 0.046). Conversely, females had a mean probability of returning to the study area of 0.196 (95% c.i.: 0.169– 0.225), which was significantly lower than for males (mean of 0.274 (95% c.i.: 0.237– 0.313)). This difference indicated that females tended to be found more frequently outside the study area than males. This sex bias in movements would lead to an average proportion of females inside the study area of 43.6%, from an initial population with equal number of males and females, and equal survival rates.

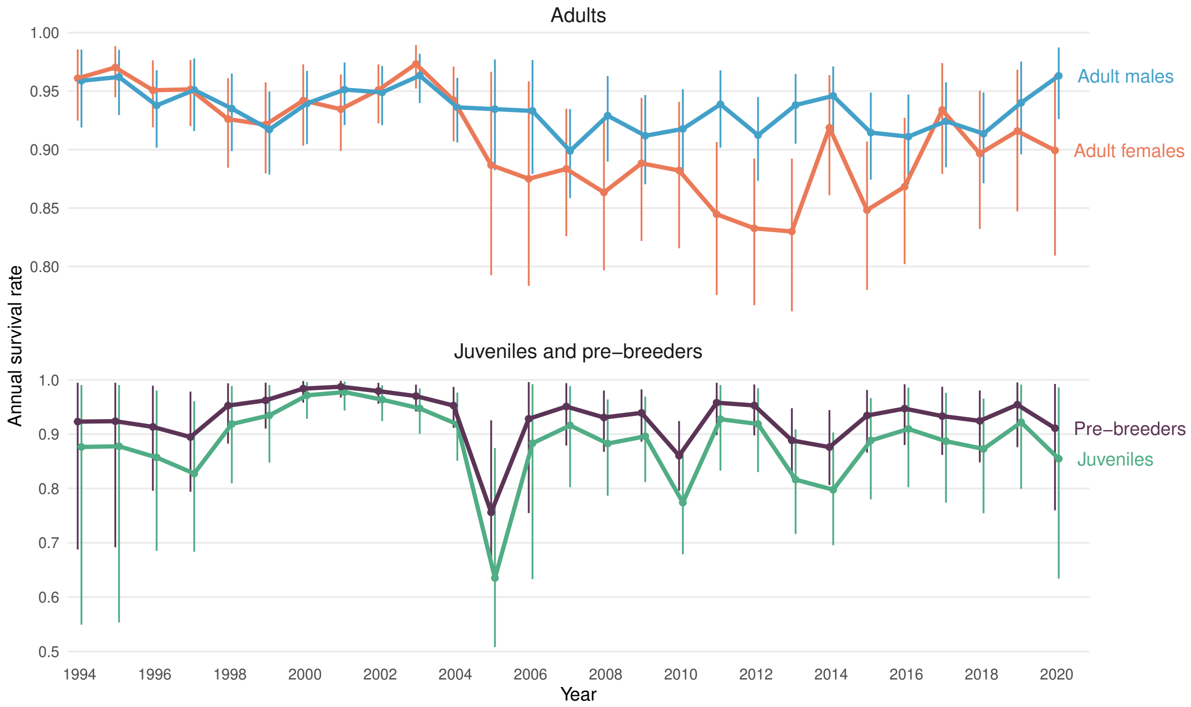

Figure 8: Annual survival rate of Antipodean albatross estimated by the population model, by population class and year. The points and lines indicate mean values, and vertical bars the 95% credible interval.

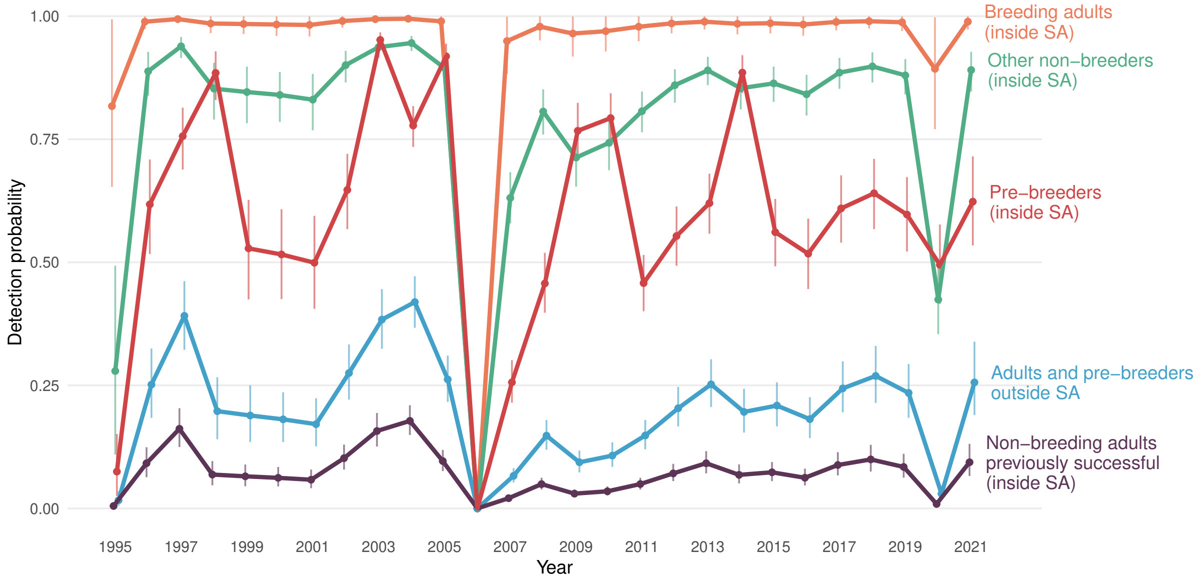

Figure 9: Detection probability of Antipodean albatross by category and by year as estimated by the population model. The points and lines indicate the mean values, and the vertical bars show the 95% credible interval. SA: study area. The detection probabilities were set to zero in 2006 as there was no survey that year. A small offset along the x-axis was added to prevent overlapping data.

The population structure of Antipodean albatross for the whole of Antipodes Island was simulated from the population model (Table 3). This modelling simulated the state of each individual in the population from their first capture, and then fixed their state in 2021 as known from field surveys.

Based on these simulations, it was estimated that the mean total population size was 895 (95% c.i.: 821–961) individuals, including 363 (95% c.i.: 290– 440) females, and 532 (95% c.i.: 459– 612) males. Males were predominant in all classes, except among juveniles.

When simulating the population size for the next 50 years, based on the demographic parameters estimated for the period 2008 to 2020, the trajectory showed a considerable decrease (Figure 11); the mean annual population growth rate was -5.8% (95% c.i.: -7.3% to -4.4%). In comparison, when using

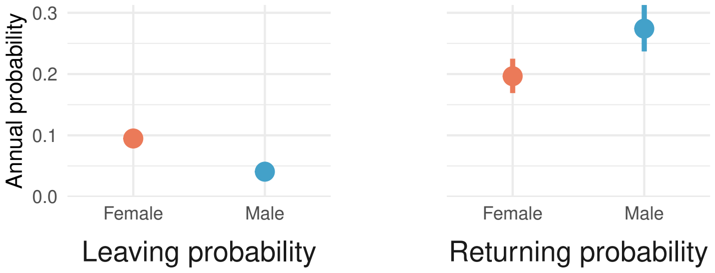

Figure 10: Annual probability that an individual leaves the study area within the colony, and returns to the study area, for both males and females, as estimated by the population model. The points and lines indicate the mean values, and the vertical bars the 95% credible interval.

Table 3: Structure of the Antipodean albatross population on Antipodes Island in 2021 as simulated from the population model.

Class	Sex	Mean	95% c.i.	
Successful breeders	Female	78	52	102
	Male	90	60	116
	Both	167	116	212
Unsuccessful breeders	Female	38	18	64
	Male	44	21	72
	Both	83	42	134
Non-breeding adults	Female	110	90	132
	Male	236	213	261
	Both	346	315	379
Pre-breeders	Female	66	41	94
	Male	94	70	122
	Both	159	135	185
Juveniles	Female	71	12	136
	Male	68	11	133
	Both	139	100	173
All	Female	363	290	440
	Male	532	459	612
	Both	895	821	961

parameters from the period 1994 to 2005, the decline was smaller, with a mean of -0.9% (95% c.i.: -3.2% to 1%), and a 19% probability of a population increase (Figure 12).

3.3 Interactions with New Zealand fisheries

The model to estimate the number of annual captures in New Zealand fisheries was fitted using data of the spatial distribution of total observed fishing effort within New Zealand's Exclusive Economic Zone (see Appendix D). The model fitted the data well, evident by the lack of a trend and considerable mixing of the MCMC chains (Appendix E, Figure E-1). There was also a clear 1:1 correlation between observed and estimated captures (Figure 13).

Comparing the vulnerabilities of Antipodean, Gibson's, and wandering albatrosses to captures in fisheries suggested that Antipodean albatross was the most vulnerable taxon in bottom-longline and trawl fisheries (Table 4). In surface longline, wandering albatross had the highest vulnerability.

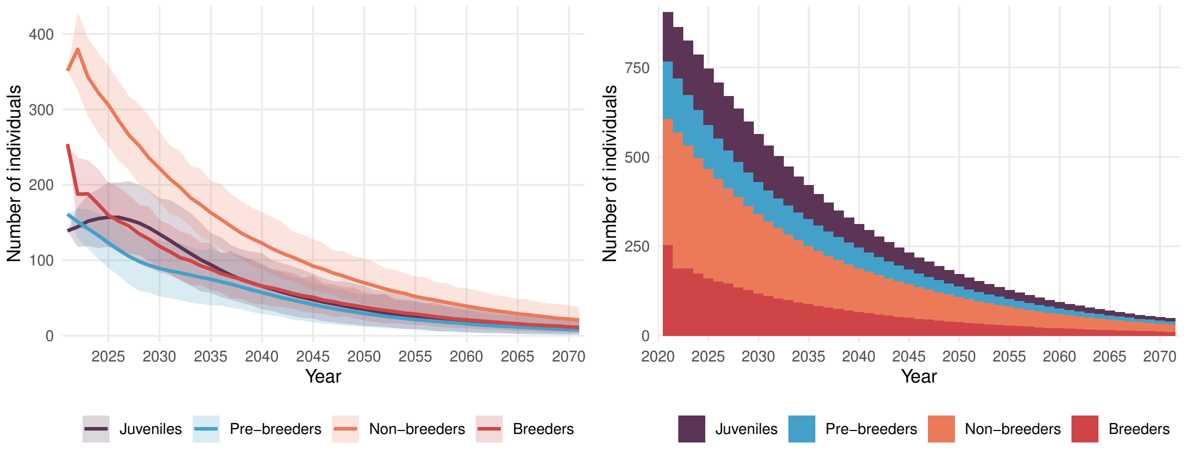

Figure 11: Simulation of the Antipodean albatross population within the study area between 2021 and 2071, based on parameters from the population model between 2008 and 2020. Left: mean (line) and 95% credible interval (shading) of each class size. Right: cumulative mean of each class.

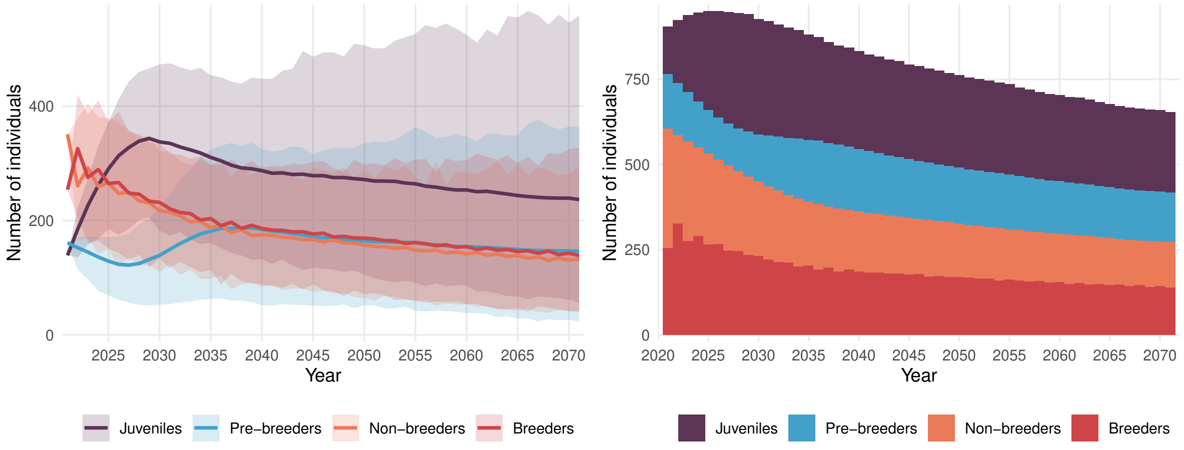

Figure 12: Simulation of the Antipodean albatross population within the study area between 2021 and 2071, based on the parameters from the population model between 1994 and 2005. Left: mean (line) and 95% credible interval (shading) of each class size. Right: cummulative mean of each class.

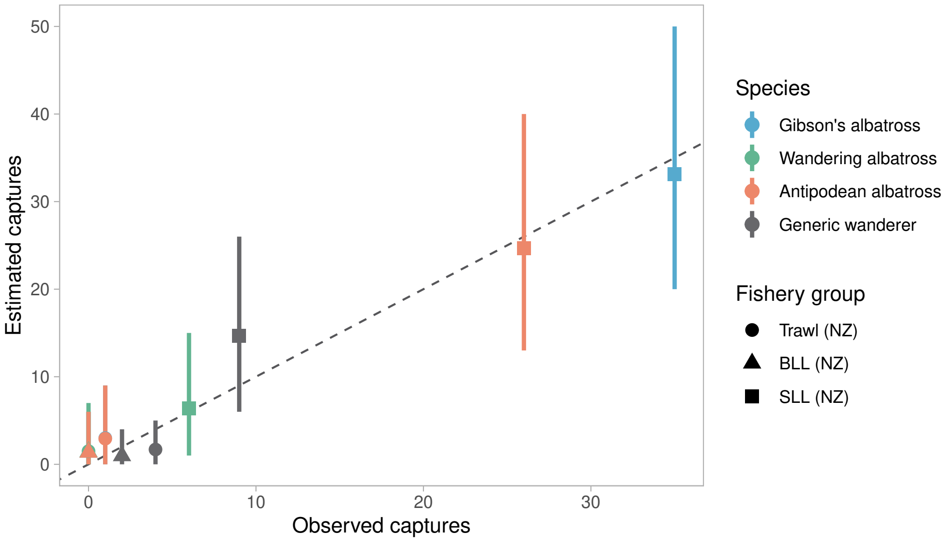

Figure 13: Comparison of the number of observed captures of wandering albatross species in New Zealand surface-longline (SLL), bottom-longline (BLL), and trawl fisheries with the associated mean number of captures predicted by the fitted model, for each 1-degree cell. The vertical lines represent the 95% credible interval of the estimate. The diagonal dashed line represents the 1:1 relationship.

Estimating captures across all fishing effort over time showed that there was a peak in for all taxa between 1999 and 2004 (Figure 14). This peak reflected a peak in fishing effort because the model did not include any variability over time in bird densities or vulnerabilities; for this reason, any temporal change in estimated captures was directly determined by changes in fishing effort.

The high vulnerability of Antipodean albatross was reflected in the relatively high number of estimated captures compared with Gibson's and wandering albatrosses (Figure 14). For the former taxon, there was a maximum mean estimate of 81 (95% c.i.: 50–116) captures in 2003. The number of estimated captures decreased after 2003, and stabilised after 2008 at around 22 captures annually.

Comparing fisheries, the majority of captures was in surface-longline fisheries (Figure 15). In these fisheries, effort peaked in 2003. The decrease in fishing effort in bottom-longline and trawl fisheries since 1993 led to a decrease in estimated captures for all taxa.

The model was also used to determine the spatial distribution of estimated captures of Antipodean albatross, based on fishing effort between 1993 and 2020 (Appendix Appendix D). This analysis showed that estimated captures were concentrated along the north-eastern coast of New Zealand's North Island, and the highest estimate was off the coast of Gisborne (Figure 16). This spatial pattern corresponded to the distribution of fishing effort (see Figures D-1 and D-2). Captures of Gibson's albatross were spread between the north-eastern coast of New Zealand's North Island and the South Island west coast, with the highest estimate off Hokitika. For wandering albatross, the captures were estimated to occur predominantly off the north-eastern coast of North Island, and also off the North Island west coast and around Chatham Islands.

Table 4: Vulnerability (mean and 95% credible interval, c.i.) of wandering albatross species to New Zealand surface-longline (SLL), bottom-longline (BLL), and trawl fisheries, as estimated by the current model. (Note that vulnerabilities cannot be compared between fishing methods, because of different units of fishing effort (hook sets for longline fisheries, trawl sets for trawl fisheries).)

Fishery	Species	Mean	95% c.i.	
BLL	Antipodean albatross	0.0148	0.0020	0.0386
	Gibson's albatross	0.0042	0.0005	0.0104
	Wandering albatross	0.0169	0.0005	0.0575
SLL	Antipodean albatross	0.0731	0.0018	0.2490
	Gibson's albatross	0.0450	0.0012	0.1495
	Wandering albatross	0.1889	0.0058	0.6533
Trawl	Antipodean albatross	3.5384	2.3673	4.9190
	Gibson's albatross	1.0603	0.7615	1.4213
	Wandering albatross	1.7760	0.6849	3.3305

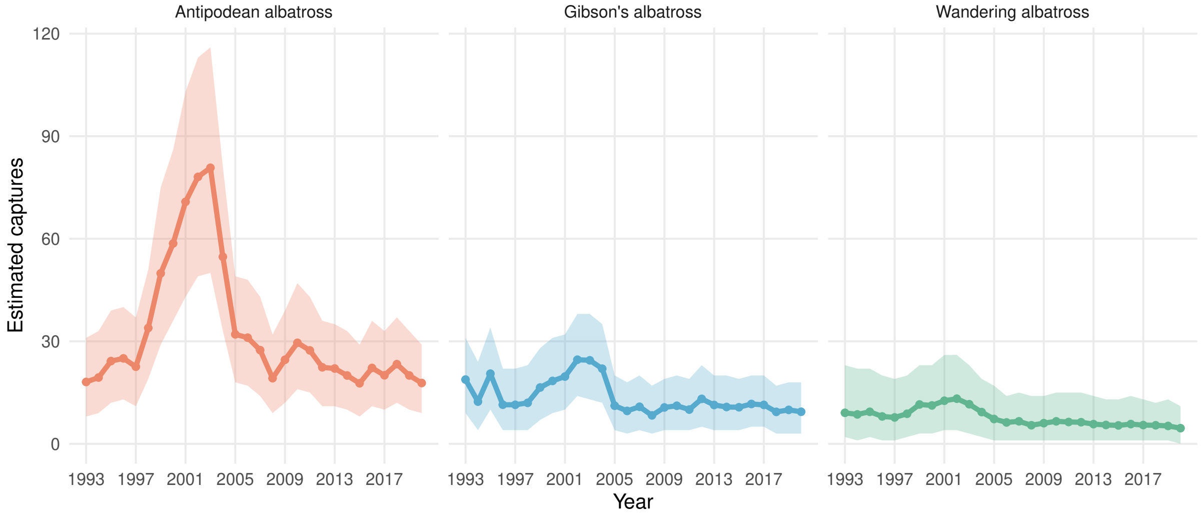

Figure 14: Total estimated captures of wandering albatross taxa in New Zealand commercial surface-longline, bottom-longline, and trawl fisheries by year. The line shows the mean, shading the 95% credible interval.

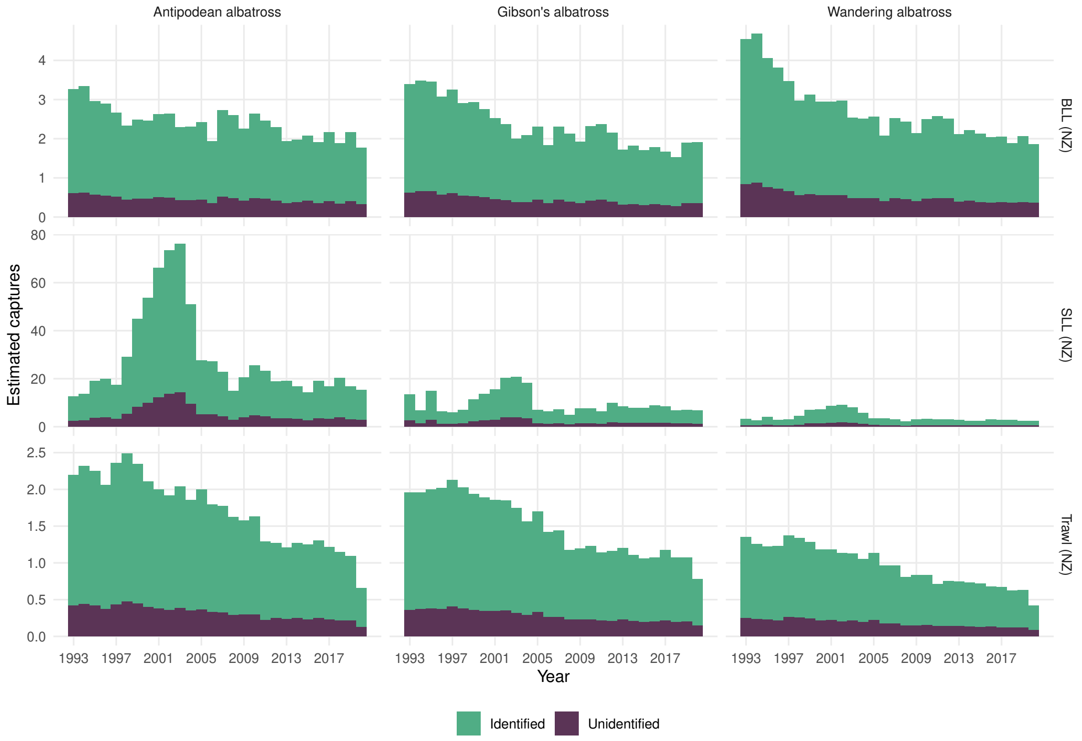

Figure 15: Mean estimated captures of wandering albatross taxa in New Zealand surface-longline (SLL), bottom-longline (BLL), and trawl fisheries by year. The captures that would be expected to be recorded as unidentified wandering albatross are shown in purple.

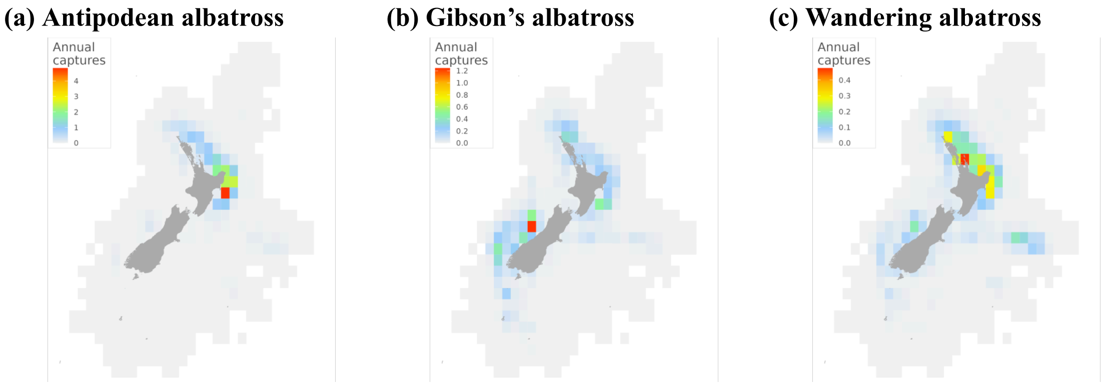
(a) Antipodean albatross

(b) Gibson's albatross

(c) Wandering albatross
Annual captures
4
3
2
1
0
Annual captures
1.2
1.0
0.8
0.6
0.4
0.2
0.0
Annual captures
0.4
0.3
0.2
0.1
0.0

Figure 16: Mean estimated number of annual captures of wandering albatross taxa in New Zealand surface-longline (SLL), bottom-longline (BLL), and trawl fisheries, between 1993 and 2020. (Note the different colour scales among taxa.)

3.4 Interactions with international fisheries

Surface-longline fisheries in the South Pacific Ocean have mostly operated in tropical waters, with no overlap with Antipodean albatross (Figure 17). Nevertheless, fishing activities overlapped with its distribution in several areas: in the Tasman Sea, vessels flagged to Japan, Chinese Taipei, China, Vanuatu, and also vessels of unknown flag overlap with Antipodean albatross; between New Zealand and South America, there was mostly overlap with the Spanish fleet, and also with the Chinese Taipei, Vanuatuan, and Chinese fleets; off the coast of Chile, most of the overlap was with the Japanese and Spanish fleets.

The overlap with international fisheries varied greatly between population classes and across years (Figure 18). Juveniles of both sexes had the greatest overlap with fisheries, and the overlap of juvenile females was almost 20 times higher than that of unsuccessful male breeders in 2019. Among pre-breeders and adults, the overlap of females of all classes with international fisheries was significantly higher than the overlap of males. In 2019, the mean overlap among females was three times higher than the overlap of males. Although the ranking of overlaps was consistent among classes over time, the overlap varied considerably across years. After an increase between 1995 and 2003, the overall overlap peaked in 2003, and then decreased markedly until 2008; in this year, it decreased to a quarter of its peak value, below the 1995 level. It then slowly increased again to reach a level in 2019 that was similar to the overlap in 1995.

There were also distinct differences when examining the overlap of Antipodean albatross across fleets distinguished by vessel flag (Figure 19). Early in the reporting period, most of the overlap was with the Japanese surface-longline fishery, and to a lesser extent with Chinese Taipei and New Zealand surface-longline effort. All fisheries except vessels flagged to China shared a similar peak in overlap between 2001 and 2005. After 2005, the overlap with New Zealand and Spanish fisheries decreased until 2019, but remained stable for Japanese fisheries; it increased for vessels flagged to China, Chinese Taipei, Vanuatu, and for fisheries of unknown origin.

In 2019, the Chinese Taipei fishery had the highest overlap with Antipodean albatross, representing 32% of the total overlap across all population classes, followed by the Vanuatuan fleet (19%), and the Japanese fleet (16%). These patterns of overlap over time remained similar when limiting the analysis to the Tasman Sea (see Appendix F, Figure F-1), where the sex ratio is skewed towards females.

The current analysis also examined the relationship between annual overlap of Antipodean albatross and annual survival rates estimated by the population model (Figure 20). Overall, there was no detectable negative impact of fishery overlap on survival. Among the 25 correlations that were significant (at a level of $\alpha = 0.05$ using the Pearson method), there were twenty correlations that were positive, and only the remaining five significant correlations were negative. The correlations were significantly positive for all population classes in New Zealand fisheries. The negative relationships were in the Chinese fleet overlapping with adult females (non-breeders, unsuccessful breeder, and successful breeders). There was also a negative relationship with the Japanese fleet and male breeders (successful and non-successful). The application of the Bonferroni correction to compensate for multiple tests suggested an α-level of 0.055% (0.05/90). Using this significance level, only two correlations were significant, and both were positive: in the Japanese fleet, and in the minor (“Other”) fisheries, both with non-breeding adult females.

(a) Japan **(b) New Zealand** **(c) Chinese Taipei**

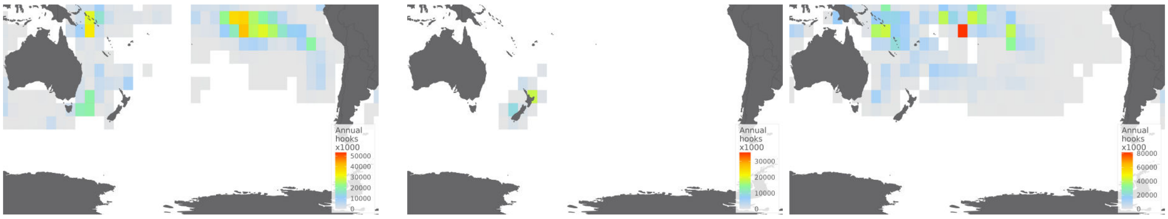
Annual hooks x1000
50000
40000
30000
20000
10000
0
Annual hooks x1000
30000
20000
10000
0
Annual hooks x1000
80000
60000
40000
20000
0

(d) Unknown flag **(e) Vanuatu** **(f) Spain**

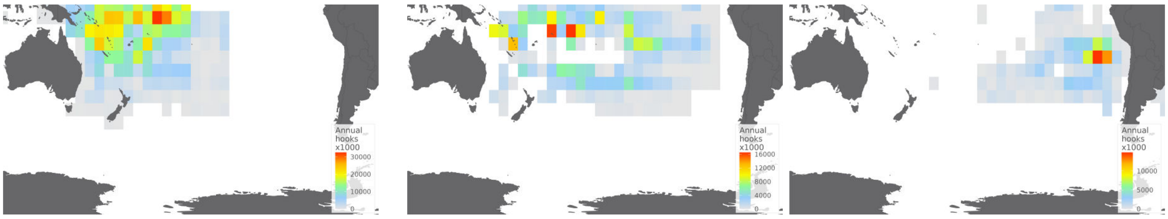
Annual hooks x1000
30000
20000
10000
0
Annual hooks x1000
16000
12000
8000
4000
0
Annual hooks x1000
10000
5000
0

(g) Australia **(h) China** **(i) Other**

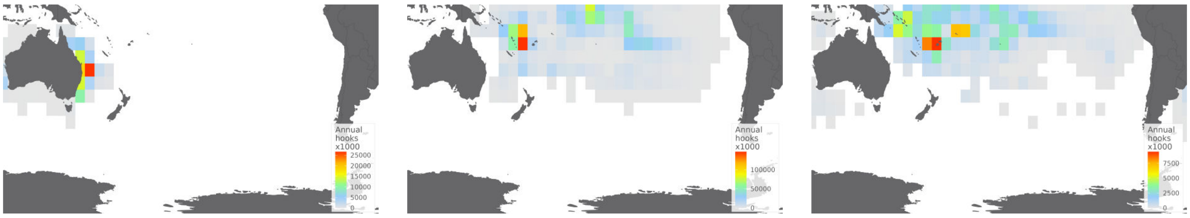
Annual hooks x1000
25000
20000
15000
10000
5000
0
Annual hooks x1000
100000
50000
0
Annual hooks x1000
7500
5000
2500
0

Figure 17: Distribution of the mean annual fishing effort within the distribution range of Antipodean albatross, for all countries and by flag. Data are sorted in decreasing order of overlap with the taxon, between 1995 and 2019. Fleets with less than 1% of the total overlap with Antipodean albatross were combined into "other" (shown in Figure G-1).

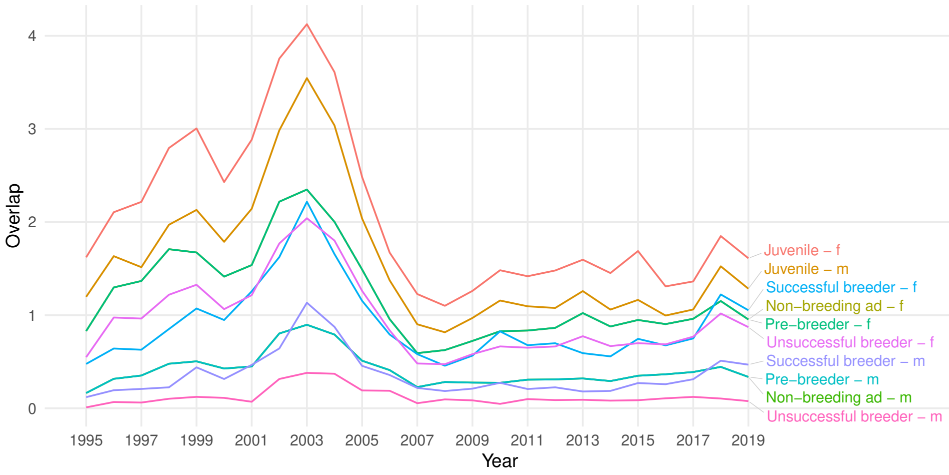

Figure 18: Total overlap of Antipodean albatross with surface-longline fisheries in the Southern Hemisphere, by year and by population class (f: female; m: male). Overlap is the product of fishing effort (in thousands of hooks) and bird density (in birds per km^2).

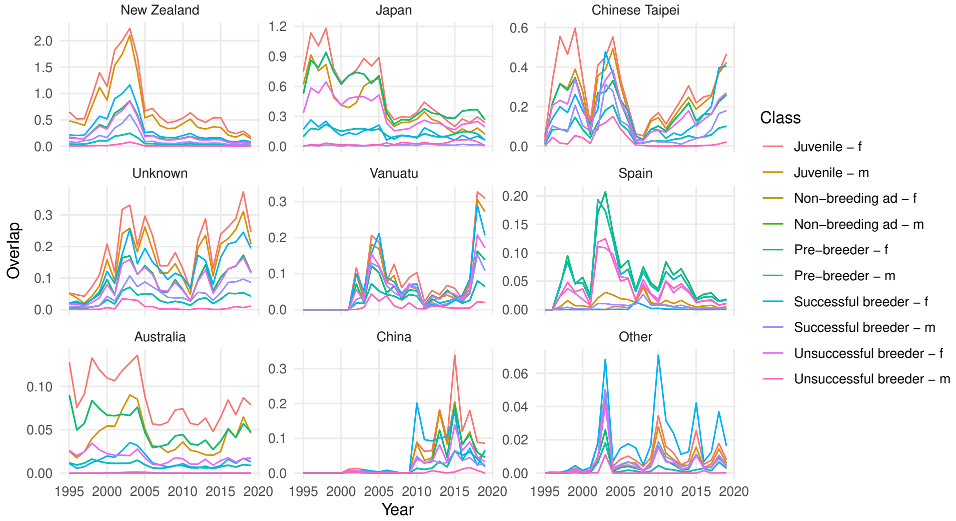

Figure 19: Overlap of Antipodean albatross with surface-longline fisheries in the Southern Hemisphere, by year and by population class (f: female; m: male). The flags responsible for less than 1% of the mean overlap across all classes were combined into "Other". The overlap is the product of fishing effort (in thousands of hooks) and bird density (in birds per km^2).

3.4.1 Comparison of catchabilities from survival rates and overlaps

The approach to calculate the catchability in a given fishery from a change in its overlap with the species and the change in annual survival rates was applied to each fishery independently. This calculation was based on the difference in annual survival rate between males and females post-2006, and the sex-specific difference between pre- and post-2006 (see Table 5 for the three estimates of catchability for each of the flag fisheries responsible for more than 99.9% of the total overlap with the species). For annual survival rate, the mean value of 0.95 was used for both females and males pre-2006, and the mean value of 0.88 and 0.93 for females and males post-2006, respectively.

There were four flag fisheries that had positive estimates for all three types of catchability: China, Vanuatu, Fiji, and Solomon Islands (Table 5). Theses four fisheries also had a low spread in their catchability estimates, with a CV of less than 0.5 for all these fisheries. The other flag fisheries had one or more negative estimate of catchability, so the differences in overlaps between sexes and periods could not explain the change in annual survival rates. For these five fisheries, the spread in catchability estimates was also high (over one in all cases).

The fishery flagged to China had the lowest catchability estimate overall, at 1.07 per 10 000 hooks. The three estimates for the fishery flagged to China were also the most consistent, varying from 0.864 to 1.238, with a coefficient of variation of 0.18. In comparison, the fisheries flagged to Vanuatu, Fiji, and Solomon Islands had higher catchability estimates, i.e., the estimates were 62%, 932%, and 1932% higher, respectively. The catchability of Antipodean albatross in the latter three flag fisheries would need to be high for them to explain the change in survival on their own.

These catchability estimates can be directly compared with the catchability estimated directly on the estimated number of captures in the New Zealand fleet and its overlap with Antipodean albatross. The current analysis estimated the number of observable captures to be around 22 individuals annually after 2006, or 44 fatalities when considering cryptic mortality. Using the same dataset on international surface-longline effort, the annual per-capita overlap with adults, O, was 671.1 hooks per square kilometre. The total adult population, N, was estimated from the demographic model to be 21 943 birds. Based on these numbers, the catchability in the New Zealand fleet was estimated to be 0.0299 per 10 000 hooks. This finding suggests that the catchability estimated for the fishery flagged to China (see Table 5) was 36

(a) All flags

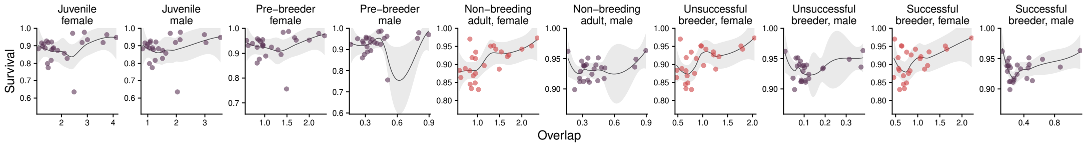

(b) Japan

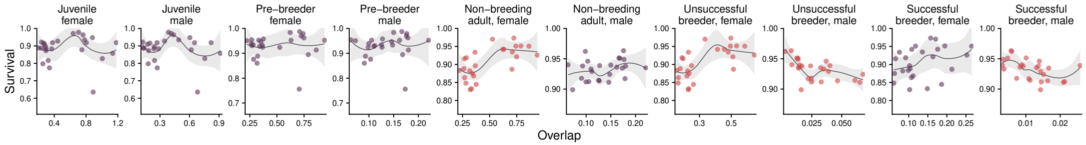

(c) New Zealand

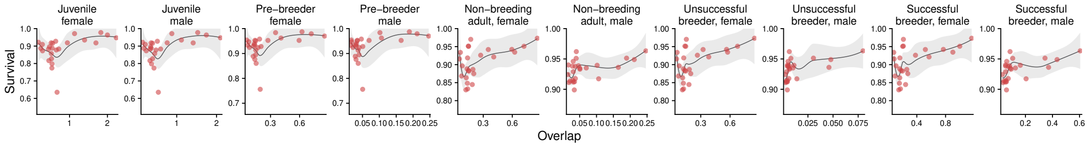

(d) Chinese Taipei

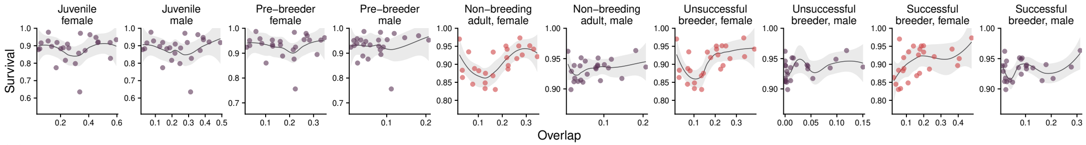

(e) Unknown

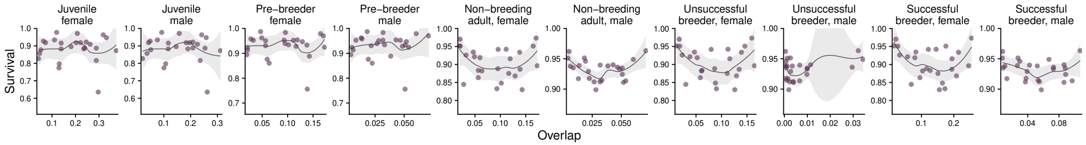

(f) Vanuatu

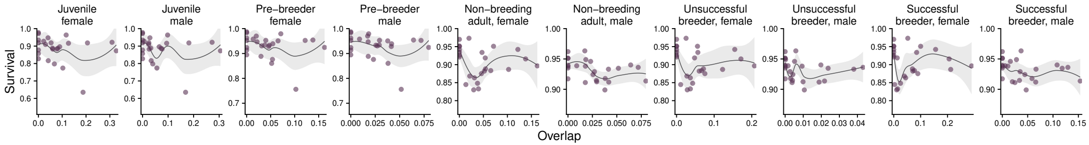

(g) Spain

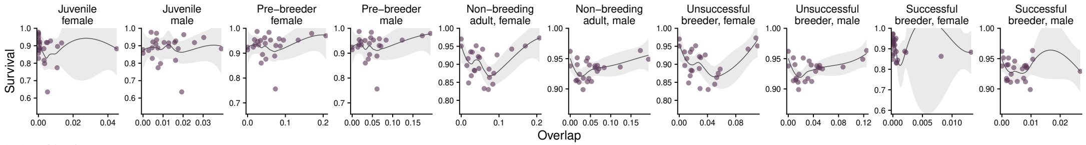

(h) China

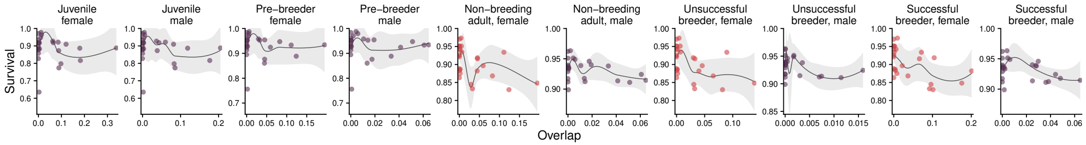

(i) Other

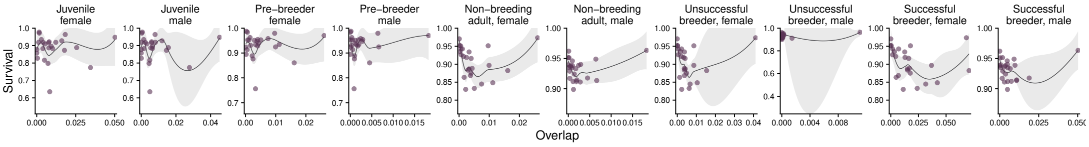

Figure 20: Relationship between the annual variability in overlap of Antipodean albatross with fisheries and the annual variability in the estimated survival rate for each population class and fishery group. The flags responsible for less than 1% of the mean overlap across all classes were combined into "Other". Points with a significant Pearson correlation (at α=0.05) are shown in orange, and in purple otherwise.

Table 5: Comparison for each flag fishery of the catchability estimates (q) calculated from the difference in per-capita overlaps (O) and annual survival rates of Antipodean albatross, between the pre- and post-2006 periods for each sex ($q_{♂}$ and $q_{♀}$), and between females and males ($q_{♀-♂}$) post-2006. The mean and absolute value of the coefficient of variation (CV) across three catchability estimates are also shown. Fisheries were sorted in decreasing order of mean catchability: fisheries with one or more negative catchability estimates are separated at the bottom and considered implausible. Per-capita overlap is in hooks per square kilometre, catchability is in per 10 thousand hooks.

	Females			Males					
Flag	O_{pre}	O_{post}	$q_{♀}$	O_{pre}	O_{post}	$q_{♂}$	$q_{♀-♂}$	Mean	|CV|
China	19.4	647.5	1.115	12.2	243.7	0.864	1.238	1.072	0.18
Vanuatu	362.2	647.4	2.454	169.0	347.3	1.122	1.666	1.747	0.38
Fiji	18.7	80.5	11.319	5.5	20.2	13.607	8.284	11.070	0.24
Solomon Islands	0.0	35.1	19.955	0.0	7.3	27.406	17.998	21.786	0.23
New Zealand	4 432.2	1 255.6	-0.220	1 275.6	313.3	-0.208	0.531	0.034	12.60
Japan	4 867.5	2 179.6	-0.260	1 102.6	785.3	-0.630	0.359	-0.177	2.82
Chinese Taipei	2 267.4	1 350.1	-0.763	1 048.0	415.7	-0.316	0.535	-0.181	3.64
Australia	431.1	250.6	-3.879	76.9	46.8	-6.641	2.453	-2.689	1.73
Spain	458.9	273.7	-3.779	531.3	299.4	-0.862	-19.464	-8.035	1.25
Panama	0.0	2.7	263.276	0.0	5.2	38.434	-196.467	35.081	6.55

times the catchability estimate of vessels flagged to New Zealand. The catchability estimated for vessels flagged to Vanuatu, Fiji, and Solomon Islands was 58, 370, and 729 times higher than for vessels flagged to New Zealand, respectively. This analysis assumes that all the change in Antipodean albatross survival is caused by a single fleet. If all four fleets (China, Vanuatu, Fiji, and Solomon Islands) contributed to the mortality of Antipodean albatross, with the same catchability, then the catchability required to explain the change in mortality of Antipodean albatross would be be roughly halved, to around 20 times the catchability of the New Zealand fleet. In this scenario, most of the mortality would be associated with the China and Vanuatu fleets.

3.5 Impact of climate

Using the bird density layers by population class from Richard et al. (2024), a weighted average of several climatic variables was calculated for each year and population class to assess whether a change over time could explain the variability in demographic parameters.

To examine the variability in demographic parameters of Antipodean albatross, the current study also included a number of climatic and atmospheric variables. The weighted average of these variables across the range of each population class suggested that the different classes resided in different environments (Figure 21). Compared with any of the other classes, male and female juveniles tended to be in areas with higher air temperature, lower relative humidity, higher sea-level pressure, warmer waters, and lower wind speeds. Male pre-breeders and breeders (successful and unsuccessful) were found predominantly in areas with lower air temperature, higher relative humidity, lower sea-level pressure, colder waters, higher surface lifted index, and higher wind speeds, compared with other classes.

The inter-annual variability of the climatic and atmospheric variables was lower than the variability among population classes for most variables, except for the sea surface temperature anomaly, and wind angle.

At the colony on Antipodes Island, the conditions were more variable among years than the weighted averages (Figure 21). These variables were from a single location, compared with the averages across extensive spatial areas for the population classes. The conditions at the colony were markedly colder, windier, and more humid, than across the range used by the population classes.

The relationship between yearly means of climatic variables and survival rates did not reveal any clear correlations (Figure 22). Only four correlations were significant at $\alpha = 0.05$: a positive relationship of wind speed and juvenile survival for both males and females, a negative correlation betwen omega and male successful breeders, and a negative relationship between the surface Lifted Index and male unsuccessful breeders. However, none of these relationship were significant when the Bonferroni correction was applied (α=0.055% for 90 comparisons).

At the colony, air temperature was significantly negatively correlated with the probability of breeding (at α=0.05), as was the mean annual sea surface temperature (SST) and its anomaly (Figure 23). Relative humidity was also positively correlated with breeding success, whereas SST and its anomaly was negatively correlated with it. No relationship was found between the Southern Oscillation Index (SOI) and any of the survival rates, breeding probability, or breeding success (Figure 24).

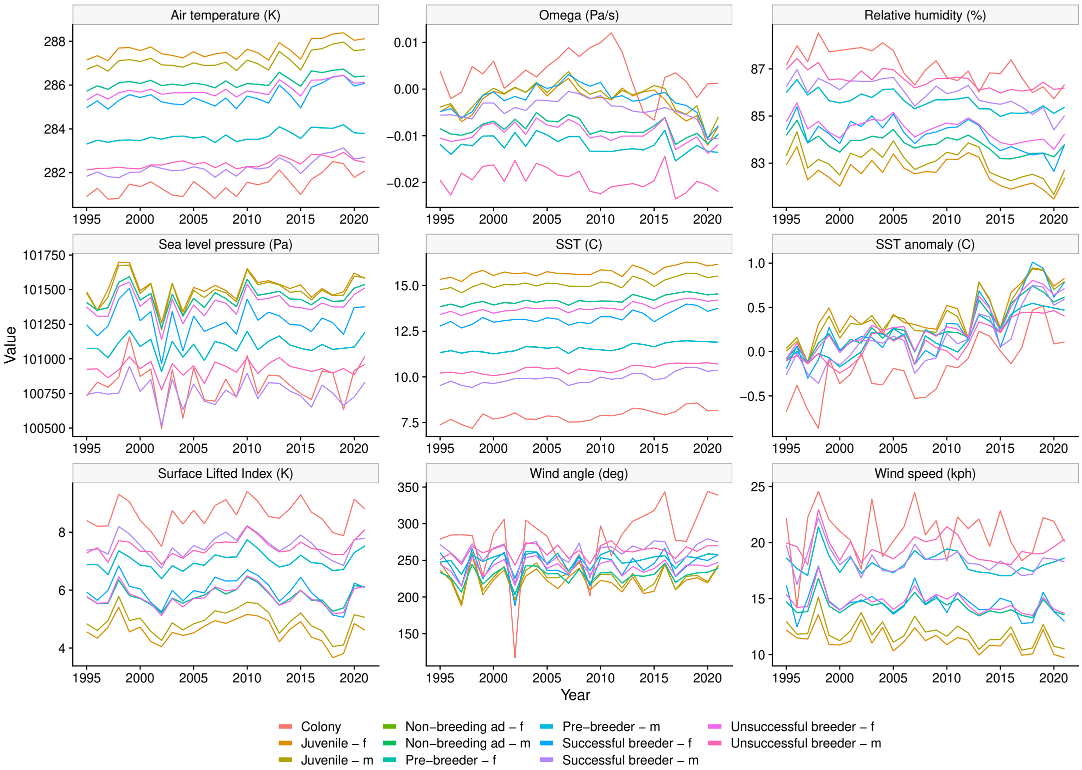

Figure 21: Annual variability of the weighted average of nine climatic and atmospheric variables by population class of Antipodean albatross (f: female; m: male), and as at the breeding colony.

(a) SST

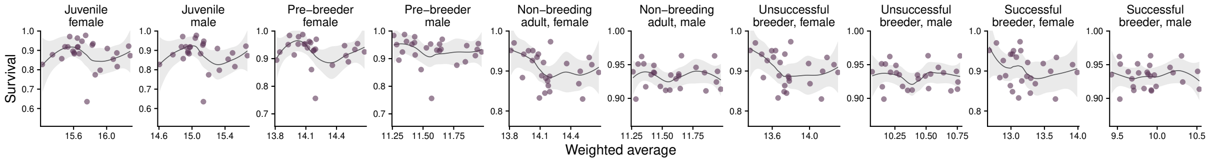

(b) SST anomaly

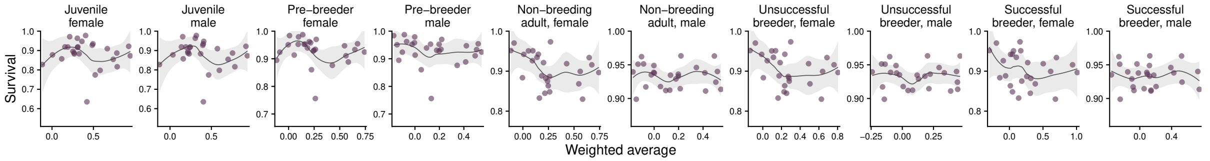

(c) Wind angle

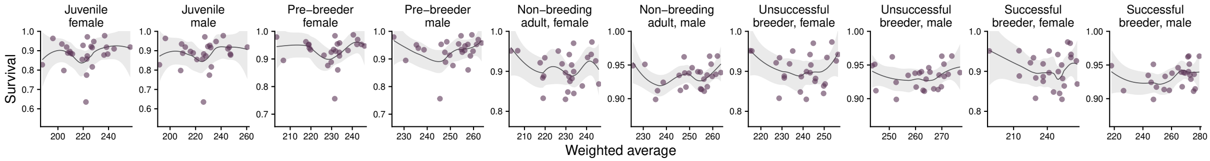

(d) Wind speed

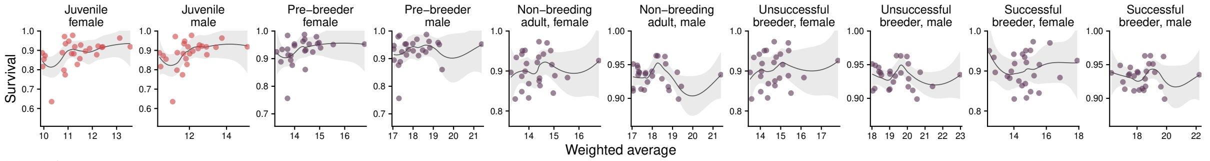

(e) Air temperature

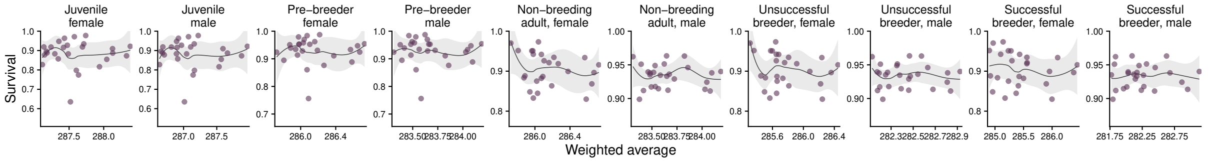

(f) Sea level pressure

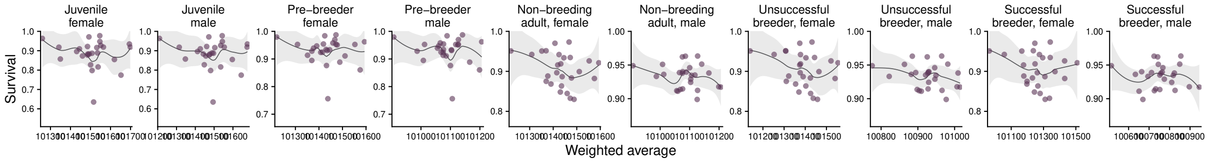

(g) Omega

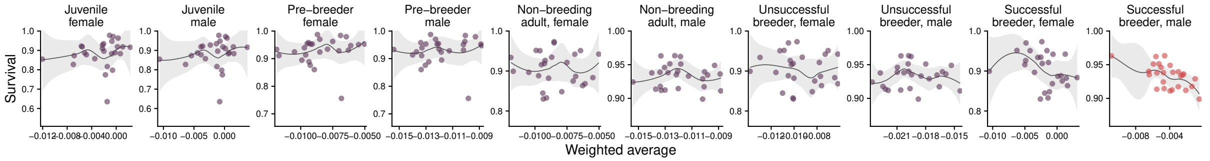

(h) Relative humidity

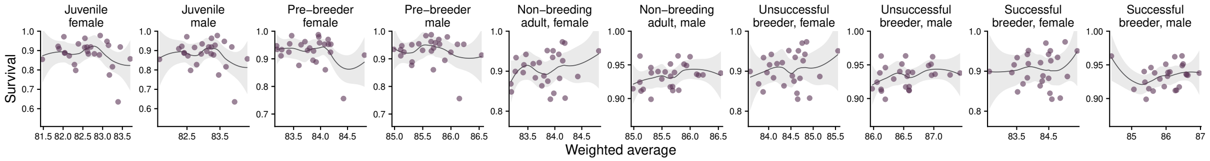

(i) Surface Lifted Index

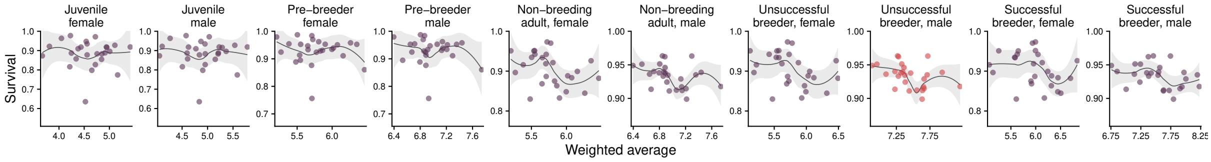

Figure 22: Relationship between the annual variability in climatic and atmospheric variables and the annual variability in the estimated survival rate for each population class of Antipodean albatross and fishery group. Points with a significant Pearson correlation (at α=0.05) are shown in orange, and in purple otherwise.

(a) Breeding probability

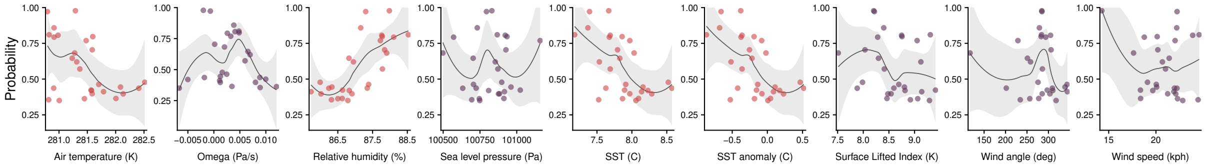

(b) Breeding success

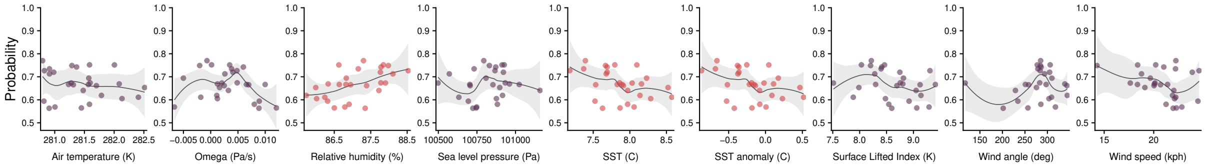

Figure 23: Relationship between the annual variability in climatic and atmospheric variables and the annual variability in the estimated breeding probability and success of Antipodean albatross. Points with a significant Pearson correlation (at α=0.05) are shown in orange, and in purple otherwise.

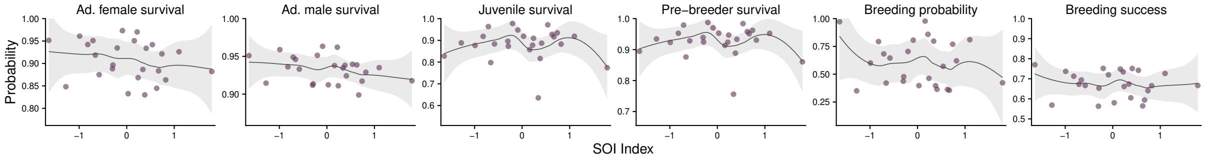

Figure 24: Relationship between the annual Southern Oscillation Index (SOI) and the estimated annual survival rate of adult females, adult males, juveniles, and pre-breeders, breeding probability, and breeding success of Antipodean albatross. Points with a significant Pearson correlation (at α=0.05) are shown in orange, and in purple otherwise.

3.6 Exploration of management scenarios

To explore the potential impact of different management scenarios on the Antipodean albatross population using the interactive tool, a workshop was held on 28 June 2023 with participants from Fisheries New Zealand and Department of Conservation. During the workshop, the results of the demographic model, the at-sea distribution analysis, and the threat analyses were presented, followed by a demonstration of the simulation tool. The tool was then used by participants to explore and test different scenarios. The focus of this exploration was on the main factors related to the decline of Antipodean albatross, specifically that females have been more affected than males; and also, and that potential factors that may responsible for the declines were significantly stronger after 2006. To support participants in this exploration, the map of spatially-varying sex ratio within the species range was made available to inform the locations of potential impacts (Appendix C, Figure C-2).

Sea surface temperature anomalies and plastic pollution were discarded as main factors of the observed patterns of decline, as they could not explain the sex bias in survival rates, nor the notable change in survival rates after 2006.

A previous risk assessment provided an estimate of annual deaths of Antipodean albatross in New Zealand fisheries, almost exclusively in surface-longline fisheries (Edwards et al. 2023a). This impact was entered into the simulation tool as an existing impact, using the upper estimate of 60 annual deaths. It was specified as a spatial impact using the New Zealand surface-longline effort distribution, and also as a non-spatial impact affecting only adult survival. Regardless of this distinction, the impact was negligible in the scenario explorer, as the outcome of the population after 30 years remained unchanged (Figure 25).

When varying the impact of different international fisheries individually, the fleet flagged to China was the only fleet that could potentially explain both the change after 2006 and the female-biased impact. When the impact factor of this fleet was set to lead to around 1450 deaths annually across the entire distributional range of the subspecies, the simulation showed a stabilisation of the population, and an even survival rate between both sexes, at around 97% (Figure 25).

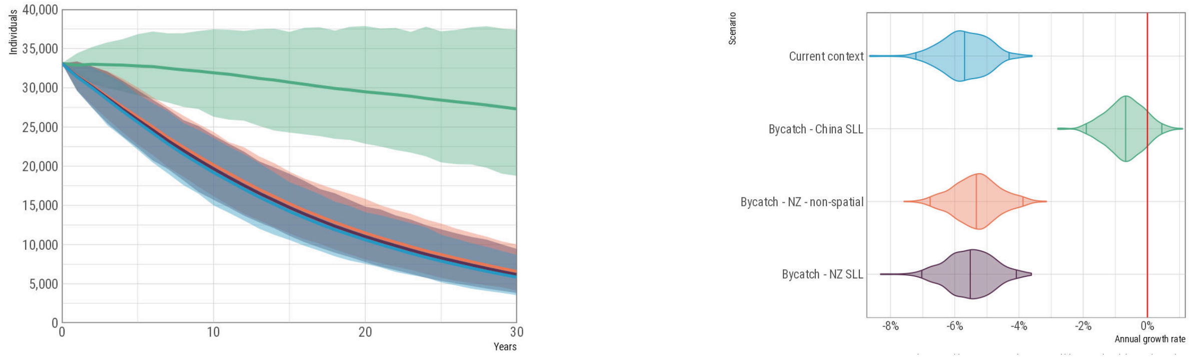

(a) Population size

(b) Population growth

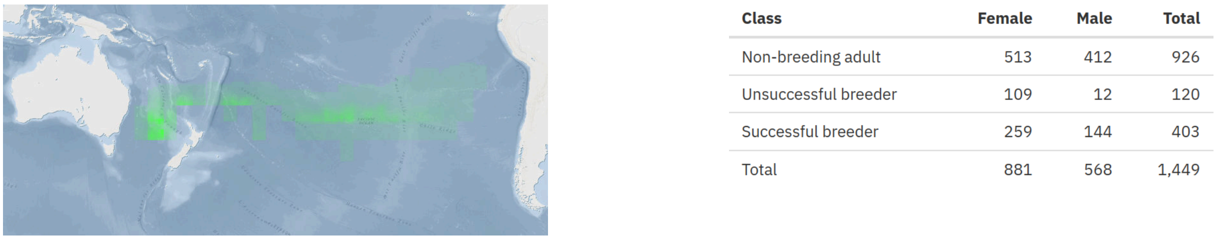

(c) Overlap with China-flagged SLL fleet

(d) Fatalities from overlap

Class	Female	Male	Total
Non-breeding adult	513	412	926
Unsuccessful breeder	109	12	120
Successful breeder	259	144	403
Total	881	568	1,449

Figure 25: Screenshots of the simulation tool exploring the demographic impact of Antipodean albatross bycatch within New Zealand's Exclusive Economic Zone, and a hypothetical impact of the China-flagged surface-longline (SLL) fleet.

4. DISCUSSION

The literature review of potential threats to Antipodean albatross found a number of potential causes for the decline of Antipodean albatross. These causes included fisheries, climate change, pollution, and diseases. For a number of these factors, detailed data are missing, with available information relevant to Antipodean albatross generally limited to fisheries bycatch.

Fitting a population model to sighting data collected at the colony since 1995 allowed the detection of patterns in demographic parameters that could be explained by variations in threats; the latter were examined across demographic classes and sex, and across years. The current results from this analysis confirmed findings from previous research (e.g., Edwards et al. 2017, Walker & Elliott 2022, Parker et al. 2023), particularly declines after 2006 of population size, survival rates (mostly of female adults), the probability of breeding, and breeding success. These demographic parameters appear to have stabilised after 2011, and may have been potentially increasing at a slow rate since then, although the inter-annual variability prevented confirmation of this trend.

The at-sea distributions of Antipodean albatross was derived in a companion study and showed that different population classes and sexes tend to use different areas (Richard et al. 2024). These differences included that the Tasman Sea and the area north-east of New Zealand's North Island are predominantly used by females, whereas males mostly forage around the Southern Pacific Ocean. Some areas of high-density, "distribution hotspots", were also clearly defined for both sexes, and were consistent across years: around Chatham Rise, an area just off the coast of Chile around 45 degrees South, and an area further north and offshore around 800 km from the Chilean coast around 33 degrees South.

In combination with information of the biology and demography of Antipodean albatross, these differences in spatial distribution allowed a preliminary analysis of threats that may contribute to the decline. For example, the lower survival of females than males suggests that the threat may be located in the area north-east of New Zealand's North Island or in the Tasman Sea. In addition, the time series of demographic parameters suggested that threats to the species may have been more pronounced around 2006, or just before this time, and impacted the breeding probability and breeding success, although no direct threat at the colony was recorded. Furthermore, the stabilisation (or potential increase) in demographic parameters after 2011 suggested that the intensity of the threats did not increase (or potentially decreased) during the subsequent period.

The analysis of Antipodean albatross captures in New Zealand surface-longline, bottom-longline, and trawl fisheries revealed a peak in estimated captures in surface longline between 2001 and 2005. This peak was followed by a marked decrease in estimated captures, and a slow continuous decline after 2006. The captures were located off the eastern and northern coast of North Island, an area predominantly used by females. This finding was supported by necropsy data of Antipodean albatross caught in surface longline: since 1998, of the 28 observed captures for which the sex was identified, 17 (61%) were females. The timing and the sex bias in the captures in New Zealand surface-longline fisheries corresponded to the pattern of decline in demographic parameters, although the peak in captures occurred just before the demographic decline.

The current estimate of 22 captures annually between 2018 and 2020 in New Zealand trawl and longline fisheries was slightly lower (but not significantly so) than the estimate of 32 (95% c.i.: 21–44) captures in the most recent seabird risk assessment for New Zealand (Edwards et al. 2023a). It is worth noting that there were two main differences in the methods between the present study and the most recent seabird risk assessment, which may explain some of this difference in estimates. First, the current model included generic wandering albatross captures, which constituted the majority of recorded captures in trawl fisheries, whereas these captures were omitted by Edwards et al. (2023a). Second, the model in the risk assessment was more complex, because it was fitted to all New Zealand seabirds simultaneously and vulnerability was estimated for different fishery groups (see Edwards et al. 2023a).

The analysis of spatial overlap of Antipodean albatross with international fisheries indicated that the overlap with fleets, other than the New Zealand fleet, also peaked in the period around 2001 to 2005. This peak was particularly notable for the Japanese, Chinese Taipei, Vanuatuan, and Spanish fleets. The increase in overlap with the Chinese Taipei, Chinese, Vanuatuan, and with unknown flag fleets was not clearly reflected in the demographic parameters, although there was a negative correlation between adult survival and the overlap with vessels flagged to China. In contrast, for adult female albatross, there was a significant positive correlation between the total annual overlap across all fleets and annual survival rate. This correlation was consistent across the Japanese, New Zealand, and Chinese Taipei fleets, which all had the highest overlap with females. This correlation may be coincidental, caused by a considerable decrease in fishing effort and a concomitant decrease in survival rate. The population class that had the highest overlap with international fisheries were juveniles, but there was no clear effect on their survival. It is possible that the model constraint, that juveniles share the same annual variability as pre-breeders, may have obscured the relationship; juveniles are not recorded at the colony for several years after fledgling, and the lack of information prevented the separate estimation of their annual variability.

Direct correlative analyses of overlap and demographic parameters gave limited insight, and the results need to be interpreted with caution. For example, the comparison of overlaps assumed that the catchability of seabirds was similar across different fleets; however, bycatch rates might be higher in some fleets due to differences in the use of mitigation measures and fishing operations. In addition, separating fleets according to vessel flag use is difficult, because some vessels swap flags regularly to access different fishing areas or respond to changes in regulations (Petrossian et al. 2020).

An alternative method was developed to assess whether a difference in overlaps for a given fishery could explain the difference in survival rates, between sexes and between the periods pre- and post-2006. For the fleets flagged to China, Vanuatu, Fiji, and the Solomon Islands, changes in overlap were consistent with the changes in survival of both males and females. The changes in survival could be explained by captures in the China-flagged fleet, if its catchability was around 36 times that of New Zealand. This difference in catchability is not implausible, as catchability can vary considerably depending on the fishing gear configuration or practices (e.g., waste discharge regime, Pierre et al. 2012). For example, use of a net sonde cable by some vessels in the Chilean trawl factory fleet has been estimated to increase the capture rate by a factor of 30 (Richard & Adasme 2019), and the estimated catchability among New Zealand trawl fisheries can vary by a factor of 15 (Richard & Abraham 2020). If the captures were occurring on the fleets flagged to China, Vanuatu, Solomon Islands, and Fiji, then the catchability required to explain the differences in survival would be around 20 times the catchability associated with the New Zealand fleet.

The temporal pattern in climatic variables did not explain the decline observed in the population and demographic parameters of Antipodean albatross. The weighted averages by population class suggested that individuals can exist across a range of climatic conditions, which is greater than their inter-annual variability. In particular, the increase in sea surface temperature measured across the range of the subspecies was not found to have affected its demography.

A lack of quantitative information about the effect of other potential threats prevented a direct analysis of their impact on the subspecies demography. Some threats such as plastic pollution were identified as being significant in albatross species of the Northern Hemisphere, but no Antipodean albatross fatalities have been observed to be directly caused by it, neither at the colony (K. Walker, pers. comm.), nor from the necropsy of birds caught in fisheries (B. Bell, pers. comm.). Large albatrosses appear to be efficient at regurgitating plastic debris, and obstruction may not cause significant direct mortalities. Nevertheless, their feeding mode and foraging behaviour puts them at relatively high risk of ingesting marine plastics (Roman et al. 2016). In addition, it is possible that the toxicity of plastics may have an impact (e.g., see Yamashita et al. 2021), although observations and assessments of this aspect are difficult.

The analysis of different threats did not reveal a clear cause of the demographic decline of Antipodean albatross observed over the study period. The main potential change in threat levels identified was in fishing effort, especially in the Tasman Sea. This change may explain the greater decline for females. The surface-longline fleet flagged to China that started operating within the range of the species after 2007 overlapped particularly with female Antipodean albatross. A high bycatch level in this fleet could potentially explain the patterns of decline that have been identified, and would explain the negative correlation between the annual overlap of this fleet and the annual estimates of female survival. There were similar patterns with the fleets flagged to Vanuatu, Fiji, and Solomon Islands, and they may all be contributing to the mortality.

In this context, both males and females of Gibson's wandering albatross (*D. antipodensis gibsoni*) also forage in the Tasman Sea, with a similar decline in population size, survival rate, and breeding success recorded in 2005 and 2006 (Walker et al. 2023).

International collaboration is essential to gain insight into the relative contribution of different fisheries to the decline of Antipodean albatross, and this entails the comprehensive collection and sharing of data on their capture in the Tasman Sea across the diverse fleets.

5. ACKNOWLEDGEMENTS

We are grateful to Igor Debski and Johannes Fischer at the Department of Conservation for providing their inputs into the project and the team at Wildlife Management International for sharing their knowledge on the threats to Antipodean albatross.

The Aquatic Environment Working Group (hosted by Fisheries New Zealand) provided valuable feedback on an earlier version of this analysis. This project was funded under Fisheries New Zealand project PRO2021-03.

6. REFERENCES

Abraham, E.; Richard, Y.; Walker, N.; Gibson, W.; Daisuke, O.; Tsuji, S.; Kerwarth, S.; Winkler, H.; Parsa, M.; Small, C.; Waugh, S. (2019). Assessment of the risk of surface longline fisheries in the Southern Hemisphere to albatrosses and petrels, for 2016. https://www.ccsbt.org/en/system/files/ERSWG13_17_NZ_Assessment_RiskOfSurfaceLonglineFisheries_SouthernHemisphere.pdf Prepared for the 13th meeting of the Ecologically Related Species Working Group (ERSWG13) of the Commission for the Conservation of Southern Bluefin Tuna (CCSBT).

Agreement on the Conservation of Albatrosses and Petrels (2009). Species assessment: Antipodean albatross *Diomedea antipodensis*. http://www.acap.aq/en/acap-species/289-antipodean-albatross.

Alexander, D. (2003). Current situation of avian influenza in poultry in Great Britain. *Avian diseases. Vol. 47, Special Issue. First International Symposium on Avian Influenza. 1981 Proceedings (2003)*: 35–45.

Alfaro-Shigueto, J.; Mangel, J.C.; Valenzuela, K.; Arias-Schreiber, M. (2016). The intentional harvest of waved albatrosses *Phoebastria irrorata* by small-scale offshore fishermen from Salaverry port, Peru. *Pan-American Journal of Aquatic Sciences 11 (1)*: 70–77.

Arthur, C.; Bamford, H.; Baker, J. (2008). The occurrence, effects and fate of small plastic debris in the oceans. *Proceedings of the International Research Workshop on the occurrence, effects and fate of microplastic marine debris. 9–11 September, NOAA Technical Memorandum NOS-OR&R-30.*

Bertrand, S.; Joo, R.; Smet, C.A.; Tremblay, Y.; Barbraud, C.; Weimerskirch, H. (2012). Local depletion by a fishery can affect seabird foraging. *Journal of Applied Ecology 49*: 1168–1177.

BirdLife International (2018). *Diomedea antipodensis. In*: The IUCN Red List of Threatened Species 2018: e.T22728318A132656045. IUCN. https://www.iucnredlist.org/species/22728318/132656045

Blévin, P.; Carravieri, A.; Jaeger, A.; Chastel, O.; Bustamante, P.; Cherel, Y. (2013). Wide range of mercury contamination in chicks of Southern Ocean seabirds. *PLoS One 8 (1)*: e54508.

Bose, S.; Debski, I. (2020). Antipodean albatross spatial distribution and fisheries overlap 2019. Prepared by the Department of Conservation. 23 p.

Bose, S.; Debski, I. (2021). Antipodean albatross spatial distribution and fisheries overlap 2020. Prepared by the Department of Conservation. 36 p.

Brothers, N.; Duckworth, A.R.; Safina, C.; Gilman, E.L. (2010). Seabird bycatch in pelagic longline fisheries is grossly underestimated when using only haul data. *PLoS ONE 5*: e12491. https://doi.org/10.1371/journal.pone.0012491

Caccavo, J.; Christiansen, H.; Constable, A.; Ghigliotti, L.; Trebilco, R.; Brooks, C.; Cotte, C.; Desvignes, T.; Dornan, T.; Jones, C.; Koubbi, P.; Saunders, R.; Strobel, A.; Vacchi, M.; van de Putte, A.; Walters, A.; Waluda, C.; Woods, B.; Xavier, J. (2021). Productivity and change in fish and squid in the Southern Ocean. *Frontiers in Ecology and Evolution 9*: 1–25.

Carpenter, B.; Gelman, A.; Hoffman, M.; Lee, D.; Goodrich, B.; Betancourt, M.; Brubaker, M.A.; Guo, J.; Li, P.; Riddell, A. (2017). Stan: A probabilistic programming language. *Journal of Statistical Software 76*.

Carpenter-Kling, T.; Reisinger, R.R.; Orgeret, F.; Connan, M.; Stevens, K.L.; Ryan, P.G.; Makhado, A.; Pistorius, P.A. (2020). Foraging in a dynamic environment: response of four sympatric sub-Antarctic albatross species to interannual environmental variability. *Ecology and Evolution 10 (20)*: 1–19.

Chamberlain, S. (2023). Rerddap: General purpose client for 'ERDDAP' servers. https://docs.ropensci.org/rerddap/,%20https://github.com/ropensci/rerddap.

Cherel, Y.; Barbraud, C.; Lahournat, M.; Jaeger, A.; Jaquemet, S.; Wanless, R.M.; Phillips, R.A.; Thompson, D.R.; Bustamante, P. (2018). Accumulate or eliminate? Seasonal mercury dynamics in albatrosses, the most contaminated family of birds. *Environmental Pollution 241*: 124–135.

Cherel, Y.; Klages, N. (1997). A review of the food of albatrosses. *In*: Albatross biology and conservation (pp. 113–136). Surrey Beatty & Sonds, Chipping Norton.

Cherel, Y.; Xavier, J.; de Grissac, S.; Trouvé, C.; Weimerskirch, H. (2017). Feeding ecology, isotopic niche, and ingestion of fishery-related items of the wandering albatross *Diomedea exulans* at Kerguelen and Crozet Islands. *Marine Ecology Progress Series 565*: 197–215.

Chilvers, B.L.; Hiscock, J.A. (2019). Significant decline of endangered Antipodes Island penguins: Is extreme weather an additional impact? *Aquatic Conservation: Marine and Freshwater Ecosystems 29*: 546–553.

Chilvers, B.L.; Ruoppolo, V. (2019). Planning for an offshore oiled wildlife response: case studies from New Zealand and Brazil. *Environmental Science and Pollution Research 30 (19)*: 54351–54361.

Convention on Migratory Species (2020). Concerted Action for the Antipodean albatross (*Diomedea antipodensis*). *UNEP/CMS/Concerted Action 13.12*. https://www.cms.int/cami/en/document/concerted-action-antipodean-albatross-diomedea-antipodensis. 8 p.

Cózar, A.; Echevarría, F.; González-Gordillo, J.I.; Irigoien, X.; Úbeda, B.; León, S.H.; Palma, Á.T.; Navarro, S.; García-de-Lomas, J.; Ruiz, A.; et al. (2014). Plastic debris in the open ocean. *Proceedings of the National Academy of Sciences 111*: 10239–10244.

Department of Conservation (2018). Million Dollar Mouse successfully eradicates mice from Antipodes Island. http://www.doc.govt.nz/news/media-releases/2018/million-dollar-mouse-successfully-eradicates-mice-from-antipodes-island//

Dias, M.; Martin, R.; Pearmain, E.; Burfield, I.; Small, C.; Phillips, R.; Yates, O.; Lascelles, B.; Borboroglu, P.; Croxall, J. (2019). Threats to seabirds: A global assessment. *Biological Conservation 237*: 525–537.

Dunn, O.J. (1961). Multiple comparisons among means. *Journal of the American Statistical Association 56 (293)*: 52–64.

Edwards, C.T.T.; Peatman, T.; Goad, D.; Webber, D.N. (2023a). Update to the risk assessment for New Zealand seabirds. *New Zealand Aquatic Environment and Biodiversity Report No. 314*. 66 p.

Edwards, C.T.T.; Peatman, T.; Roberts, J.O.; Devine, J.A.; Hoyle, S.D. (2023b). Southern Hemisphere seabird risk assessment. *New Zealand Aquatic Environment and Biodiversity Report No. 321*. 103 p.

Edwards, C.T.T.; Roberts, J.O.; Walker, K.; Elliott, G. (2017). Quantitative modelling of Antipodean wandering albatross. *New Zealand Aquatic Environment and Biodiversity Report No. 180*. 32 p.

Elliott, G.; Walker, K.J. (2013). Antipodean albatross [updated 2022] [www.nzbirdsonline.org.nz]. *In*: C.M. Miskelly (Ed.), New Zealand Birds Online.

Eriksen, M.; Lebreton, L.C.M.; Carson, H.S.; Thiel, M.; Moore, C.J.; Borerro, J.C.; Galgani, F.; Ryan, P.G.; Reisser, J. (2014). Plastic pollution in the world's oceans: More than 5 trillion plastic pieces weighing over 250,000 tons afloat at sea. *PLOS ONE 9 (12)*. https://doi.org/10.1371/journal.pone.0111913

Eriksen, M.; Maximenko, N.; Thiel, M.; Cummins, A.; Lattin, G.; Wilson, S.; Hafner, J.; Zellers, A.; Rifman, S. (2013). Plastic pollution in the South Pacific subtropical gyre. *Marine Pollution Bulletin 68*: 71–76.

Fayet, A.L.; Clucas, G.V.; Anker-Nilssen, T.; Syposz, M.; Hansen, E.S. (2021). Local prey shortages drive foraging costs and breeding success in a declining seabird, the Atlantic puffin. *Journal of Animal Ecology 90*: 1152–1164.

Freedman, D.; Pisani, R.; Purves, R. (2007). *Statistics (international student edition), 4th edn.* WW Norton & Company, New York.

Gall, S.C.; Thompson, R.C. (2015). The impact of debris on marine life. *Marine Pollution Bulletin 92*: 170–179.

Gianuca, D.; Bugoni, L.; Jiménez, S.; Daudt, N.W.; Miller, P.; Canani, G.; Silva-Costa, A.; Faria, F.A.; Bastida, J.; Pon, J.P.S.; et al. (2020). Intentional killing and extensive aggressive handling of albatrosses and petrels at sea in the southwestern Atlantic Ocean. *Biological Conservation 252*: 108817.

Goutte, A.; Barbraud, C.; Meillère, A.; Carravieri, A.; Bustamante, P.; Labadie, P.; Budzinski, H.; Delord, K.; Cherel, Y.; Weimerskirch, H.; et al. (2014). Demographic consequences of heavy metals and persistent organic pollutants in a vulnerable long-lived bird, the wandering albatross. *Proceedings of the Royal Society B: Biological Sciences 281 (1787)*: 20133313.

Grémillet, D.; Ponchon, A.; Paleczny, M.; Palomares, M.-L.D.; Karpouzi, V.; Pauly, D. (2018). Persisting worldwide seabird-fishery competition despite seabird community decline. *Current Biology 28 (24)*: 4009–4013.

Horn, S.; Greene, T.; Elliott, G. (2019). Eradication of mice from Antipodes Island, New Zealand. *In*: C.R. Veitch, M.N. Clout, A.R. Martin, J.C. Russel; C.J. West (Eds.), Island invasives: scaling up to meet the challenge. Occasional Paper of the IUCN Special Survival Commission No. 62 (pp. 131–137). IUCN, Gland, Switzerland.

Hunter, S.A.; Tennyson, A.J.D.; Bartle, J.A.S.; Miskelly, C.M.; Waugh, S.M.; McConnell, H.M.; Morgan, K.J.; Finlayson, S.T.; Baylis, S.M.; Chilvers, B.L.; et al. (2019). Assessing avian mortality during oil spills: a case study of the New Zealand MV 'Rena' oil spill, 2011. *Endangered Species Research 39*: 303–314.

Jaeger, A.; Lebarbenchon, C.; Bourret, V.; Bastien, M.; Lagadec, E.; Thiebot, J.-B.; Boulinier, T.; Delord, K.; Barbraud, C.; Marteau, C.; Dellagi, K.; Tortosa, P.; Weimerskirch, H. (2018). Avian cholera outbreaks threaten seabird species on Amsterdam Island. *PLoS ONE 13 (5)*: 1–17.

King, M.D.; Elliott, J.E.; Williams, T.D. (2021). Effects of petroleum exposure on birds: A review. *Science Of The Total Environment 755*: 142834.

Krüger, L.; Ramos, J.A.; Xavier, J.C.; Grémillet, D.; González-Solı́s, J.; Petry, M.V.; Phillips, R.A.; Wanless, R.M.; Paiva, V.H. (2018). Projected distributions of Southern Ocean albatrosses, petrels and fisheries as a consequence of climatic change. *Ecography 41*: 195–208.

Leighton, F.A. (1993). The toxicity of petroleum oils to birds. *Environmental Reviews 1 (2)*: 92–103.

Leotta, G.A.; Chinen, I.; Vigo, G.B.; Pecoraro, M.; Rivas, M. (2006). Outbreaks of avian cholera in Hope Bay, Antarctica. *Journal of Wildlife Diseases 42 (2)*: 259–270.

Matias, R.S.; Guı́maro, H.R.; Bustamante, P.; Seco, J.; Chipev, N.; Fragão, J.; Tavares, S.; Ceia, F.R.; Pereira, M.E.; Barbosa, A.; et al. (2022). Mercury biomagnification in an Antarctic food web of the Antarctic Peninsula. *Environmental Pollution 304*: 119–199.

Mills, W.F.; Bustamante, P.; McGill, R.A.R.; Anderson, O.R.J.; Bearhop, S.; Cherel, Y.; Votier, S.C.; Phillips, R.A. (2020). Mercury exposure in an endangered seabird: Long-term changes and relationships with trophic ecology and breeding success. *Proceedings of the Royal Society B: Biological Sciences 287 (1941)*: 20202683.

Nicholls, D.G.; Robertson, C.J.R.; Prince, P.A.; Murray, M.D.; Walker, K.J.; Elliott, G.P. (2002). Foraging niches of three *Diomedea* albatrosses. *Marine Ecology Progress Series 231*: 269–277.

Oliver, E.C.J.; Benthuysen, J.A.; Bindoff, N.L.; Hobday, A.J.; Holbrook, N.J.; Mundy, C.N.; Perkins-Kirkpatrick, S.E. (2017). The unprecedented 2015/16 Tasman Sea marine heatwave. *Nature Communications 8*: 16101.

Ostle, C.; Thompson, R.C.; Broughton, D.; Gregory, L.; Wootton, M.; Johns, D.G. (2019). The rise in ocean plastics evidenced from a 60-year time series. *Nature Communications 10*: 1622.

Pardo, D.; Forcada, J.; Wood, A.G.; Tuck, G.N.; Ireland, L.; Pradel, R.; Croxall, J.P.; Phillips, R.A. (2017). Additive effects of climate and fisheries drive ongoing declines in multiple albatross species. *Proceedings of the National Academy of Sciences of the United States of America 114 (50)*: 9 p.

Parker, G.C.; Rexer-Huber, K.; Walker, K.; Elliott, G. (2023). Antipodean wandering albatross population study 2023. https://www.doc.govt.nz/globalassets/documents/conservation/marine-and-coastal/marine-conservation-services/meetings/2023/twg-8-jun/pop2022-10-antipodes-island-antipodean-albatross-draft-report.pdf. Draft final report to the Department of Conservation. Parker Conservation, Dunedin. 20 p.

Petrossian, G.A.; Sosnowski, M.; Miller, D.; Rouzbahani, D. (2020). Flags for sale: An empirical assessment of flag of convenience desirability to foreign vessels. *Marine Policy 116*: 103937.

Phillips, R.A.; Gales, R.; Baker, G.B.; Double, M.C.; Favero, M.; Quintana, F.; Tasker, M.L.; Weimerskirchi, H.; Uhart, M.; Wolfaardt, A. (2016). The conservation status and priorities for albatrosses and large petrels. *Biological Conservation 201*: 169–183.

Pierre, J.P.; Abraham, E.R.; Richard, Y.; Cleal, J.; Middleton, D.A.J. (2012). Controlling trawler waste discharge to reduce seabird mortality. *Fisheries Research 131–133*: 30–38. https://doi.org/10.1016/j.fishres.2012.07.005

Pinaud, D.; Weimerskirch, H. (2002). Ultimate and proximate factors affecting the breeding performance of a marine top-predator. *Oikos 99*: 141–150.

Queirós, J.; Hilário, A.; Thompson, D.; Ceia, F.; Elliott, G.; Walker, K.; Cherel, Y.; Xavier, J. (2021). From warm to cold waters: new insights into the habitat and trophic ecology of Southern Ocean squids throughout their life cycle. *Marine Ecology Progress Series 659*: 113–126.

R Core Team (2021). *R: A language and environment for statistical computing*. R Foundation for Statistical Computing. Vienna, Austria. https://www.R-project.org/

Richard, Y. (2021). Integrated population model of Antipodean albatross for simulating management scenarios. BCBC2020-09 final report prepared by Dragonfly Data Science for the Conservation Services Programme, Department of Conservation, Wellington. 31 p.

Richard, Y.; Abraham, E.R. (2020). Assessment of the risk of commercial fisheries to New Zealand seabirds, 2006–07 to 2016–17. *New Zealand Aquatic Environment and Biodiversity Report No. 237*. https://mpi.govt.nz/dmsdocument/39407. 61 p.

Richard, Y.; Adasme, L. (2019). Assessment of the risk of trawl and longline fisheries to ACAP-listed seabirds in Chile. *In*: Ninth meeting of the seabird bycatch working group. florianópolis, brazil, 6–8 may 2019 (23 p). https://www.acap.aq/documents/working-groups/seabird-bycatch-working-group/seabird-bycatch-wg-meeting-9/sbwg9-information-papers/3363-sbwg9-inf-08-assessment-of-the-risk-of-trawl-and-longline-fisheries-to-acap-listed-seabirds-in-chile/file

Richard, Y.; Tremblay-Boyer, L.; Berkenbusch, K.; Wilkinson, N.; Walker, K.; Elliot, G. (2024). Assessing inter-annual variability in Antipodean albatross distribution. *Draft New Zealand Aquatic Environment and Biodiversity Report*. 24 p.

Robertson, C.J.R.; Bell, E.; Scofield, P. (2001). Autopsy report for seabirds killed and returned from New Zealand fisheries. 1 October 2000 to 30 September 2001. *DOC Science Internal Series 96*. Department of Conservation, Wellington, New Zealand.

Robertson, H.A.; Baird, K.; Elliott, G.P.; Hitchmough, R.A.; McArthur, N.; Makan, T.D.; Miskelly, C.M.; O'Donnell, C.F.J.; Sagar, P.M.; Scofield, R.P.; Taylor, G.A.; Michel, P. (2021). Conservation status of birds in Aotearoa New Zealand, 2021. *New Zealand Threat Classification Series 36*: 43 p. Department of Conservation.

Rodríguez, A.; Arcos, J.M.; Bretagnolle, V.; Dias, M.P.; Holmes, N.D.; Louzao, M.; Provencher, J.; Raine, A.F.; Ramirez, F.; Rodriguez, B.; et al. (2019). Future directions in conservation research on petrels and shearwaters. *Frontiers in Marine Science 6*: 1–27.

Rolland, V.; Weimerskirch, H.; Barbraud, C. (2010). Relative influence of fisheries and climate on the demography of four albatross species. *Global Change Biology 16*: 1910–1922.

Roman, L.; Bell, E.; Wilcox, C.; Hardesty, B.D.; Hindell, M. (2019). Ecological drivers of marine debris ingestion in Procellariiform seabirds. *Scientific Reports 9 (916).*

Roman, L.; Butcher, R.G.; Stewart, D.; Hunter, S.; Jolly, M.; Kowalski, P.; Hardesty, B.D.; Lenting, B. (2021). Plastic ingestion is an underestimated cause of death for Southern Hemisphere albatrosses. *Conservation Letters 14 (3)*: e12785.

Roman, L.; Schuyler, Q.A.; Hardesty, B.D.; Townsend, K.A. (2016). Anthropogenic debris ingestion by avifauna in eastern Australia. *PLoS ONE 11 (8)*: e0158343.

Ryan, P.G. (2015). How quickly do albatrosses and petrels digest plastic particles? *Environmental Pollution 207*: 438–440.

Selin, N.E. (2009). Global biogeochemical cycling of mercury: A review. *Annual Review of Environment and Resources 34*: 43–63.

Stan Development Team (2020). RStan: the R interface to Stan. R package version 2.19.3. http://mc-stan.org/

Stewart, F.M.; Phillips, R.A.; Bartle, J.A.; Craig, J.; Shooter, D. (1999). Influence of phylogeny, diet, moult schedule and sex on heavy metal concentrations in New Zealand Procellariiformes. *Marine Ecology Progress Series 178*: 295–305.

Tavares, S.; Xavier, J.C.; Phillips, R.A.; Pereira, M.E.; Pardal, M.A. (2013). Influence of age, sex and breeding status on mercury accumulation patterns in the wandering albatross *Diomedea exulans*. *Environmental Pollution 181*: 315–320.

Thompson, D.R.; Hamer, K.C. (2000). Stress in seabirds: Causes, consequences and diagnostic value. *Journal of Aquatic Ecosystem Stress and Recovery 7*: 91–109.

Thomson, R.B.; Alderman, R.L.; Tuck, G.N.; Hobday, A.J. (2015). Effects of climate change and fisheries bycatch on shy albatross (*Thalassarche cauta*) in Southern Australia. *PLoS One 10*: e0127006.

Uhart, M.; Vanstreels, R.E.T.; Serafini, P. (2022). Guidelines for working with albatrosses and petrels during the on-going high-pathogenicity H5N1 avian Influenza outbreak. ACAP Conservation Guideline. 4 p.

Uhart, M.M.; Gallo, L.; Quintana, F. (2018). Review of diseases (pathogen isolation, direct recovery and antibodies) in albatrosses and large petrels worldwide. *Bird Conservation International 28*: 169–196.

Ventura, F.; Stanworth, A.; Crofts, S.; Kuepfer, A.; Catry, P. (2023). Local-scale impacts of extreme events drive demographic asynchrony in neighbouring top predator populations. *Biology Letters 19 (2)*: 20220408.

Walker, K.; Elliott, G. (2022). Antipodean wandering albatross satellite tracking and population study on Antipodes Island in 2021 and 2022. https://www.doc.govt.nz/globalassets/documents/conservation/marine-and-coastal/marine-conservation-services/reports/non-csp-reports/antipodean-wandering-albatross-satellite-tracking-and-population-study-on-antipodes-island-in-2021-and-2022-final-report.pdf Report prepared for the Department of Conservation by Albatross Research

Walker, K.; Elliott, G.; Parker, G.; Rexer-Huber, K. (2023). Gibson's wandering albatross: population study and assessment of potential for drone-based whole-island census. https://www.doc.govt.nz/globalassets/documents/conservation/marine-and-coastal/marine-conservation-services/reports/202223-annual-plan/pop2022-08-gibsons-albatross-final-report.pdf Report prepared for the Department of Conservation. Conservation Services Programme POP2022-08 Auckland Islands seabird research

Weimerskirch, H. (2004). Diseases threaten southern ocean albatrosses. *Polar Biology 24*: 374–379.

Weimerskirch, H.; Louzao, M.; Grissac, S.D.; Delord, K. (2012). Changes in wind pattern alter albatross distribution and life-history traits. *Science 335 (6065)*: 211–214.

Wilcox, C.; Sebille, E.V.; Hardesty, B.D. (2015). Threat of plastic pollution to seabirds is global, pervasive, and increasing. *Proceedings of the National Academy of Sciences 112 (38)*: 11899–11904.

Wille, M.; McBurney, S.; Robertson, G.J.; Wilhelm, S.I.; Blehert, D.S.; Soos, C.; Dunphy, R.; Whitney, H. (2016). A pelagic outbreak of avian cholera in north american gulls: Scavenging as a primary mechanism for transmission? *Journal of Wildlife Diseases 52*: 793–802.

Wolfaardt, A.; Crofts, S.; Baylis, A. (2012). Effects of a storm on colonies of seabirds breeding at the Falkland Islands. *Marine Ornithology 40*: 129–133.

Wong, C. (2024). Bird-flu threat disrupts antarctic penguin studies. *Nature*. https://doi.org/https://doi.org/10.1038/d41586-024-00807-0

Xavier, J.C.; Walker, K.; Elliott, G.; Cherel, Y.; Thompson, D. (2014). Cephalopod fauna of South Pacific waters: new information from breeding New Zealand wandering albatrosses. *Marine Ecology Progress Series 513*: 131–142.

Yamashita, R.; Hiki, N.; Kashiwada, F.; Takada, H.; Mizukawa, K.; Hardesty, B.D.; Roman, L.; Hyrenbach, D.; Ryan, P.G.; Dilley, B.; et al. (2021). Plastic additives and legacy persistent organic pollutants in the preen gland oil of seabirds sampled across the globe. *Environmental Monitoring and Contaminants Research 1*: 97–112.

APPENDIX A: STAN MODELS

A.1 Model of population dynamics of Antipodean albatross

```
functions {

  row_vector trans_probs1(int instate, int nstates, real s_ad, real s_ado, real s_juv,
                                          real p_mv_out, real p_mv_in, int succ, array[] real p_breed,
                                          real p_rec, real p_bead, real p_succ) {
    /** TRANSITIONS and SURVIVAL **/

    // 1: adults breeding inside SA
    // 2: adults breeding outside SA
    // 3: adults non-breeding inside SA
    // 4: adults non-breeding outside SA
    // 5: ados inside SA
    // 6: ados outside SA
    // 7: juvs inside SA
    // 8: juvs outside SA
    // 9: deads
        row_vector[nstates] tmat1;

        if (instate == 1) { //* ADULTS PREVIOUSLY BREEDING WITHIN STUDY AREA *//
          // re-breeding in SA (SA = study area)
          tmat1[1] = succ == 2 ?
                0 :
                (succ == 1 ?
                 p_breed[1] * s_ad * (1-p_mv_out) :
                 (1-p_succ) * p_breed[1] * s_ad * (1-p_mv_out));
          // re-breeding outside SA
          tmat1[2] = succ == 2 ?
                0 :
                (succ == 1 ?
                 p_breed[1] * s_ad *    p_mv_out  :
                 (1-p_succ) * p_breed[1] * s_ad *    p_mv_out);
          // non-breeding in SA
          tmat1[3] = succ == 2 ?
                s_ad * (1-p_mv_out) :
                (succ == 1 ?
                 (1-p_breed[1]) * s_ad * (1-p_mv_out) :
                 (1-p_succ) * (1-p_breed[1]) * s_ad * (1-p_mv_out) +
                 p_succ * s_ad * (1-p_mv_out));
          // non-breeding outside SA
          tmat1[4] = succ == 2 ?
                s_ad * p_mv_out :
                (succ == 1 ?
                 (1-p_breed[1]) * s_ad * p_mv_out :
                 (1-p_succ) * (1-p_breed[1]) * s_ad * p_mv_out +
                 p_succ * s_ad * p_mv_out);
          // ados inside SA
          tmat1[5] = 0;
          // ados outside SA
          tmat1[6] = 0;
          // juvs inside SA
          tmat1[7] = 0;
          // juvs outside SA
          tmat1[8] = 0;
          // dead
          tmat1[9] = 1-s_ad;

        } else if (instate == 2) { //* ADULTS PREVIOUSLY BREEDING OUTSIDE STUDY AREA *//
          // re-breeding in SA (SA = study area)
          tmat1[1] = succ == 2 ?
                0 :
                (succ == 1 ?
                 p_breed[1] * s_ad * p_mv_in :
                 (1-p_succ) * p_breed[1] * s_ad * p_mv_in);
          // re-breeding outside SA
          tmat1[2] = succ == 2 ?
                0 :
                (succ == 1 ?
                 p_breed[1] * s_ad * (1-p_mv_in) :
                 (1-p_succ) * p_breed[1] * s_ad * (1-p_mv_in));
          // non-breeding in SA
          tmat1[3] = succ == 2 ?
                s_ad * p_mv_in :
                (succ == 1 ?
                 (1-p_breed[1]) * s_ad * p_mv_in :
                 (1-p_succ) * (1-p_breed[1]) * s_ad * p_mv_in  +  p_succ * s_ad * p_mv_in);
          // non-breeding outside SA
          tmat1[4] = succ == 2 ?
                s_ad * (1-p_mv_in) :
                (succ == 1 ?
                 (1-p_breed[1]) * s_ad * (1-p_mv_in) :
                 (1-p_succ) * (1-p_breed[1]) * s_ad * (1-p_mv_in)  +  p_succ * s_ad * (1-p_mv_in));
          // ados inside SA
          tmat1[5] = 0;
          // ados outside SA
          tmat1[6] = 0;
          // juvs
          tmat1[7] = 0;
          // juvs outside SA
          tmat1[8] = 0;
          // dead
          tmat1[9] = 1-s_ad;

        } else if (instate == 3) { //* ADULTS PREVIOUSLY NOT BREEDING WITHIN STUDY AREA *//
          // breeding in SA (SA = study area)
          tmat1[1] =    p_breed[2]  * s_ad * (1-p_mv_out);
          // breeding outside SA
          tmat1[2] =    p_breed[2]  * s_ad *    p_mv_out;
          // non-breeding in SA
          tmat1[3] = (1-p_breed[2]) * s_ad * (1-p_mv_out);
          // non-breeding outside SA
          tmat1[4] = (1-p_breed[2]) * s_ad *    p_mv_out;
          // ados inside SA
          tmat1[5] = 0;
          // ados outside SA
          tmat1[6] = 0;
          // juvs inside SA
          tmat1[7] = 0;
          // juvs outside SA
          tmat1[8] = 0;
          // dead
          tmat1[9] = 1-s_ad;

        } else if (instate == 4) { //* ADULTS PREVIOUSLY NOT BREEDING OUTSIDE THE STUDY AREA *//
          // breeding in SA (SA = study area)
          tmat1[1] =    p_breed[2]  * s_ad *    p_mv_in;
          // breeding outside SA
          tmat1[2] =    p_breed[2]  * s_ad * (1-p_mv_in);
          // non-breeding in SA
          tmat1[3] = (1-p_breed[2]) * s_ad *    p_mv_in;
          // non-breeding outside SA
          tmat1[4] = (1-p_breed[2]) * s_ad * (1-p_mv_in);
          // ados inside SA
          tmat1[5] = 0;
          // ados outside SA
          tmat1[6] = 0;
          // juvs inside SA
          tmat1[7] = 0;
          // juvs outside SA
          tmat1[8] = 0;
          // dead
          tmat1[9] = 1-s_ad;

        } else if (instate == 5) { //* ADOLESCENTS INSIDE THE STUDY AREA *//
          // breeding in SA (SA = study area)
          tmat1[1] = s_ado * p_bead * (1-p_mv_out);
          // breeding outside SA
          tmat1[2] = s_ado * p_bead *    p_mv_out;
          // non-breeding in SA
          tmat1[3] = 0;
          // non-breeding outside SA
          tmat1[4] = 0;
          // ados inside SA
          tmat1[5] = s_ado * (1-p_bead) * (1-p_mv_out);
          // ados outside SA
          tmat1[6] = s_ado * (1-p_bead) *    p_mv_out;
          // juvs inside SA
          tmat1[7] = 0;
          // juvs outside SA
          tmat1[8] = 0;
          // dead
          tmat1[9] = 1-s_ado;

        } else if (instate == 6) { //* ADOLESCENTS OUTSIDE THE STUDY AREA *//
          // breeding in SA (SA = study area)
          tmat1[1] = s_ado * p_bead *    p_mv_in;
          // breeding outside SA
          tmat1[2] = s_ado * p_bead * (1-p_mv_in);
          // non-breeding in SA
          tmat1[3] = 0;
          // non-breeding outside SA
          tmat1[4] = 0;
          // ados inside SA
          tmat1[5] = s_ado * (1-p_bead) *    p_mv_in;
          // ados outside SA
          tmat1[6] = s_ado * (1-p_bead) * (1-p_mv_in);
          // juvs inside SA
          tmat1[7] = 0;
          // juvs outside SA
          tmat1[8] = 0;
          // dead
          tmat1[9] = 1-s_ado;

        } else if (instate == 7) { //* JUVENILES INSIDE SA *//
          // breeding in SA (SA = study area)
          tmat1[1] = 0;
          // breeding outside SA
          tmat1[2] = 0;
          // non-breeding in SA
          tmat1[3] = 0;
          // non-breeding outside SA
          tmat1[4] = 0;
          // ados inside SA
          tmat1[5] = s_juv * p_rec * (1-p_mv_out);
          // ados outside SA
          tmat1[6] = s_juv * p_rec *    p_mv_out;
          // juvs inside SA
          tmat1[7] = s_juv * (1-p_rec);
          // juvs outside SA
          tmat1[8] = 0;
          // dead
          tmat1[9] = 1-s_juv;

        } else if (instate == 8) { //* JUVENILES OUTSIDE SA *//
          // breeding in SA (SA = study area)
          tmat1[1] = 0;
        // breeding outside SA
        tmat1[2] = 0;
        // non-breeding in SA
        tmat1[3] = 0;
        // non-breeding outside SA
        tmat1[4] = 0;
        // ados inside SA
        tmat1[5] = s_juv * p_rec * p_mv_in;
        // ados outside SA
        tmat1[6] = s_juv * p_rec * (1-p_mv_in);
        // juvs inside SA
        tmat1[7] = 0;
        // juvs outside SA
        tmat1[8] = s_juv * (1-p_rec);
        // dead
        tmat1[9] = 1-s_juv;

      } else if (instate == 9) { //* DEADS *//
        // breeding in SA (SA = study area)
        tmat1[1] = 0;
        // breeding outside SA
        tmat1[2] = 0;
        // non-breeding in SA
        tmat1[3] = 0;
        // non-breeding outside SA
        tmat1[4] = 0;
        // ados inside SA
        tmat1[5] = 0;
        // ados outside SA
        tmat1[6] = 0;
        // juvs inside SA
        tmat1[7] = 0;
        // juvs outside SA
        tmat1[8] = 0;
        // dead
        tmat1[9] = 1;

      }
      return tmat1;
  }


  row_vector obs_probs1(int latstate, int n_obs_states, array[] real p_obs, real p_detect_juv, real p_detect_dead,
                                      real p_female, real p_succ, int succ, int no_visit) {

      /** OBSERVED STATES **/

      // 1: adults breeding in SA
      // 2: adults non-breeding in SA
      // 3: adults outside SA
      // 4: ados inside SA
      // 5: ados outside SA
      // 6: juvs inside SA
      // 7: juvs outside SA
      // 8: dead
      // 9: not seen

    row_vector[n_obs_states] pmat1;
    real withvisit;

      if (no_visit == 1) {
        withvisit = 0;
      } else withvisit = 1;

      if (latstate == 1) { //* ADULTS BREEDING WITHIN STUDY AREA *//
        // ad breeding in SA (SA = study area)
        pmat1[1] = withvisit * p_obs[1];
        // ad non-breeding in SA
        pmat1[2] = 0;
        // ad outside SA
        pmat1[3] = 0;
        // ados inside SA
        pmat1[4] = 0;
        // ados outside SA
        pmat1[5] = 0;
        // juvs inside SA
        pmat1[6] = 0;
        // juvs outside SA
        pmat1[7] = 0;
        // dead
        pmat1[8] = 0;
        // not seen
        pmat1[9] = 1 - pmat1[1];

      } else if (latstate == 2) { //* ADULTS BREEDING OUTSIDE STUDY AREA *//
        // ad breeding in SA (SA = study area)
        pmat1[1] = 0;
        // ad non-breeding in SA
        pmat1[2] = 0;
        // ad outside SA
        pmat1[3] = withvisit * p_obs[5];
        // ados inside SA
        pmat1[4] = 0;
        // ados outside SA
        pmat1[5] = 0;
        // juvs inside SA
        pmat1[6] = 0;
        // juvs outside SA
        pmat1[7] = 0;
        // dead
```

```
          pmat1[8] = 0;
          // not seen
          pmat1[9] = 1 - pmat1[3];

        } else if (latstate == 3) { //* ADULTS NON-BREEDING INSIDE STUDY AREA *//
          // ad breeding in SA (SA = study area)
          pmat1[1] = 0;
          // ad non-breeding in SA
          pmat1[2] = no_visit == 1 ?
                0 :
                (succ == 2 ?
                 p_obs[2] :
                 (succ == 1 ?
                  p_obs[3] :
                  p_succ * p_obs[2] + (1-p_succ) * p_obs[3]));
          // ad outside SA
          pmat1[3] = 0;
          // ados inside SA
          pmat1[4] = 0;
          // ados outside SA
          pmat1[5] = 0;
          // juvs inside SA
          pmat1[6] = 0;
          // juvs outside SA
          pmat1[7] = 0;
          // dead
          pmat1[8] = 0;
          // not seen
          pmat1[9] = 1 - pmat1[2];

        } else if (latstate == 4) { //* ADULTS NON-BREEDING OUTSIDE STUDY AREA *//
          // ad breeding in SA (SA = study area)
          pmat1[1] = 0;
          // ad non-breeding in SA
          pmat1[2] = 0;
          // ad outside SA
          pmat1[3] = withvisit * p_obs[5];
          // ados inside SA
          pmat1[4] = 0;
          // ados outside SA
          pmat1[5] = 0;
          // juvs inside SA
          pmat1[6] = 0;
          // juvs outside SA
          pmat1[7] = 0;
          // dead
          pmat1[8] = 0;
          // not seen
          pmat1[9] = 1 - pmat1[3];

        } else if (latstate == 5) { //* ADOS INSIDE STUDY AREA *//
          // ad breeding in SA (SA = study area)
          pmat1[1] = 0;
          // ad non-breeding in SA
          pmat1[2] = 0;
          // ad outside SA
          pmat1[3] = 0;
          // ados inside SA
          pmat1[4] = withvisit * p_obs[4];
          // ados outside SA
          pmat1[5] = 0;
          // juvs inside SA
          pmat1[6] = 0;
          // juvs outside SA
          pmat1[7] = 0;
          // dead
          pmat1[8] = 0;
          // not seen
          pmat1[9] = 1 - pmat1[4];

        } else if (latstate == 6) { //* ADOS OUTSIDE STUDY AREA *//
          // ad breeding in SA (SA = study area)
          pmat1[1] = 0;
          // ad non-breeding in SA
          pmat1[2] = 0;
          // ad outside SA
          pmat1[3] = 0;
          // ados inside SA
          pmat1[4] = 0;
          // ados outside SA
          pmat1[5] = withvisit * p_obs[5];
          // juvs inside SA
          pmat1[6] = 0;
          // juvs outside SA
          pmat1[7] = 0;
          // dead
          pmat1[8] = 0;
          // not seen
          pmat1[9] = 1 - pmat1[5];

        } else if (latstate == 7) { //* JUVENILES INSIDE SA *//
          // ad breeding in SA (SA = study area)
          pmat1[1] = 0;
          // ad non-breeding in SA
          pmat1[2] = 0;
          // ad outside SA
          pmat1[3] = 0;
          // ados inside SA
          pmat1[4] = 0;
          // ados outside SA
        pmat1[5] = 0;
        // juvs inside SA
        pmat1[6] = withvisit * p_detect_juv;
        // juvs outside SA
        pmat1[7] = 0;
        // dead
        pmat1[8] = 0;
        // not seen
        pmat1[9] = 1 - pmat1[6];

      } else if (latstate == 8) { //* JUVENILES OUTSIDE SA *//
        // ad breeding in SA (SA = study area)
        pmat1[1] = 0;
        // ad non-breeding in SA
        pmat1[2] = 0;
        // ad outside SA
        pmat1[3] = 0;
        // ados inside SA
        pmat1[4] = 0;
        // ados outside SA
        pmat1[5] = 0;
        // juvs inside SA
        pmat1[6] = 0;
        // juvs outside SA
        pmat1[7] = withvisit * p_detect_juv;
        // dead
        pmat1[8] = 0;
        // not seen
        pmat1[9] = 1 - pmat1[7];

      } else if (latstate == 9) { //* DEADS *//
        // ad breeding in SA (SA = study area)
        pmat1[1] = 0;
        // ad non-breeding in SA
        pmat1[2] = 0;
        // ad outside SA
        pmat1[3] = 0;
        // ados inside SA
        pmat1[4] = 0;
        // ados outside SA
        pmat1[5] = 0;
        // juvs inside SA
        pmat1[6] = 0;
        // juvs outside SA
        pmat1[7] = 0;
        // dead
        pmat1[8] = withvisit * p_detect_dead;
        // not seen
        pmat1[9] = 1 - pmat1[8];

      }
      return pmat1;
}


matrix trans_probs(int nstates, real s_ad, real s_ado, real s_juv,
                                       real p_mv_out, real p_mv_in, int succ, array[] real p_breed,
                                       real p_rec, real p_bead, real p_succ) {

  matrix[nstates, nstates] tmat;
      for (i in 1:nstates) {
        tmat[i,] = trans_probs1(i, nstates, s_ad, s_ado, s_juv,
                                                        p_mv_out, p_mv_in, succ, p_breed,
                                                        p_rec, p_bead, p_succ);
      }
      return tmat;
}


matrix obs_probs(int n_lat_states, int n_obs_states, array[] real p_obs, real p_detect_juv, real p_detect_dead,
                                 real p_female, real p_succ, int succ, int no_visit) {

  matrix[n_lat_states, n_obs_states] pmat;

      for (i in 1:n_lat_states) {
        pmat[i,] = obs_probs1(i, n_obs_states, p_obs, p_detect_juv, p_detect_dead,
                                                      p_female, p_succ, succ, no_visit);
      }
  return pmat;
}


real log_sum_one_indiv (int N_STATES_L, int N_STATES_O, int sex, array[] int age, int MAX_T, int first_cap, int last_cap,
                                                array[] int c_hist, array[,] real s_ad, array[] real s_ado, array[] real s_juv, array[] real p_moveout,
                                                array[] real p_movein, array[] int b_success, array[,] real p_breeding,
                                                real age_rec_alpha, real age_rec_beta, real age_br_alpha, real age_br_beta,
                                                array[] real p_success, array[,] real p_obs,
                                                real p_detect_juv, real p_detect_dead, real p_female, array[] int NO_VISIT,
                                                int first_state, int ind) {

  matrix[N_STATES_L, N_STATES_L] tmat;
  matrix[N_STATES_L, N_STATES_O] pmat;
  array[MAX_T, N_STATES_L] real pz;
  array[N_STATES_L] real temp;
  real lsum;
      real p_rec;
      real p_bead;

  for (j in 1:N_STATES_L) {
      pz[first_cap, j] = (j == first_state);
    }
    for (t in (first_cap+1):last_cap) {
          p_rec  = fmin(1, fmax(0, (1 - age_rec_alpha) / (age_rec_beta - age_rec_alpha) + age[t] / (age_rec_beta - age_rec_alpha)));
          p_bead = fmin(1, fmax(0, (1 - age_br_alpha)  / (age_br_beta  - age_br_alpha)  + age[t] / (age_br_beta  - age_br_alpha)));
      tmat = trans_probs(N_STATES_L, s_ad[sex+1, t-1], s_ado[t-1], s_juv[t-1],
                                                 p_moveout[sex+1], p_movein[sex+1], b_success[t-1],
                                                 p_breeding[,t], p_rec, p_bead,
                                                 p_success[t-1]);
      pmat = obs_probs(N_STATES_L, N_STATES_O, p_obs[t-1], p_detect_juv, p_detect_dead, p_female,
                                           p_success[t-1], b_success[t-1], NO_VISIT[t]);
      for (i in 1:N_STATES_L) {
                for (j in 1:N_STATES_L) {
                  temp[j] = pz[t-1, j] * tmat[j, i] * pmat[i, c_hist[t]];
                }
                pz[t, i] = sum(temp);
      }
    }
        lsum = log(sum(pz[last_cap]));
        return lsum;
  }


  real calc_log_sum_multi (array[] int INDS, int start, int end, int N_STATES_L, int N_STATES_O, array[] int SEX,
                                                   array[,] int AGE, int MAX_T, array[] int FIRST_CAP, array[] int LAST_CAP, array[,] int C_HIST,
                                                   array[,] real s_ad, array[] real s_ado, array[] real s_juv,
                                                   array[] real p_moveout, array[] real p_movein, array[,] int B_SUCCESS, array[,] real p_breeding,
                                                   real age_rec_alpha, real age_rec_beta, real age_br_alpha, real age_br_beta,
                                                   array[] real p_success, array[,] real p_obs,
                                                   real p_detect_juv, real p_detect_dead, real p_female,
                                                   array[] int NO_VISIT, array[] int FIRST_STATE) {
        real lsum;
        lsum = 0.0;
        for (ind in start:end) {
          lsum += log_sum_one_indiv(N_STATES_L, N_STATES_O, SEX[ind], AGE[ind], MAX_T, FIRST_CAP[ind], LAST_CAP[ind], C_HIST[ind],
                                                                s_ad, s_ado, s_juv, p_moveout, p_movein,
                                                                B_SUCCESS[ind], p_breeding,
                                                                age_rec_alpha, age_rec_beta, age_br_alpha, age_br_beta,
                                                                p_success, p_obs, p_detect_juv, p_detect_dead, p_female,
                                                                NO_VISIT, FIRST_STATE[ind], ind);
        }
        return lsum;
  }
}


data{

  int<lower=1> N_INDS;
  array[N_INDS] int<lower=1> INDS;
  array[N_INDS] int<lower=1> FIRST_STATE;

  array[N_INDS] int<lower=0, upper=2> SEX;
  int<lower=1> N_SEXED;
  array[N_SEXED] int<lower=0, upper=1> IS_FEMALE;

  int<lower=1> N_NESTS;
  array[N_NESTS] int<lower=0, upper=1> NEST_SUCCESS;
  array[N_NESTS] int<lower=1> NEST_YEAR;

  array[N_INDS] int<lower=1> FIRST_CAP;
  array[N_INDS] int<lower=1> LAST_CAP;

  int<lower=1> MAX_T;
  int<lower=1> MAX_AGE;
  array[N_INDS, MAX_T] int<lower=1> AGE;

  array[MAX_T] int<lower=0, upper=1> NO_VISIT;

  int<lower=1> N_STATES_L;
  int<lower=1> N_STATES_O;
  int<lower=1> N_PDETECTS;
  array[N_INDS, MAX_T] int<lower=1, upper=N_STATES_O> C_HIST;

  array[N_INDS, MAX_T] int<lower=0, upper=2> B_SUCCESS;

  array[MAX_T] int<lower=0, upper=1> IS_LATE_YEAR;

}


transformed data {
  int<lower=1> grainsize=1;
}


parameters{

  real<lower=0, upper=1> p_female;

  array[2] real<lower=0, upper=1> pbreed_lg_mean; // 1: previously unsuccessful breeders; 2: other non-breeders
  array[MAX_T] real pbreed_lg_re;
  real<lower=0> sigma_re_pbreed;

  real bsucc_lg_mean;
  array[MAX_T] real bsucc_lg_re;
  real<lower=0> sigma_re_bsucc;

  /* Random effect on adult survival */
  array[2] real surv_ad_lg_mean;
  array[2, MAX_T-1] real surv_ad_lg_re;
  real<lower=0> sigma_re_ad_s;

  /* Random effect on adult survival */
  real surv_juv_lg_mean;
  real surv_ado_lg_mean;
  array[MAX_T-1] real surv_juvado_lg_re;
  real<lower=0> sigma_re_juvado_s;

  /* Random effect on detectability */
  real<lower=0> sigma_re_p;
  array[MAX_T-1] real p_detect_lg_re;
  array[N_PDETECTS] real p_detect_lg_mean;
  real<lower=0, upper=1> p_detect_juv;
  real<lower=0, upper=1> p_detect_dead;

  array[2] real<lower=0, upper=1> p_leave;
  array[2] real<lower=0, upper=1> p_back;

  real<lower=1> age_rec_alpha;
  real<lower=age_rec_alpha+1> age_rec_beta;
  real<lower=1> age_br_alpha;
  real<lower=age_br_alpha+1> age_br_beta;

  real beta_detect_late_year;
}


transformed parameters{

  array[2, MAX_T-1] real<lower=0, upper=1> s_adult;
  array[3, MAX_T-1] real<lower=0, upper=1> s_ad;
  array[MAX_T-1] real<lower=0, upper=1> s_juv;
  array[MAX_T-1] real<lower=0, upper=1> s_ado;

  array[N_PDETECTS, MAX_T-1] real<lower=0, upper=1> p_detect; // 1: breeding ad (inside sa); 2: non-breeding ad previously successful (inside sa); 3: other non-breeders (inside sa); 4: ado inside SA; 5: ad or ado outside SA

  array[2, MAX_T] real<lower=0, upper=1> p_breeding;
  array[MAX_T] real<lower=0, upper=1> p_success;

  array[3] real<lower=0, upper=1> p_moveout;
  array[3] real<lower=0, upper=1> p_movein;

  array[MAX_T-1, N_PDETECTS] real<lower=0, upper=1> p_obs;

  for (t in 1:(MAX_T-1)) {
    for (s in 1:N_PDETECTS) { // t=1 here means year 2!
          if (s == 4) {
                p_detect[s, t] = inv_logit(p_detect_lg_mean[s] + p_detect_lg_re[t] * sigma_re_p + IS_LATE_YEAR[t+1] * beta_detect_late_year);
          } else {
                p_detect[s, t] = inv_logit(p_detect_lg_mean[s] + p_detect_lg_re[t] * sigma_re_p);
          }
    }
    for (sex in 1:2) {        // t=1 here means year 1!
          s_adult[sex, t]  = inv_logit(surv_ad_lg_mean[sex] + surv_ad_lg_re[sex, t] * sigma_re_ad_s);
    }
        s_juv[t]  = inv_logit(surv_juv_lg_mean + surv_juvado_lg_re[t] * sigma_re_juvado_s);
        s_ado[t]  = inv_logit(surv_ado_lg_mean + surv_juvado_lg_re[t] * sigma_re_juvado_s);
  }

  for (t in 1:MAX_T) {
    p_breeding[1, t] = inv_logit(pbreed_lg_mean[1] + pbreed_lg_re[t] * sigma_re_pbreed);
    p_breeding[2, t] = inv_logit(pbreed_lg_mean[2] + pbreed_lg_re[t] * sigma_re_pbreed);
    p_success[t] = inv_logit(bsucc_lg_mean + bsucc_lg_re[t] * sigma_re_bsucc);
  }

  for (sex in 0:2) {
    p_moveout[sex+1] = sex != 0 ? p_leave[sex] : p_female * p_leave[1] + (1-p_female) * p_leave[2];
    p_movein[sex+1]  = sex != 0 ? p_back[sex]  : p_female * p_back[1]  + (1-p_female) * p_back[2];
    for (t in 1:(MAX_T-1)) {
      s_ad[sex+1, t] = sex != 0 ? s_adult[sex, t] : p_female * s_adult[1, t] + (1-p_female) * s_adult[2, t];
    }
  }

  for (s in 1:N_PDETECTS) {
    for (t in 1:(MAX_T-1)) {
          p_obs[t, s] = p_detect[s, t];
    }
  }

}


model{

  matrix[N_STATES_L, N_STATES_L] tmat;
  matrix[N_STATES_O, N_STATES_O] pmat;

  array[N_STATES_L] real temp;

  p_female  ~ beta(1, 1);
  IS_FEMALE ~ bernoulli(p_female);

  /* Probability of adult to breed (1: failed breeders; 2: non-breeders) */
  pbreed_lg_mean ~ normal(0, 2);
  pbreed_lg_re   ~ normal(0, 1);
  sigma_re_pbreed ~ cauchy(0, 2);

  /* Adult survival */
  for (sex in 1:2) {
    surv_ad_lg_mean[sex] ~ normal(0, 5);
    for (t in 1:(MAX_T-1)) {
      surv_ad_lg_re[sex, t] ~ normal(0, 5); // Time effect varies by sex
    }
  }
  sigma_re_ad_s ~ cauchy(0, 2);

  /* Juv + ado survival */
  surv_juv_lg_mean ~ normal(0, 5);
  surv_ado_lg_mean ~ normal(0, 5);
  for (t in 1:(MAX_T-1)) {
        surv_juvado_lg_re[t] ~ normal(0, 5); // Time effect varies by sex
  }
  sigma_re_juvado_s ~ cauchy(0, 2);

  /* P(successful breeding) */
  for (n in 1:N_NESTS) {
    NEST_SUCCESS[n] ~ bernoulli(p_success[NEST_YEAR[n]]);
  }
  bsucc_lg_mean ~ normal(0, 2);
  bsucc_lg_re   ~ normal(0, 1);
  sigma_re_bsucc ~ cauchy(0, 2);

  /* P(leaving/returning the study area) */
  p_leave ~ beta(1, 1);
  p_back  ~ beta(1, 1);

  /* Detectability */
  for (s in 1:N_PDETECTS) {
    p_detect_lg_mean[s] ~ normal(0, 5);
  }
  p_detect_juv ~ beta(1, 10);
  p_detect_dead ~ beta(1, 10);

  beta_detect_late_year ~ normal(0, 5);

  // Same time effect for all classes and sexes (reflects changes in surveys)
  for (t in 1:(MAX_T-1)) {
    p_detect_lg_re[t] ~ normal(0, 5);
  }
  sigma_re_p ~ cauchy(0, 2);

  /* Age at first return and first breeding */
  age_rec_alpha ~ gamma(3, 1);
  age_rec_beta ~ gamma(10, 1);
  age_br_alpha ~ gamma(10, 1);
  age_br_beta ~ gamma(20, 1);

  /* Likelihood */
  target += reduce_sum(calc_log_sum_multi, INDS, grainsize, N_STATES_L, N_STATES_O, SEX, AGE, MAX_T,
                                           FIRST_CAP, LAST_CAP, C_HIST,
                                           s_ad, s_ado, s_juv, p_moveout, p_movein,
                                           B_SUCCESS, p_breeding,
                                           age_rec_alpha, age_rec_beta, age_br_alpha, age_br_beta,
                                           p_success,
                                           p_obs, p_detect_juv, p_detect_dead, p_female,
                                           NO_VISIT, FIRST_STATE);

}
```

A.2 Estimation of captures in New Zealand fisheries

```
data {
  int<lower=1>  N_ROW_O; /* rows in dataset of observed fishing effort */
  int<lower=1>  N_ROW_T; /* rows in dataset of total fishing effort */
  int<lower=1> N_SPECIES; /* number of species considered */
  vector<lower=0> [N_SPECIES] OVERLAP_O [N_ROW_O]; /* observed overlap */
  vector<lower=0> [N_SPECIES] OVERLAP_T [N_ROW_T]; /* total overlap */
  int<lower=0>  CAPTURES [N_ROW_O]; /* number of observed captures */
  int<lower=0>  SPECIES_I [N_ROW_O]; /* index of species captured */
  int<lower=1> N_FISHERY_GROUPS; /* number of fishery groups */
  int<lower=1>  FISHERY_GROUP_O [N_ROW_O]; /* fishery group of dataset of observed effort */
  int<lower=1>  FISHERY_GROUP_T [N_ROW_T]; /* fishery group of dataset of total effort */
}

parameters{
  vector<lower=0> [N_SPECIES] vulnerability [N_FISHERY_GROUPS]; /* vulnerability parameters */
  real<lower=0, upper=1> p_unident; /* probability that a capture is identified at the species level */
}

transformed parameters{ /* mean number of captures by species and fishery group */
  vector<lower=0> [N_ROW_O] poisson_mean;
  for (i in 1:N_ROW_O) {
    if (SPECIES_I[i] > 0) {
      poisson_mean[i] = (1 - p_unident) * vulnerability[FISHERY_GROUP_O[i]][SPECIES_I[i]] * OVERLAP_O[i][SPECIES_I[i]];
    } else {
      poisson_mean[i] =  p_unident * sum(vulnerability[FISHERY_GROUP_O[i]] .* OVERLAP_O[i]);
    }
  }
}

model{ /* priors */
  p_unident ~ beta(1, 1);
  CAPTURES ~ poisson(poisson_mean);
}

generated quantities{ /* predicted captures */
  matrix<lower=0> [N_ROW_T, N_SPECIES] ecapts_i; /* identified */
  matrix<lower=0> [N_ROW_T, N_SPECIES] ecapts_u; /* unidentified */
  matrix<lower=0> [N_ROW_T, N_SPECIES] ecapts_t; /* total: identified + unidentified */
  for (i in 1:N_ROW_T) {
    for (s in 1:N_SPECIES) {
      if (OVERLAP_T[i][s] > 0) {
        ecapts_i[i,s] = poisson_rng((1 - p_unident) * vulnerability[FISHERY_GROUP_T[i]][s] * OVERLAP_T[i][s]);
        ecapts_u[i,s] = poisson_rng(     p_unident  * vulnerability[FISHERY_GROUP_T[i]][s] * OVERLAP_T[i][s]);
        ecapts_t[i,s] = poisson_rng(                  vulnerability[FISHERY_GROUP_T[i]][s] * OVERLAP_T[i][s]);
      } else {
        ecapts_i[i,s] = 0;
        ecapts_u[i,s] = 0;
        ecapts_t[i,s] = 0;
      }
    }
  }
}
```

APPENDIX B: POPULATION MODEL DIAGNOSTICS

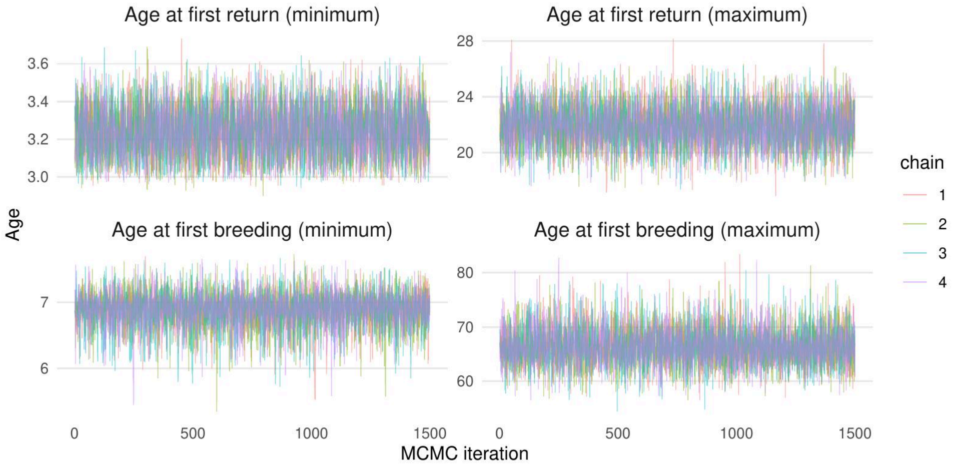

Figure B-1: Markov chain Monte Carlo traces for the age at first return to the colony and the age at first breeding parameters of Antipodean albatross.

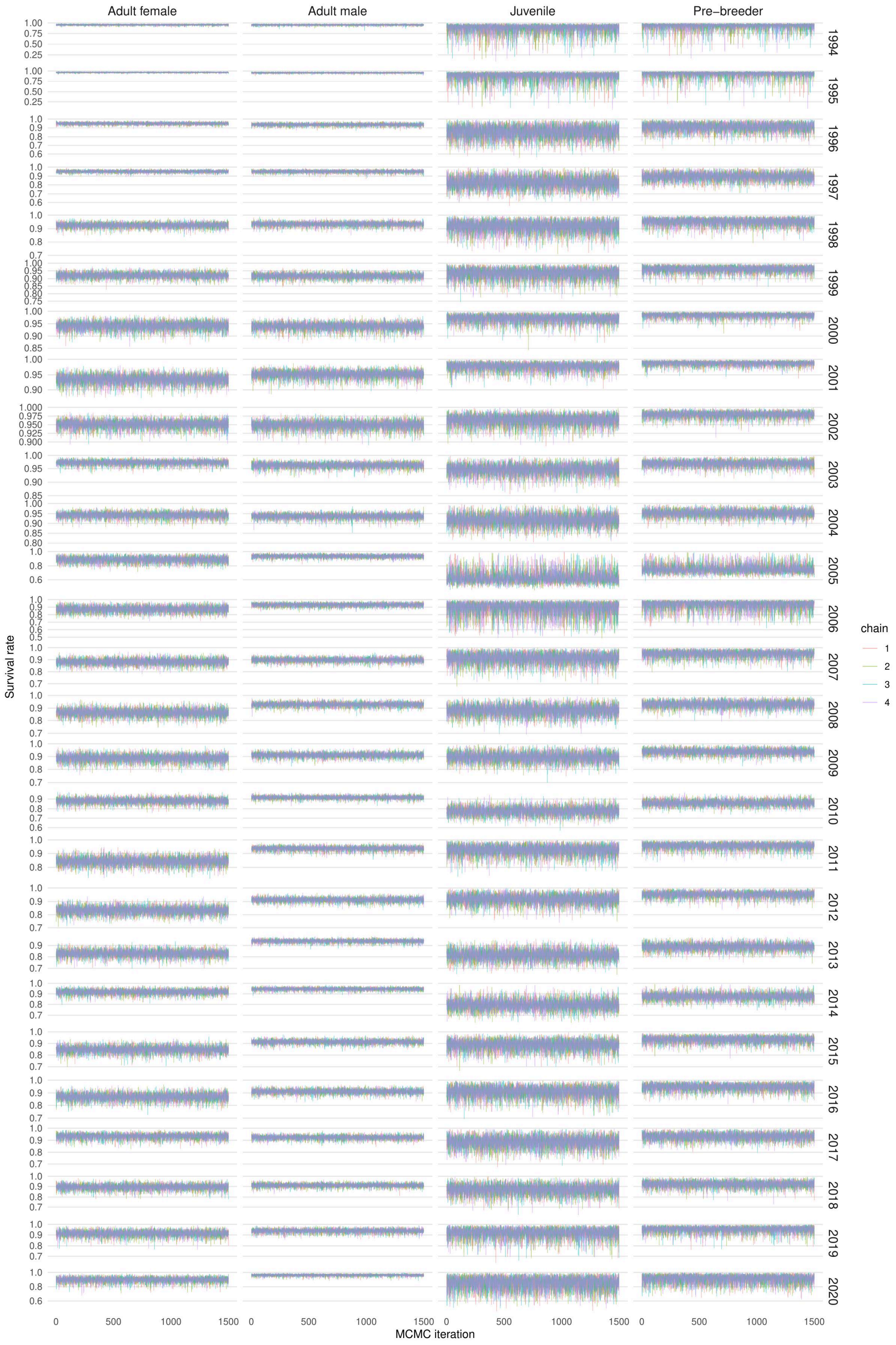

Figure B-2: Markov chain Monte Carlo traces for the annual survival parameters of Antipodean albatross, by population class and by year.

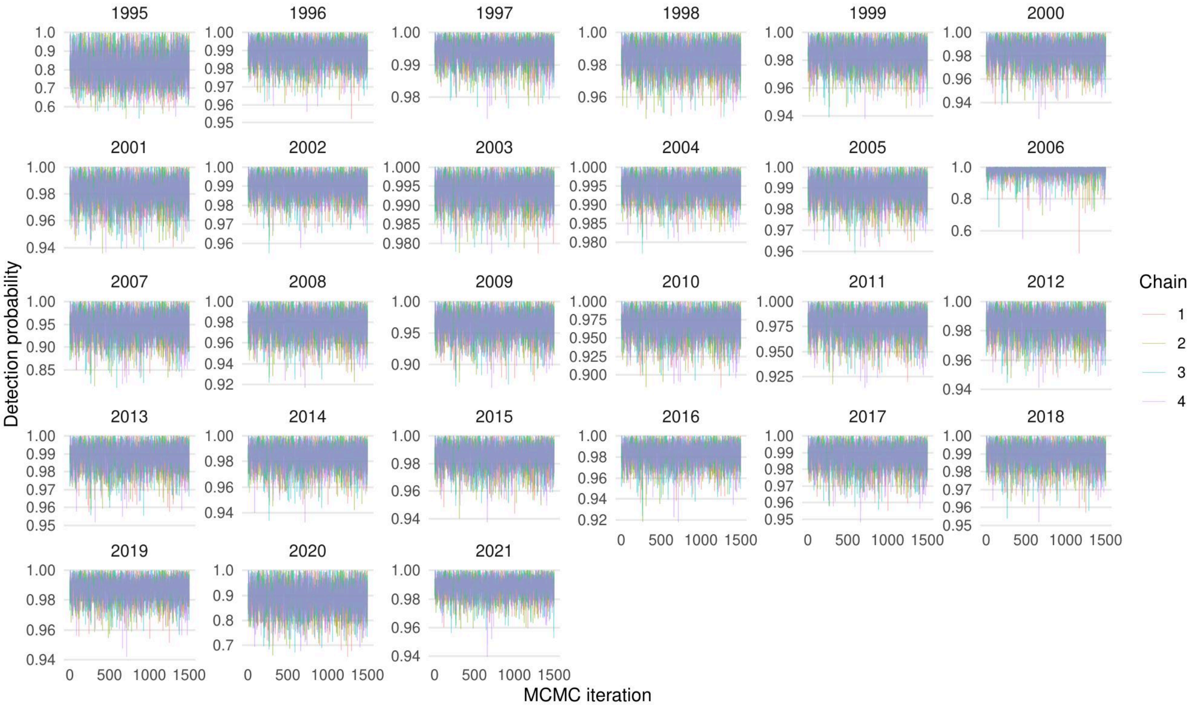

Figure B-3: Markov chain Monte Carlo traces for the detection probability of breeding adults of Antipodean albatross by year, as estimated by the population model.

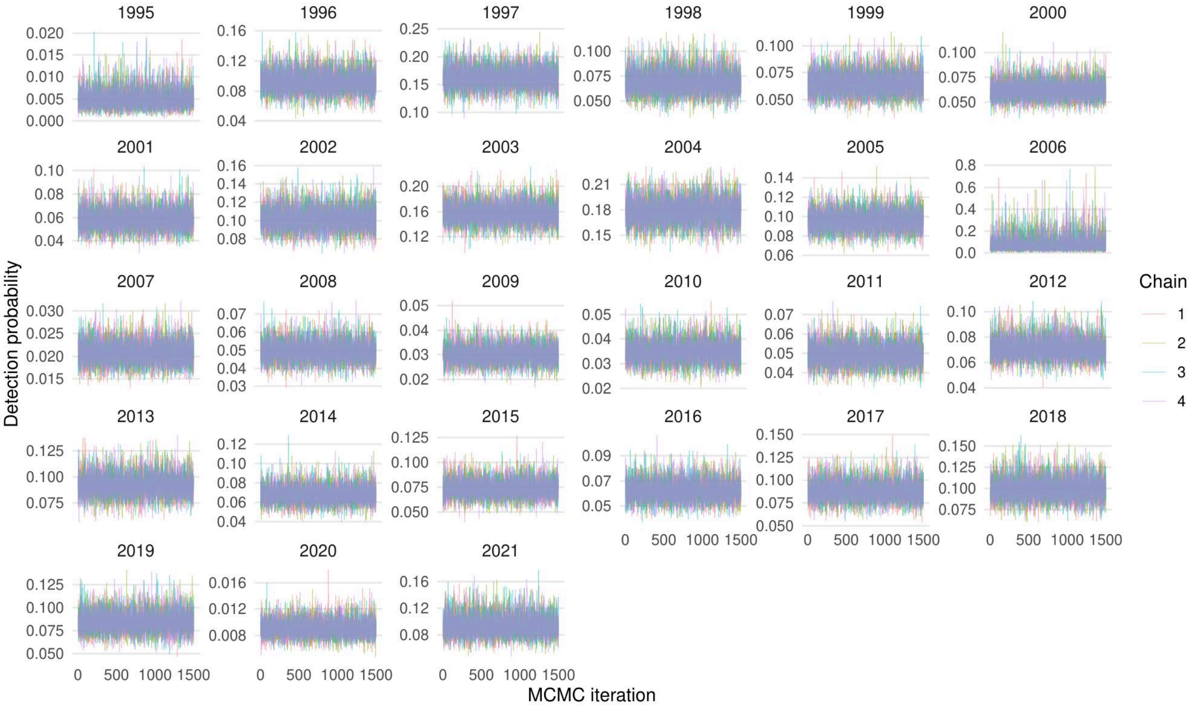

Figure B-4: Markov chain Monte Carlo traces for the detection probability of non-breeding adults of Antipodean albatross that were previously failed breeders, for each year, as estimated by the population model.

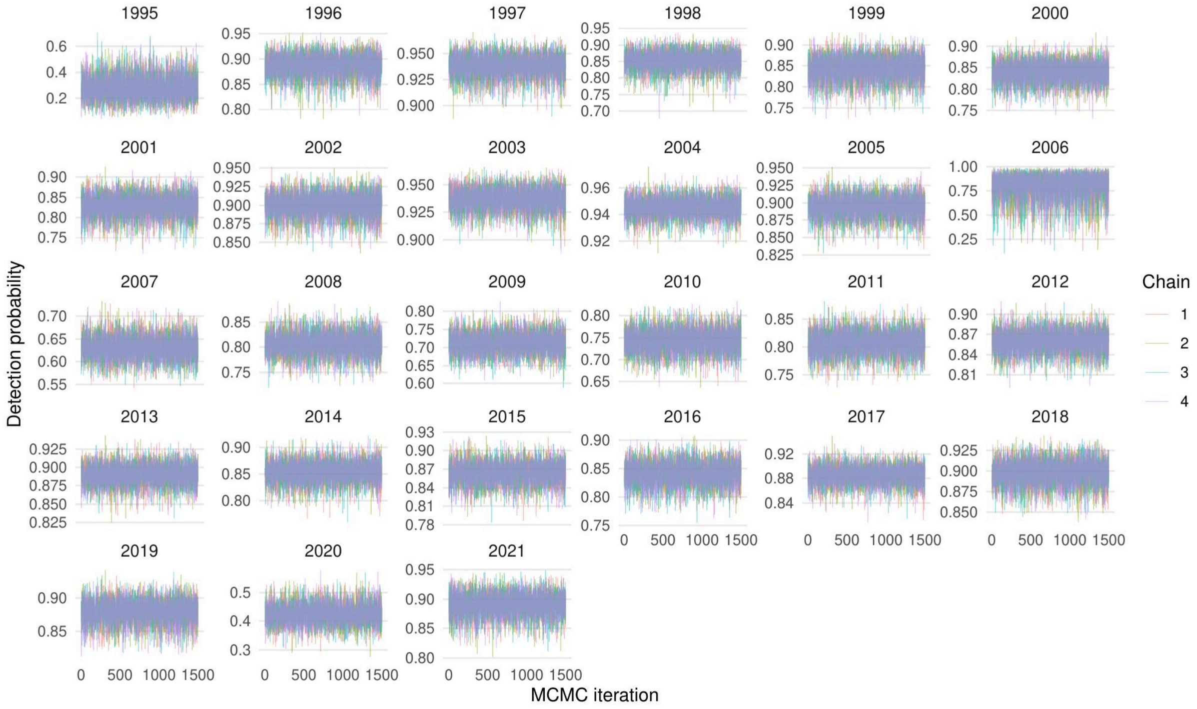

Figure B-5: Markov chain Monte Carlo traces for the detection probability of non-breeding adults of Antipodean albatross that were not previously failed breeders, for each year, as estimated by the population model.

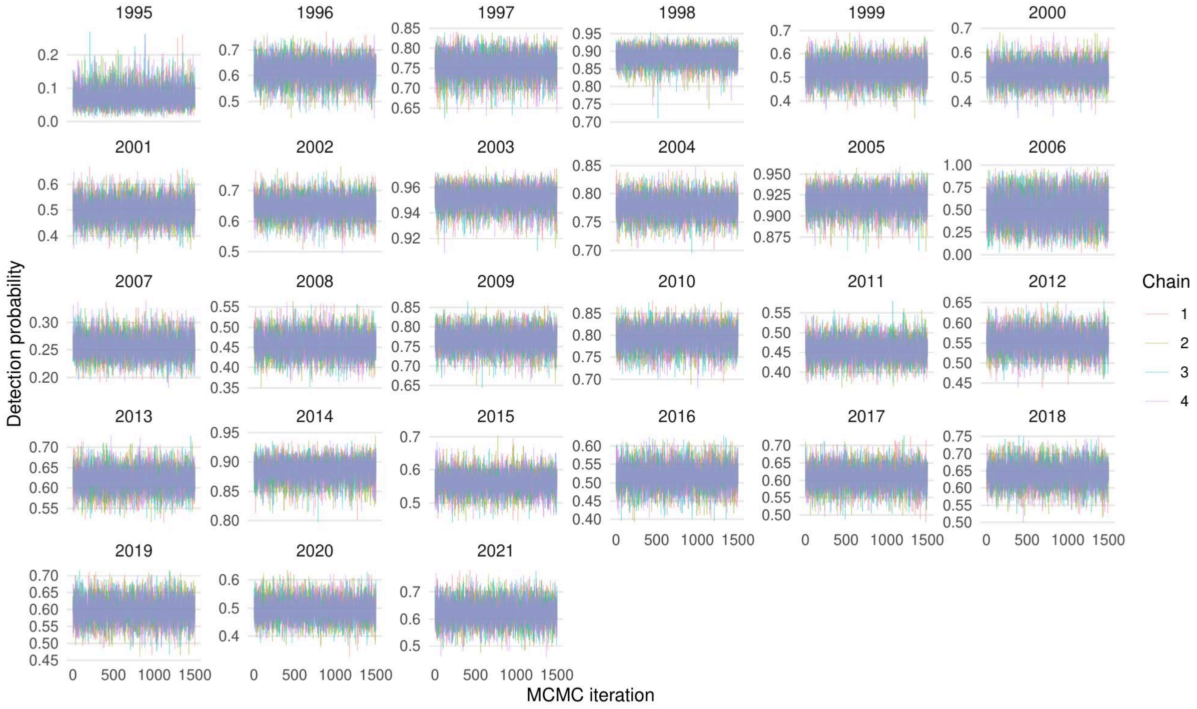

Figure B-6: Markov chain Monte Carlo traces for the detection probability of pre-breeders of Antipodean albatross by year, as estimated by the population model.

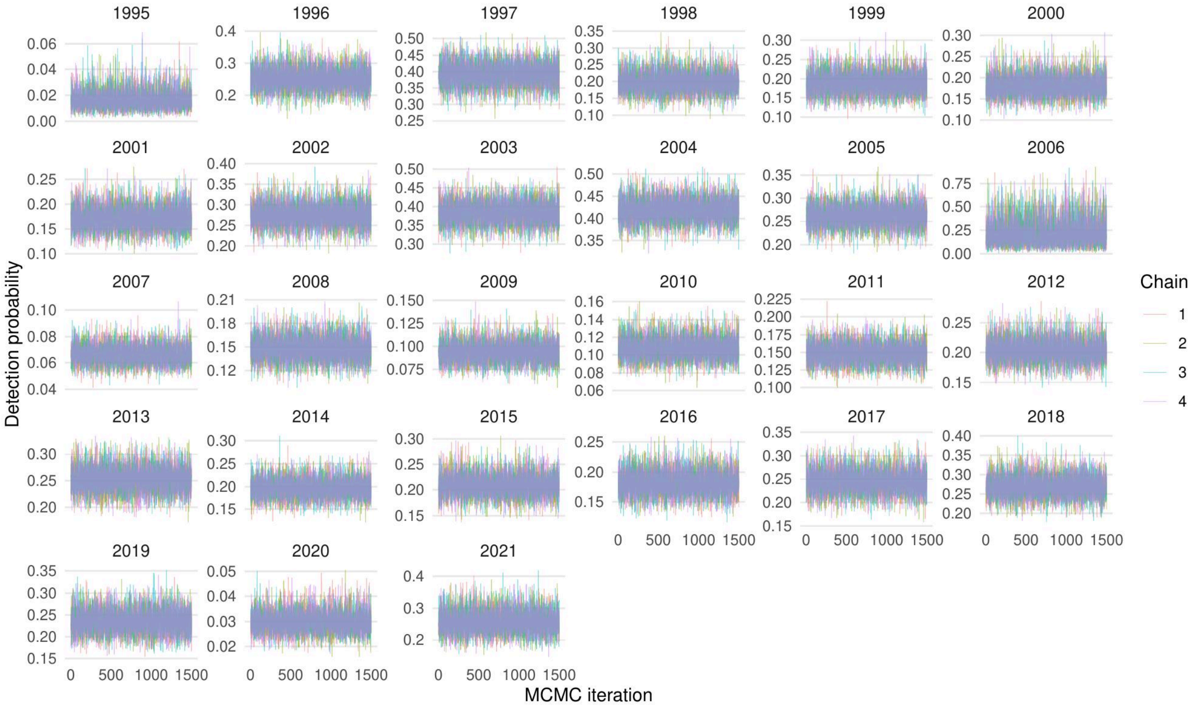

Figure B-7: Markov chain Monte Carlo traces for the detection probability of pre-breeders and non-breeders of Antipodean albatross outside the study area by year, as estimated by the population model.

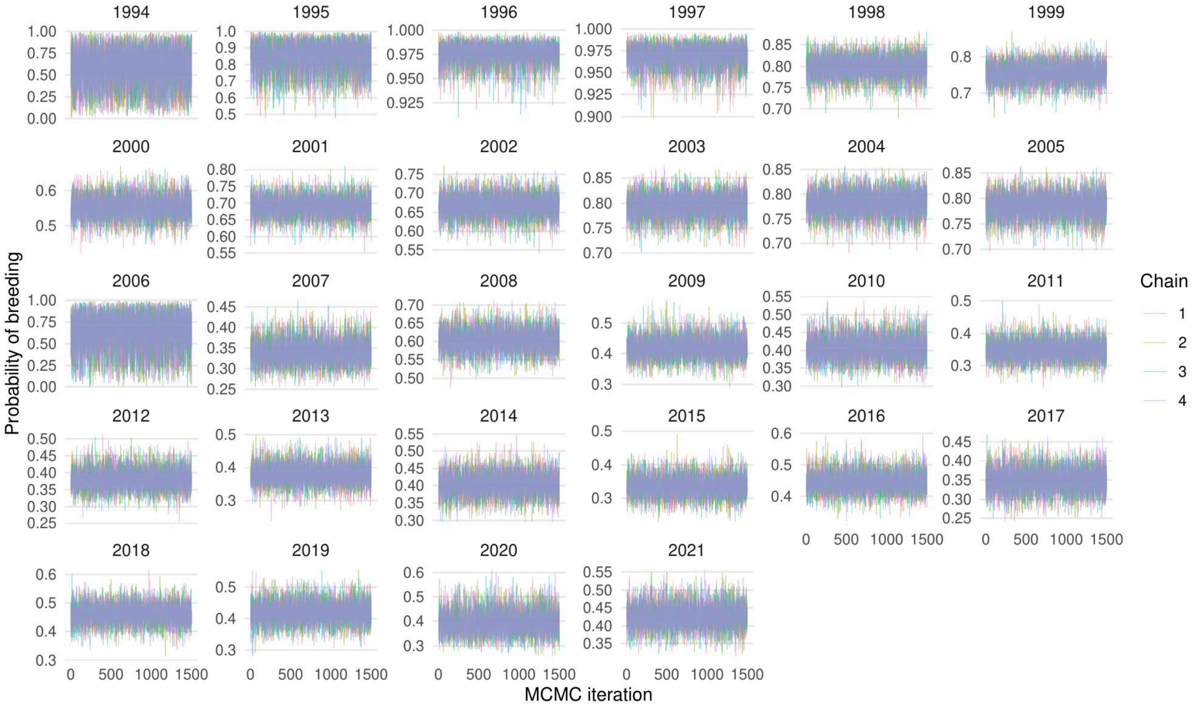

Figure B-8: Markov chain Monte Carlo traces for the probability of breeding for adults of Antipodean albatross that were previously unsuccessful breeders, as estimated by the population model.

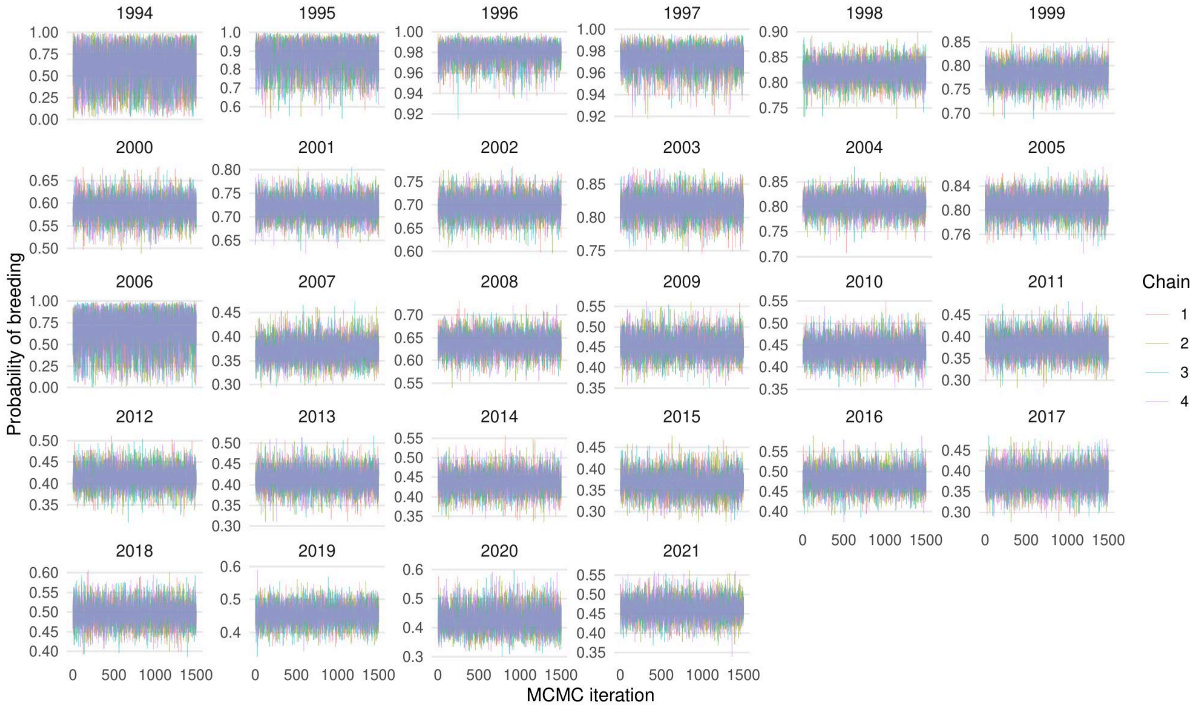

Figure B-9: Markov chain Monte Carlo traces for the probability of breeding for adults of Antipodean albatross that were not previously unsuccessful breeders, as estimated by the population model.

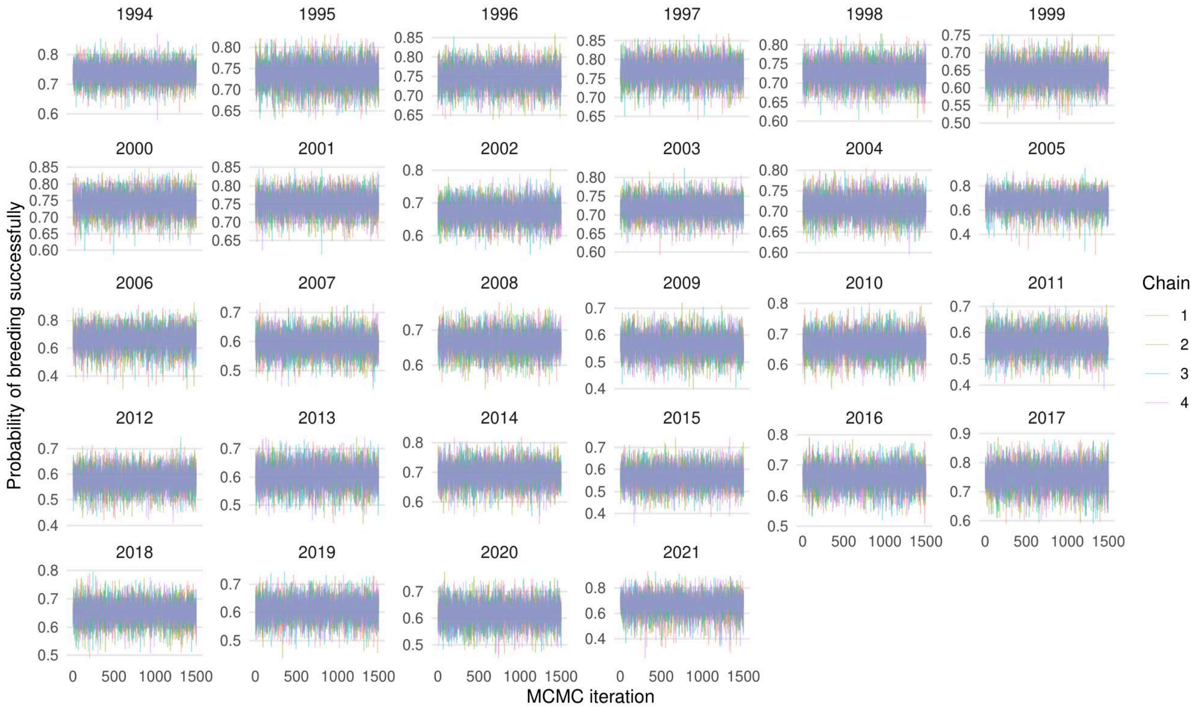

Figure B-10: Markov chain Monte Carlo traces for the breeding success of Antipodean albatross by year, as estimated by the population model.

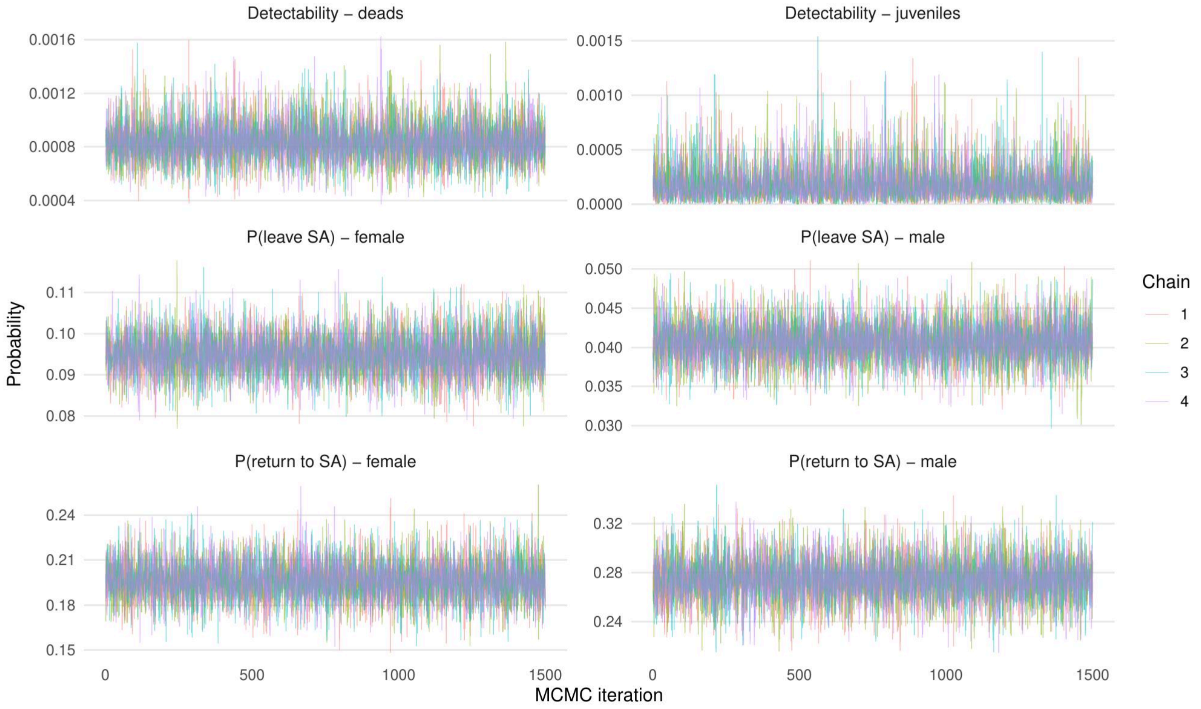

Figure B-11: Markov chain Monte Carlo traces for the detection probability of juveniles and dead individuals of Antipodean albatross, for the annual probability that an individual leaves the study area within the colony, and that an individual returns to the study area, as estimated by the population model.

APPENDIX C: AT-SEA DISTRIBUTION OF ANTIPODEAN ALBATROSS

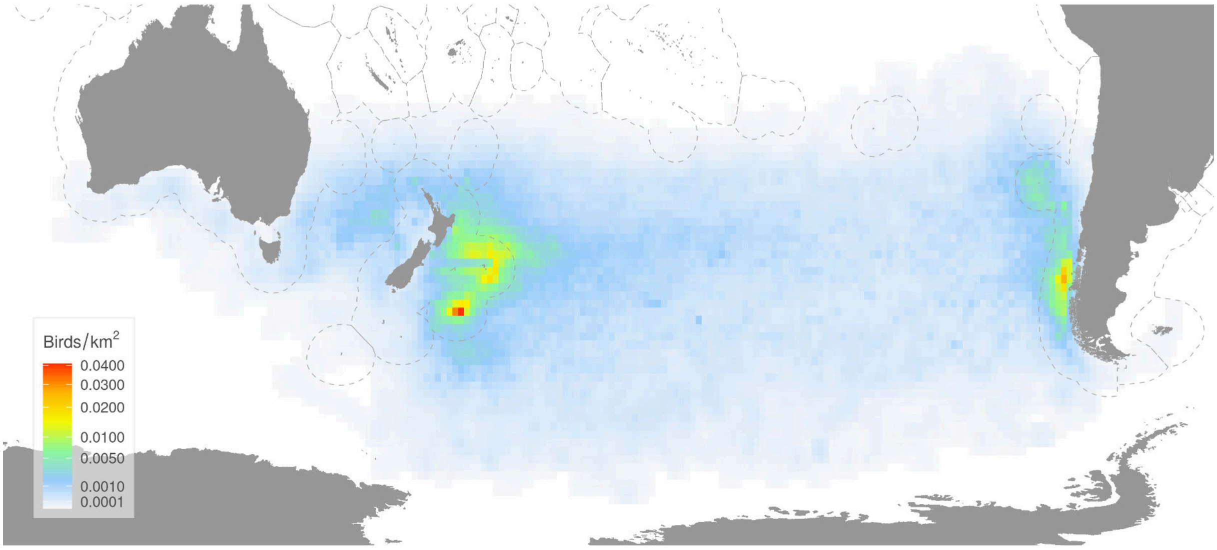

Figure C-1: At-sea distribution of Antipodean albatross, from Richard et al. (2024). The densities, in birds per square kilometre, were summed across all population classes. The colour scale was transformed by the square-root to highlight low-density areas. The dashed lines indicate the countries' Economic Exclusive Zone boundaries.

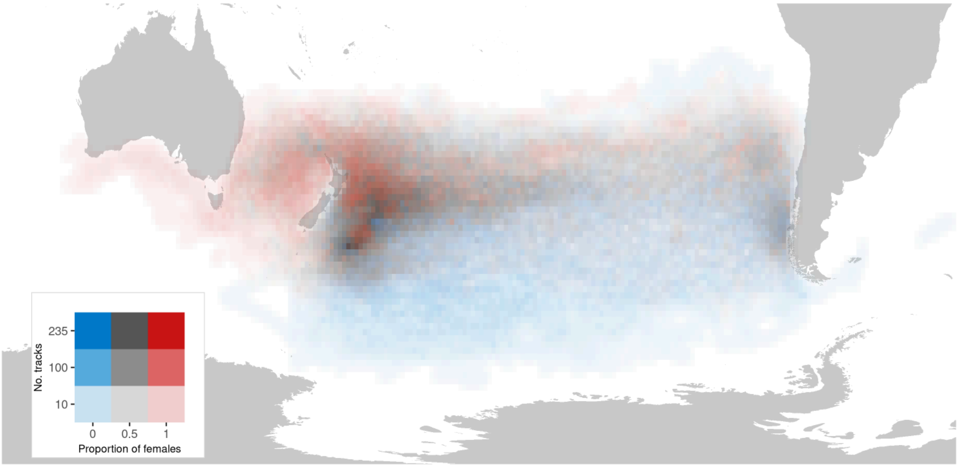
No. tracks
235
100
10
0
0.5
1
Proportion of females

Figure C-2: Spatial variability in the sex ratio of Antipodean albatross, derived from tracking data prepared by Richard et al. (2024). The hue shows the sex ratio, the colour intensity indicates the number of tracks from which the sex ratio was calculated.

APPENDIX D: NEW ZEALAND FISHING EFFORT

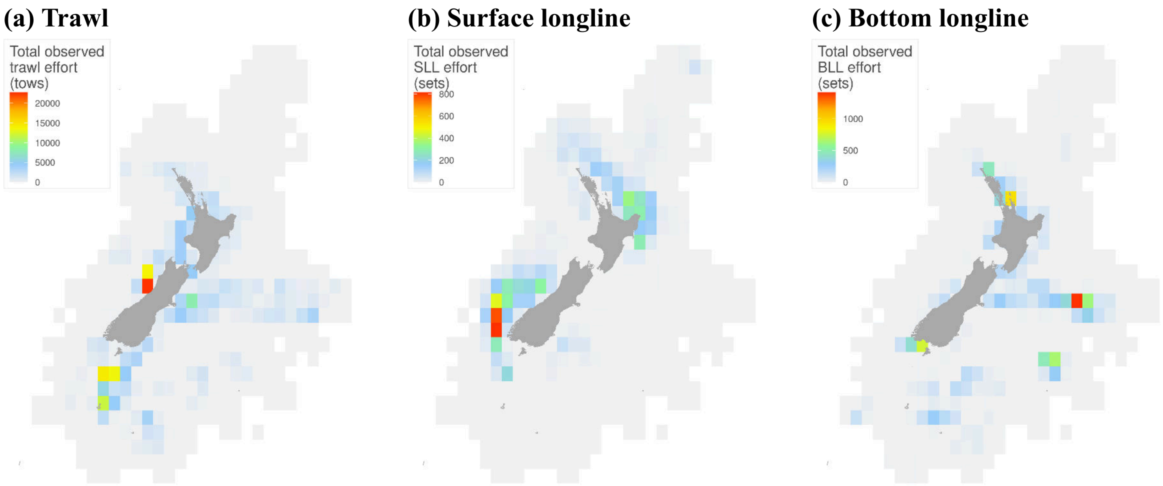
(a) Trawl

(b) Surface longline

(c) Bottom longline
Total observed trawl effort (tows)
20000
15000
10000
5000
0
Total observed SLL effort (sets)
800
600
400
200
0
Total observed BLL effort (sets)
1000
500
0

Figure D-1: Distribution of the total observed fishing effort within New Zealand’s Exclusive Economic Zone, for trawl, surface-longline, and bottom-longline fisheries. Data were from the period between 2003 and 2020, and used to fit the model of vulnerability. Fishing effort is in tows for trawl, and hook sets for longline fisheries.

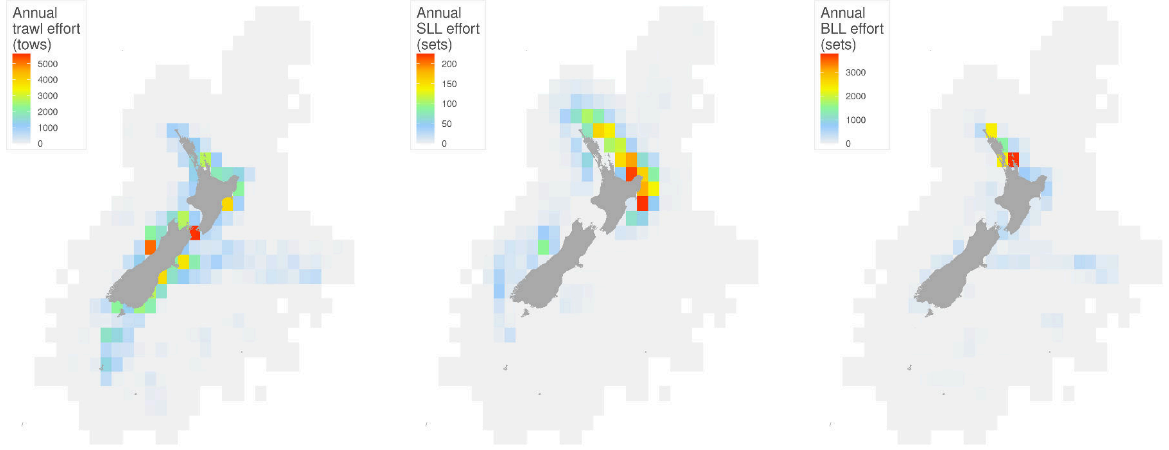
Annual
trawl effort
(tows)
5000
4000
3000
2000
1000
0
Annual
SLL effort
(sets)
200
150
100
50
0
Annual
BLL effort
(sets)
3000
2000
1000
0

(a) Trawl **(b) Surface longline** **(c) Bottom longline**

Figure D-2: Distribution of the mean annual fishing effort within New Zealand's Exclusive Economic Zone, for trawl, surface-longline, and bottom-longline fisheries. Data were from the period between 2003 and 2020, and used to predict captures. Fishing effort is in tows for trawl, and hook sets for longline fisheries.

APPENDIX E: MODEL DIAGNOSTICS FOR NEW ZEALAND FISHERY IMPACT

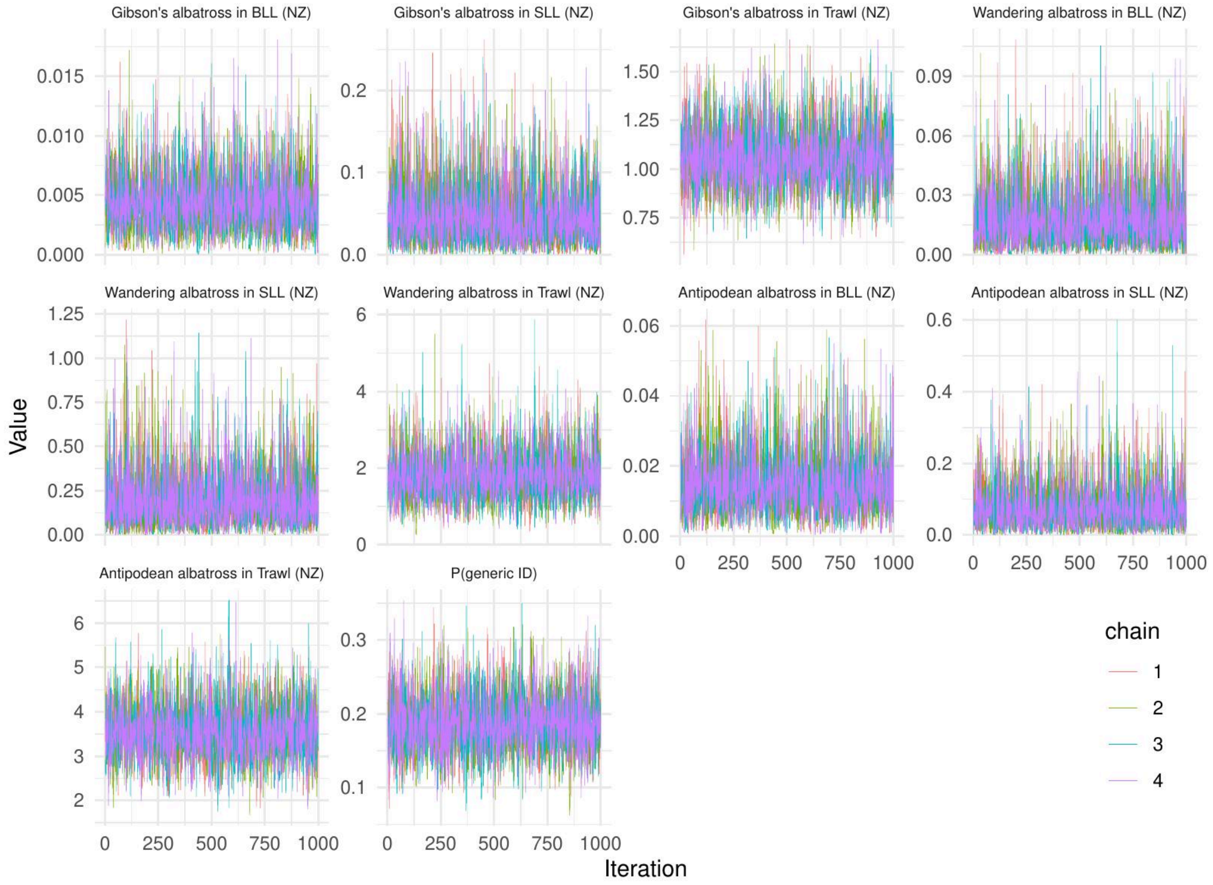

Figure E-1: Markov chain Monte Carlo traces for the model estimating the number of Antipodean albatross captures in New Zealand fisheries. The parameters shown are the vulnerabilities of the three taxa to the three fishing methods included in the model. SLL: surface longline, BLL: bottom longline, P(generic ID): probability of an observed capture to be identified at the species level.

APPENDIX F: OVERLAP BY YEAR AND FLAG IN THE TASMAN SEA

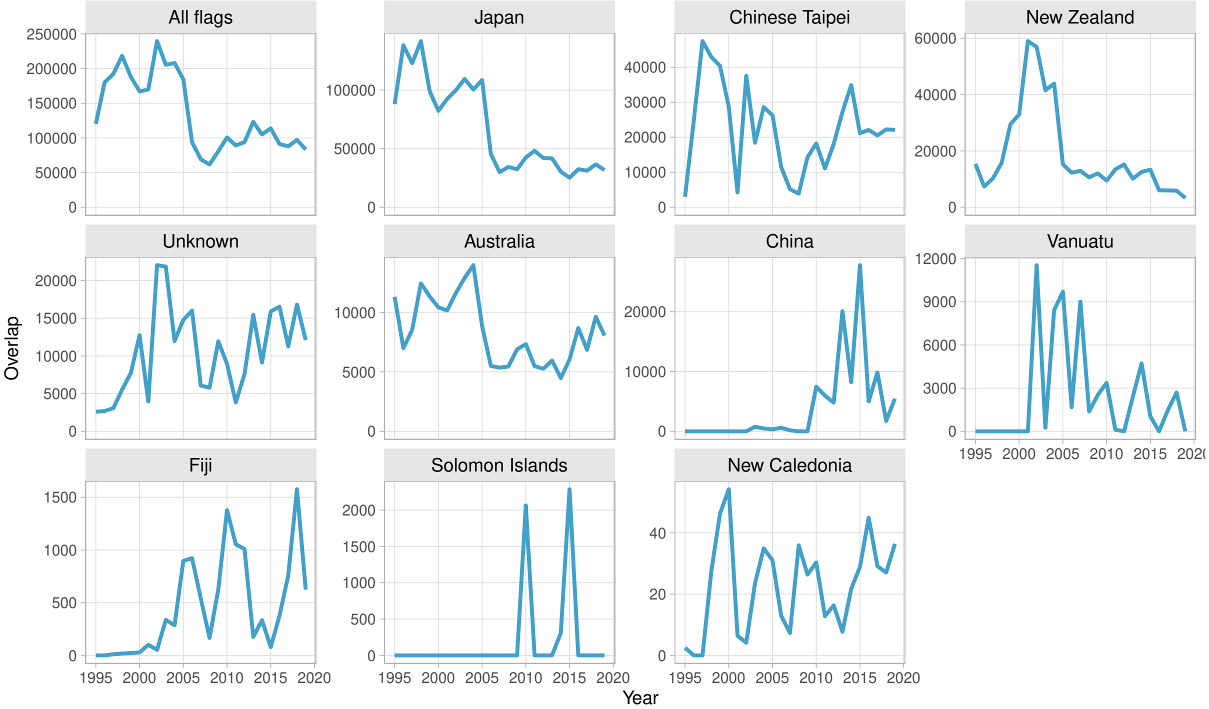

Figure F-1: Overlap by year between Antipodean albatross and the fishing effort by vessel flag, across all population classes, within the Tasman Sea.

APPENDIX G: INTERNATIONAL FISHERIES CATEGORISED AS “OTHER”

(a) South Korea (b) Fiji (c) French Polynesia (d) Solomon Islands

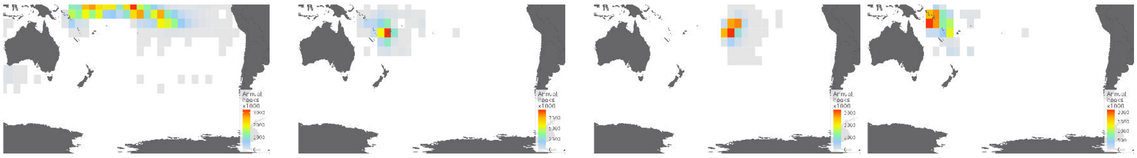

(e) United States (f) Samoa (g) Cook Islands (h) Papua New Guinea

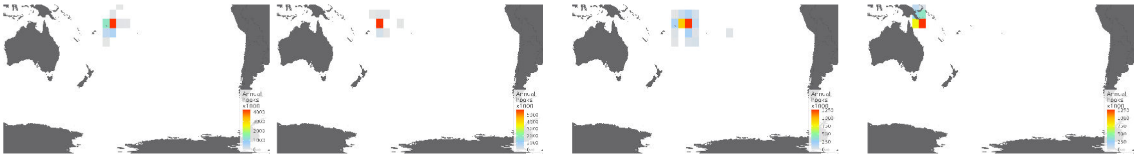

(i) New Caledonia (j) Micronesia (k) Panama (l) Belize

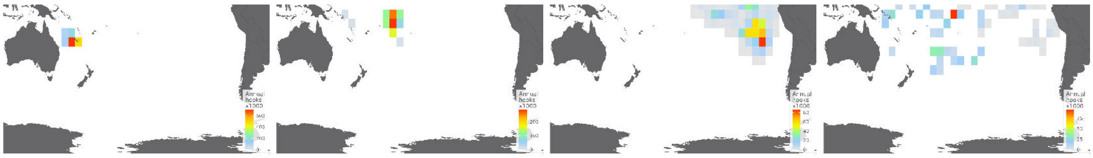

(m) Tonga (n) Uruguay (o) Kiribati (p) Brazil

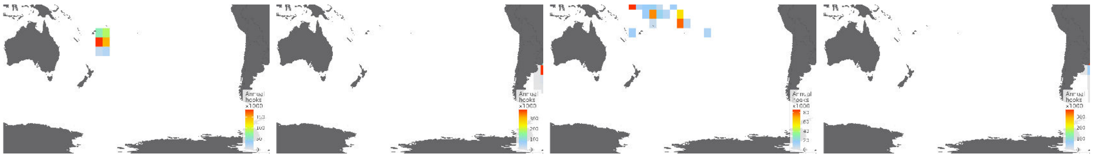

(q) Tuvalu (r) Portugal (s) Indonesia (t) Niue

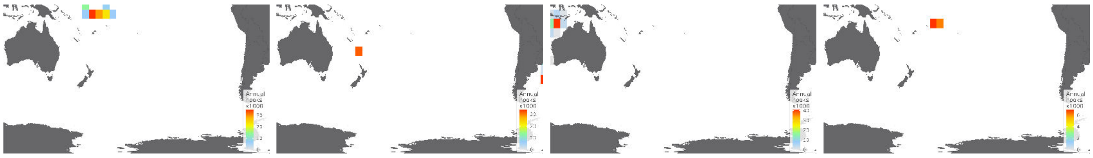

(u) Seychelles (v) St. Vincent & Grenadines (w) Thailand

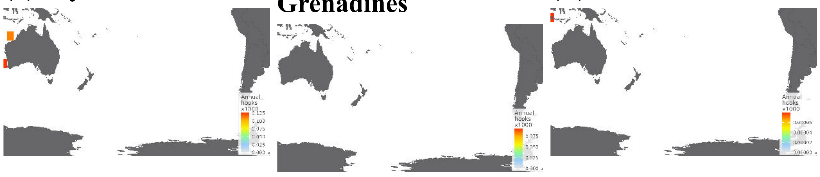

Figure G-1: Distribution of the mean annual fishing effort within the Antipodean albatross distribution range, for all vessel flags that were categorised as “Other” in the analysis. Vessel flags are sorted in decreasing order of mean fishing effort within the species range, between 1995 and 2019.